A TRNSYS Model of a Hybrid Lighting System

by

Greg Schlegel

A thesis submitted in partial fulfillment of the
requirements for the degree of:

Master of Science
Mechanical Engineering

University of Wisconsin – Madison
2003

Abstract

A TRNSYS Model of a Hybrid Lighting System
by Greg Schlegel
Under the supervision of William A. Beckman and Sandy A. Klein

During the past two years, considerable effort has been expended in developing the TRNSYS Hybrid Lighting Model. The work has resulted in a software tool that can simulate impacts associated with utilizing the hybrid lighting technology. All of the physical parameters of a hybrid lighting system are included as variables within the software. By utilizing this work, the hybrid lighting team can make design decisions based upon computer predictions of the performance of a hybrid lighting system.

The hybrid lighting system is modeled using the transient system simulation program TRNSYS. The TRNSYS model is implemented using interconnected components, which include a weather generator, radiation processors, a hybrid lighting model, a building model, building schedules, utility rate schedules, and output components. The results from the simulation include the annual energy and monetary savings gained from the hybrid lighting system. An economic model has been incorporated into the hybrid lighting model to calculate the break-even capital cost of a hybrid lighting system based on the annual savings.

A narrow-band and wide-band hybrid lighting model has been developed. The wide-band model uses direct normal solar radiation from either a TMY2 data file or the TRNSYS weather generator. The incoming direct normal radiation is weighted by the average spectral properties of the hybrid lighting components which include concentrator reflectance, secondary element transmittance and reflectance, thermal photovoltaic quantum efficiency, light fiber attenuation, and luminaire efficiency.

The narrow-band model uses TMY2 data or the TRNSYS weather generator to obtain the magnitude of the direct normal radiation, but the direct normal spectral distribution is predicted based on the atmospheric transmission model SMARTS. The narrow-band model predicts the direct normal spectral radiation at five nanometer bandwidths. Next it reads the available spectral component data, applies the component data to the solar spectral distribution, and calculates the amount of light and electricity that is generated by the system. The outputs from

both models include the light produced by the hybrid lighting system as well as electricity generated by the TPV.

Within TRNSYS, the light output from the hybrid lighting system model is sent to the building model. The building is modeled using the TRNSYS type 56 multi-zone building model. Type 56 is a FORTRAN subroutine which is designed to provide detailed thermal models of buildings. The model consists of two windowless 2500 m^2 zones. One zone uses efficient fluorescent lighting and the other zone uses hybrid lighting with dimmable fluorescent auxiliary lighting. Identical schedules in the two zones simulate the heating, cooling, and ventilation of a typical mixed-use environment. Gains in the model account for the people, computers, and lights in the building. Cooling in the building is supplied using a chiller with a constant COP of 3 and heating loads are met using an 80 % efficient natural gas furnace. Using local utility rate schedules, energy costs can be calculated for the two zones of the building model with the difference representing the energy savings due to the hybrid lighting system.

The hybrid lighting model calculates the break-even capital cost of a hybrid lighting system based on the system energy savings. The break-even capital cost is defined as the initial cost of the hybrid lighting system that will provide a life cycle savings (LCS) of zero over the economic lifetime. At this point in the design stage, realistic component prices are not available for determining economic parameters such as years to payback, LCS, or return on investment. Instead the break-even capital cost was calculated to be used as a price target where the energy savings predicted by the TRNSYS model will economically compensate for the system components.

Simulations were performed to determine effectiveness of the hybrid lighting technology across the United States. Hybrid lighting systems located in Tucson, AZ and Honolulu, HI performed best with break-even capital costs of $2050 and $2800 based on a 10 year analysis period.

Other daylighting strategies were evaluated to determine their cost competitiveness with hybrid lighting. Photovoltaics and toplighting were both evaluated using TRNSYS models. The break-even capital cost of the hybrid lighting system was approximately five times that of a toplighting or photovoltaic system. Photovoltaics are not an economic alternative, but the low cost and simple nature of toplighting makes it a very competitive alternative to hybrid lighting.

Acknowledgements

I would like to thank my advisors, Bill Beckman and Sandy Klein, for their support, guidance, and motivation throughout this project. Thanks for always having time to answer questions and spending time to ensure that the answers were understood. It has been a rewarding and unique experience to work and study in the Solar Energy Lab.

Thanks must also be extended to Michael Kummert, without his help I am not sure if my TRNSYS model would ever have worked. Michael not only provided constant support fixing TRNSYS and lab related problems, but he always had time to discuss new ideas and better ways to address problems.

A very special thanks goes out all of the students and faculty who make the Solar Energy Laboratory a great place to learn. I will treasure the friendships and cultural experiences that I have taken from my time here.

But most important of all, I would like to thank Leslie. Thank you for your understanding, patience, and love.

Table of Contents

List of Figures

List of Tables

Nomenclature

β_{act}	Actual Turbidity Value
β_{low}	Lower of Two Turbidity Fit Values
Δ_{β}	Difference between Turbidity Fit Values
ε	Band Gap of GaSb Semi-conductor
$\eta_{QE, \lambda}$	Quantum Efficiency
K_{λ}	Exponential Decay Coefficients
κ_1	Air Mass Decay Coefficient
κ_2	Turbidity Decay Coefficient
λ	Wavelength
μ_{SC}	Temperature Coefficient of the Short Circuit Current,
μ_{OC}	Temperature Coefficient of the Open Circuit Voltage,
ν_{λ}	1924 Standard CIE Visibility Curve
ρ_{λ}	Spectral Reflectance
$\rho_{\text{ light well}}$	Reflectance of Light Well Walls
τ_{λ}	Spectral Transmittance
$\tau_{skylight}$	Overall Transmittance of Skylight
A_{λ}	Spectral Attenuation of 3M Light Fiber
AM	Air Mass
Area $_{skylight}$	Area of Skylight Module
c	Speed of Light
C_{AREA}	Concentrator Area
dis	Discount Rate
Down	Initial Down Payment
e	Electron Charge
E	Equation of time
E_i	Illuminance
G_{λ}	Solar Irradiance
h	Planck's Constant

I_{SC}	Short Circuit Current
I_{MAX}	Current at Maximum Power Point
inf	General Inflation Rate
$Power_{IN}$	Total Input Power
L	Overall Light Fiber Length
LLOC	Longitude of the Location in Question
LST	Standard Meridian for the Local Time Zone
m	Mortgage Rate
M_s	Ratio of First Year Miscellaneous Costs to Initial Cost
n	Years of Analysis
PR_{tx}	Property Tax Rate
R_β	Turbidity Ratio
R_v	Ratio of Resale Value at the End of the Analysis to Initial Cost
$T_{C,REF}$	Reference Cell Temperature
t bar	Income Tax Rate
V_{MAX}	Voltage at Maximum Power Point
V_{OC}	Open Circuit Voltage
Val	Ratio of Initial Valuation to Initial Cost
Y_D	Years of Depreciation
Y_L	Years of Loan

Chapter 1 Introduction

1.1 Overview

Hybrid lighting represents an alternative renewable technology that has the potential to reduce building energy consumption due to lighting. In the U.S. commercial building sector, lighting is the single highest user of energy with current annual lighting energy estimates of about four quadrillion kilojoules (4 Quads) of primary energy (Department of Energy, 2000). With a domestic energy consumption of that level, hybrid lighting systems could provide significant reductions in demand and energy usage.

By dividing and utilizing different portions of the light spectrum, hybrid lighting has an advantage over other daylighting technologies. The first component of the system is a concentrating collector that collects light and focuses it onto a secondary element. The secondary element divides the light into the visible and infrared spectra. The visible spectrum is used directly to light the interior of the building while the infrared radiation is used to generate electricity.

Using sunlight to directly light the building, hybrid lighting overcomes the inefficiencies of indirect solar lighting systems such as photovoltaics. Photovoltaics use light to generate electricity, and the electricity from photovoltaic panels can be used to power interior lighting. Unfortunately commercially available photovoltaics generally operate at an overall efficiency of less than 15 %. Adding up all of the losses which include energy conversion losses, transmission losses, and losses due to electric lighting, the overall PV lighting system efficiency would be less than 5 %. According to Oak Ridge National Laboratory a hybrid lighting system will operate with efficiencies in the range of 20-30 % (Muhs, 2000a) while our studies indicate that system efficiencies will range from 31 -32 %.

Hybrid lighting also has advantages over daylighting techniques. Toplighting typically results in uneven light distribution, additional cooling loads, and the inability to maximize the amount of incident solar radiation collected. Daylighting techniques have been developed to overcome these problems but most of these techniques require significant and expensive building modifications. Hybrid lighting systems use two axis concentrating collectors to maximize collected beam solar energy and the systems distribute the light evenly throughout the lighted

space using large core optical fibers. Heat load effects are minimized by removing the infrared portion of the solar spectrum and using it for energy generation. Hybrid lighting systems also do not require major building modifications aside from a small roof penetration, optical fiber layout, and light fixture modifications. By overcoming some of the drawbacks of toplighting, daylighting, and PV lighting systems, hybrid lighting technology has the potential to bring solar energy into mainstream use.

1.2 The Atmosphere

In order to determine the quantity of energy that is available to the system, a thorough understanding of how light is transmitted through the atmosphere is needed. Light leaves the sun and is transmitted through space until it reaches the edge of the earth's atmosphere. At the edge of our atmosphere the energy from the sun has been reduced to the annual average value of 1367 W/m^2, the solar constant (Duffie and Beckman, 1991). The solar constant represents the power at the top of the earth's atmosphere integrated over all wavelengths. As the solar radiation is transmitted through the atmosphere, a portion of the energy, ranging from nearly 0 to 80 %, is either absorbed or scattered by different components of the atmosphere.

The amount of atmosphere that radiation passes through directly impacts the amount of radiation received at the earth's surface. The radiation path is represented by a value of air mass, the amount of atmosphere the radiation must travel through to get to the surface of the earth. An air mass of one is defined as the atmosphere the radiation must travel through to get to the equator when the sun is directly overhead. An air mass two is defined when the sun is at solar zenith angle of 60 degrees relative to the horizontal as shown in Figure 1.1. In general, the

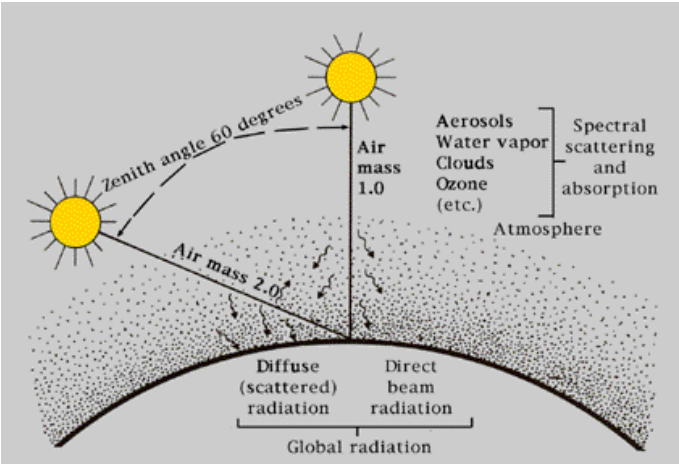

Figure 1.1: Air mass definitions

higher the location's latitude, the higher the air mass with larger values of air mass leading to smaller amounts of terrestrial radiation and more scattered radiation. Figure 1.2 shows the decrease in solar irradiance with increasing air mass.

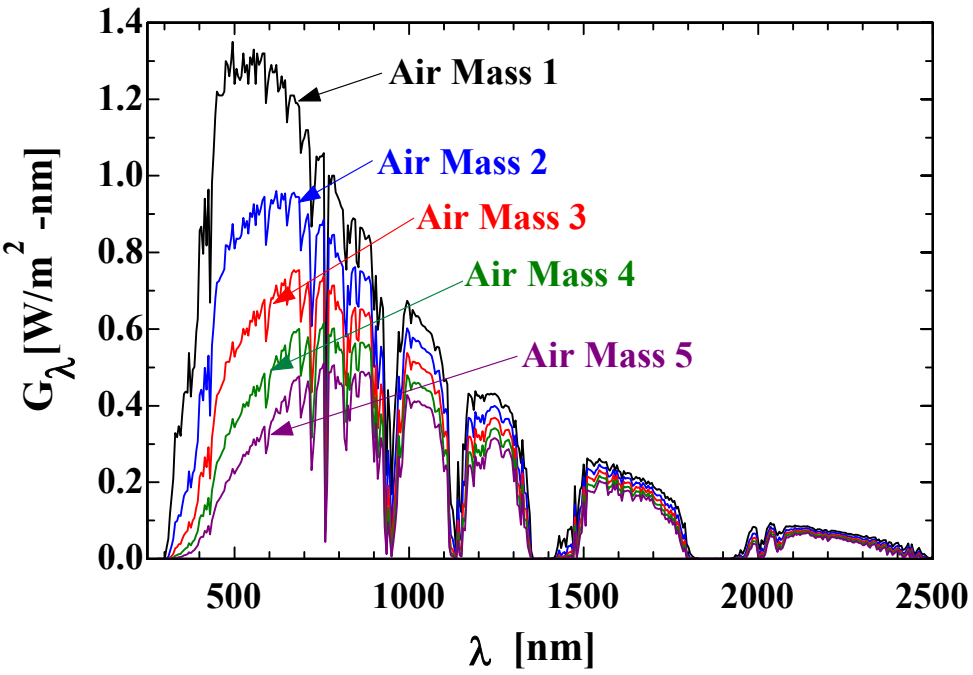

Figure 1.2: Terrestrial spectrum for various air masses

O_3=0.35, w=2 cm., β=0.1, results from SMARTS2 (Gueymard, 2000)

Ultraviolet (UV), visible, and infrared (IR) are the three radiation regions of the solar spectrum. The majority of the energy contained in the solar spectrum is transmitted at wavelengths between 0.3 μm and 2.4 μm. The visible portion of the spectrum includes wavelengths from about 0.38 μm - 0.78 μm. The wavelengths of the UV portion of the spectrum are less than 0.38 μm, while the IR portion of the spectrum has wavelengths greater than 0.78 μm. Hybrid lighting systems are designed to operate by utilizing the visible and near infrared portions of the spectrum that contain a large percentage of the sun's transmitted energy.

As radiation is transmitted through the atmosphere, some of the radiation, depending on wavelength, will be scattered, absorbed, or transmitted. Radiation attenuation can be attributed to dry air molecules, water vapor, and aerosols. While all elements of dry air scatter radiation regardless of wavelength, absorption is wavelength dependent. Ozone, oxygen, water vapor, and

carbon dioxide are some of the best absorbers of radiation in our atmosphere. At wavelengths greater than 2.5 μm, CO_2 and water vapor absorb most of the energy from the sun; less than 5 % of the total spectral energy at or above this wavelength reaches the Earth's surface (Duffie and Beckman, 1991).

Aerosols, tiny particles suspended in the atmosphere such as dirt, pollen, or soot, scatter incoming spectral radiation. The amount of aerosols in the atmosphere, or turbidity, is heavily dependent upon geographic location and weather conditions. Typically the turbidity of the atmosphere is greater over land than water and the turbidity levels are lower in drier climates and seasons. Another major contribution to increased turbidity of the atmosphere is air pollution from power generation and home heating (Iqbal, 1983).

Air mass, aerosols, water vapor, carbon dioxide, and ozone concentrations all affect the amount of radiation that passes through the atmosphere. Computer models have been created to simulate the attenuation of the solar spectrum due to the atmosphere. Models such as MODTRAN (Berk *et al*., 1989), LOWTRAN (Kneizys *et al*., 1980), and SMARTS2 (Gueymard, 2000) simulate atmospheric transmittance and scattering based on user-defined inputs of the atmosphere composition.

1.3 Beam and Diffuse Radiation

The operation of the hybrid lighting system depends on how the atmosphere scatters and absorbs the incoming radiation. The concentrating collector used with these systems gathers only the un-scattered and unabsorbed beam radiation, which is approximately 80 % of the total radiation we receive from the sun on a clear day (Muhs, 2000b). Although the diffuse radiation is useful for other solar applications like thermal heating, it is of no use to the concentrating collector used in hybrid lighting systems.

Since the diffuse radiation is of no use, it is very important to gather as much of the beam radiation as possible. The solar collection of beam radiation is maximized by tracking the sun's movement through the sky. The sun moves across the sky from east to west and reaches its highest point in the sky at noon solar time[1]. The solar azimuth angle is defined as 0 degrees when the sun is directly south, -90 degrees when the sun is directly east, and 90 degrees when the

[1] Solar time is the time used for all sun time relationships and can be thought of as noon when the sun crosses the meridian of the observer (Duffie and Beckman, 1991)

sun is pointing west (all values for the northern hemisphere). The height of the sun in the sky is defined by the zenith angle, which is the angle between the perpendicular to the surface horizontal, and the sun as shown in Figure 1.3. Changes in zenith angle throughout the day also have a significant impact on the value of air mass for that particular location and time. To maximize the amount of incident beam radiation, the collector must rotate to match the solar azimuth angle and the slope of the collector should follow the solar zenith angle. In order to track both angles a two-axis tracking system must be used.

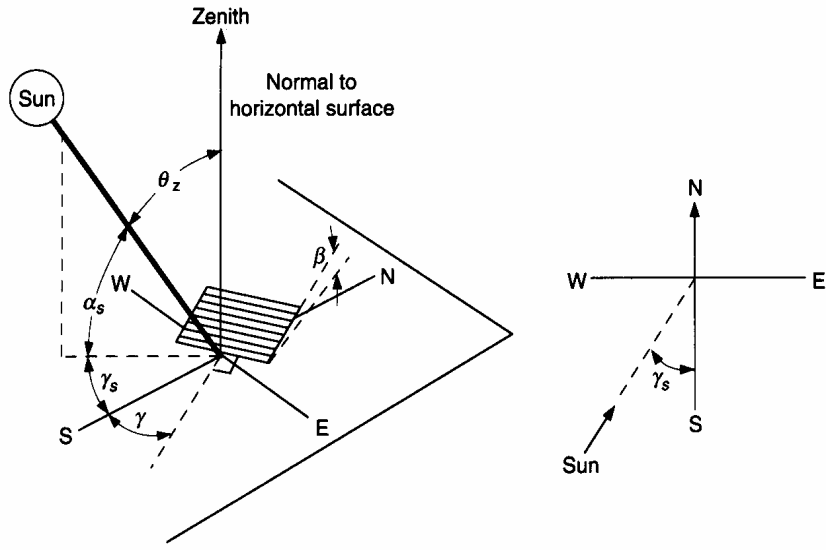

Figure 1.3: Zenith angle ϑ_z, solar altitude angle α_s, slope β, surface azimuth angle γ, and solar azimuth angle γ_s for a tilted surface (Duffie and Beckman, 1991)

1.4 Luminous Flux, the Visibility Curve, and Efficacy

In order to compare solar radiation to fluorescent lighting in commercial office buildings, both the solar radiation and the fluorescent light must be converted into a comparable unit of light. The instantaneous power of the radiation from the sky and the light output of a typical fluorescent lamp are both wavelength dependent. Since the eye views light differently depending on the power distribution at different wavelengths both the amount of solar radiation and the amount of fluorescent lighting must be weighted using response characteristics of the a typical human eye.

Luminous flux is defined as radiant power, or irradiance, weighted by the standard visibility curve as shown in Equation 1.1. The light watt is the unit of luminous flux based on this definition. Unfortunately the light watt concept was developed after the field of photometry had already named the standard unit of luminous flux to be the lumen. The lumen is based on a point source of one candela[2] at the center of a sphere. The sphere has a radius of either one meter or foot depending upon the unit system. The light per unit area, or luminous flux, on the surface of the sphere is equivalent to one lumen (lm) as shown in Figure 1.4. Light watts and lumens have been experimentally correlated to show that 683 light watts are equal to 1 lumen. Having two units of luminous flux, one historical and one scientifically derived, has created considerable confusion within the fields of photometry and illumination.

$$\text{Lumnious Flux (Light Watts)} = \int_0^\infty G_\lambda v_\lambda d\lambda \tag{1.1}$$

where

G_λ = Irradiance (W/m^2)

v_λ = 1924 standard CIE visibility curve

λ = wavelength

The eye processes light differently at varying wavelengths and illumination levels using two types of retinal receptors, the rods and the cones. The rods are used primarily under low light conditions and the cones are the receptors used under high levels of light. At luminance levels below 0.034 candelas/m^2 the eye functions almost exclusively using the rods, termed scotopic vision. Above 0.034 candelas/m^2 the eye primarily uses the cones or photopic vision. Under low illumination levels the eye's scotopic response results in heightened vision sensitivity towards smaller wavelengths or the violet end of the visible spectrum. Figure 1.5 shows a graphical representation of the photopic response (standard visibility curve). Under high illumination levels, the photopic response produces a higher sensitivity in the middle of the spectrum and is also primarily responsible for the way we see color, depth, and brightness. Due

[2] Unit of luminous intensity based on the output of a candle of standard size (IESNA, 2000).

to the different spectral power distribution of solar radiation and fluorescent light, the standard visibility curve must be included in evaluating the impact of the hybrid lighting system.

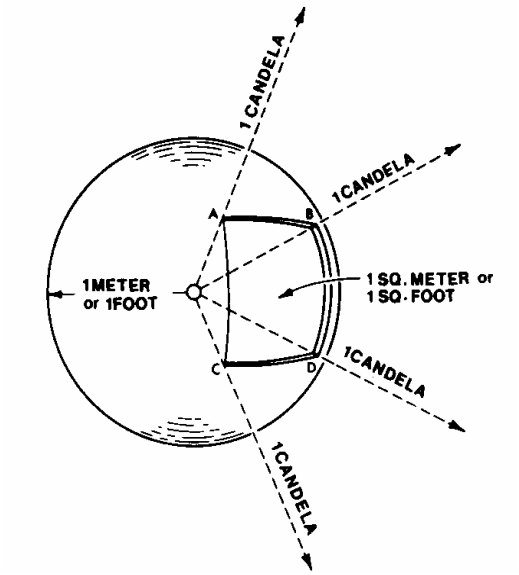

Figure 1.4: Definition of a lumen (IESNA, 2000)

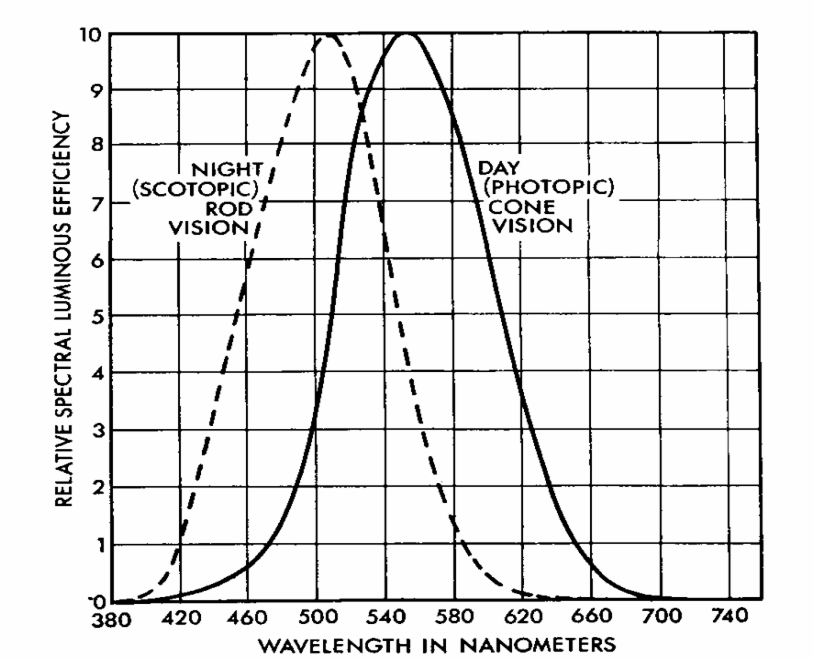

Figure 1.5: Wavelength characteristics of photopic and scotopic vision (IESNA, 2000)

Luminous efficacy of a light source is the ratio of the total emitted luminous flux and the total input power as shown in Equation 1.2. Luminous efficacy provides us with an important relationship between input power and light. To calculate the luminous efficacy of sunlight, the total solar irradiance is used as the input power and as the irradiance term, G_λ, in the numerator.

$$\text{Luminous Efficacy (lumens/watt)} = \frac{\int_0^\infty G_\lambda v_\lambda d\lambda}{Power_{IN}} \left[\frac{683\ lumens}{lightwatt} \right] \tag{1.2}$$

where

G_λ = Irradiance (W/m^2)

v_λ = 1924 standard CIE visibility curve

λ = wavelength

$Power_{IN}$ = Total input Power (W)

The efficacy of solar energy can be calculated from Equation 1.2, but as shown in Figure 1.6, air mass has a significant impact upon the solar efficacy. Increasing air mass results in decreased solar efficacy. In a hybrid lighting system, the light is actually being separated into visible and infrared portions. By reducing the limits of integration in the numerator of Equation 1.2 to the visible spectrum and below (0.38 μm - 0.78 μm), and limiting the input power to the visible and UV spectrum, the solar efficacy increases dramatically and is less affected by air mass. The increased solar efficacy is a major benefit of dividing the solar spectrum into two components and using them for separate purposes.

Fluorescent lighting is the main light source in office buildings. A fluorescent lamp converts electrical energy to light energy. The electrical energy is converted into UV light which is converted into visible light through a phosphor coating on the inside of the lamp bulb. Through each of these energy conversion steps energy is wasted and only a fraction of the initial energy is created into visible light. A perfect light source emitting monochromatic radiation at 0.555 μm could convert energy into light at an efficacy of 683 lumens/watt (lm/W). The firefly can convert energy into light at an efficacy of 560 lm/W yet in contrast, the best efficacy of a fluorescent lamp is approximately 100 lm/W. Figure 1.7 shows the efficacy of various light

sources including fluorescent and incandescent lamps.

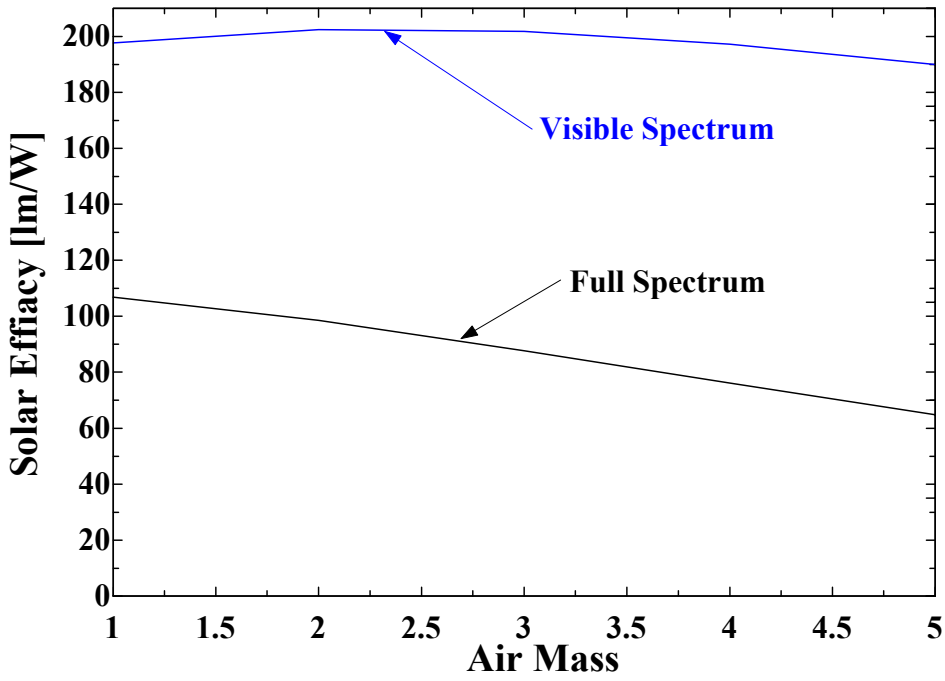

Figure 1.6: Solar efficacy versus air mass

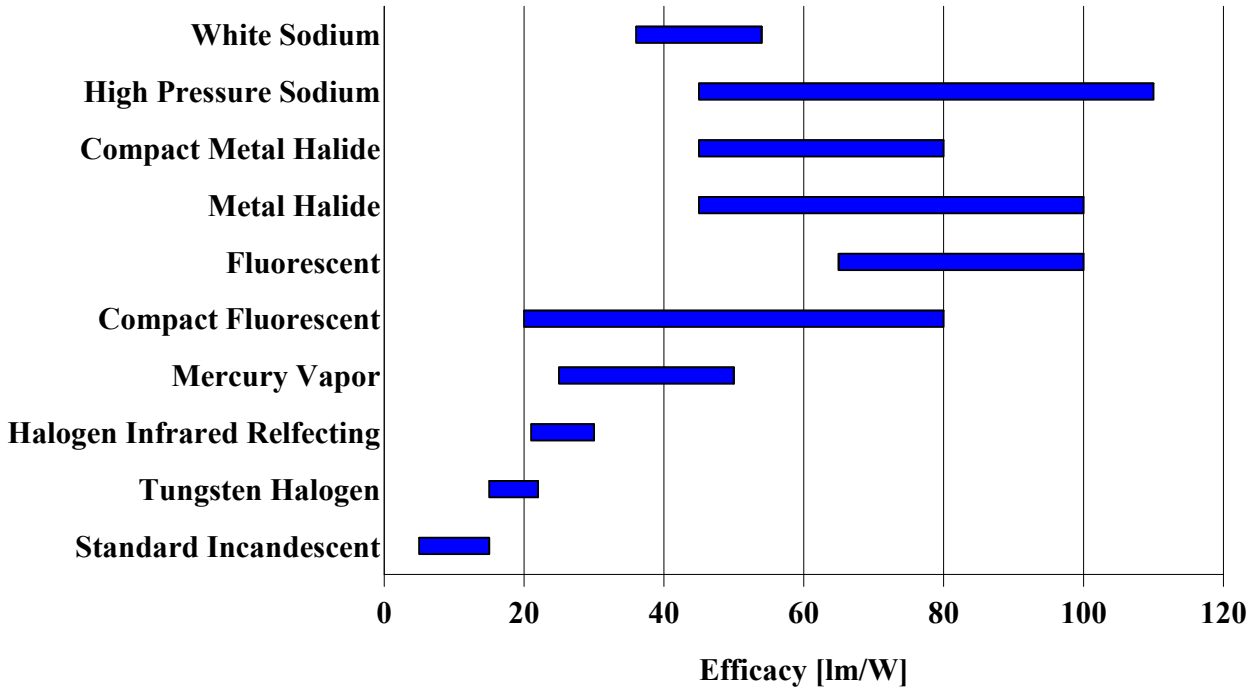

Figure 1.7: Luminous efficacy of various light sources (IESNA, 2000)

Recommendations of general lighting requirements for different areas and activities can be taken from the IESNA Lighting Handbook. Lux (lx) is the standard SI unit of illuminance. One lux is defined as 1 lumen/m^2. The IES Handbook gives a recommended value for common visual tasks as 300- 750 Lux (IESNA, 2000). Increased illumination is recommended as task become smaller in size and less defined in contrast. The recommended illumination values are used to determine the amount of light needed in an office building.

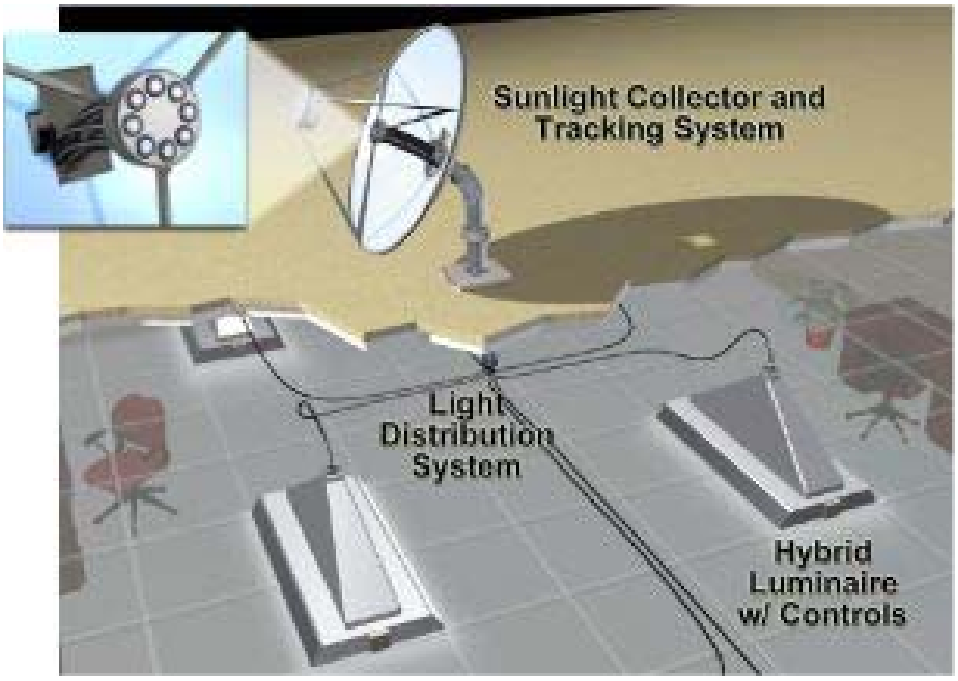

Figure 1.8: Hybrid lighting system

1.5 Hybrid Lighting Components

As shown in Figure 1.8, the radiation collection system, the light distribution system, the controls, and the luminaries are the four major components of a hybrid lighting system. The collection system is composed of a concentrating solar collector that tracks the sun and gathers solar beam radiation. The radiation is filtered into two types of radiation, the visible and the IR spectrum. The IR portion of the radiation can be harnessed to perform a number of tasks but initially it will be used for electricity generation in a thermal photovoltaic cell. Thermal photovoltaic cells are designed to operate more efficiently over the infrared spectrum than typical photovoltaic cells. The remaining visible portion of the light spectrum is channeled

through the light transmission system, out the specially configured luminaries, and into the lighted space.

1.6 Hybrid Lighting Model

The hybrid lighting system is modeled using TRNSYS (Klein *et al*., 2000). Inside the TRNSYS model, the lighting system is separated into components. The current model components include a weather generator, radiation processors, a secondary element, a building component with appropriate schedules, an economic model, utility rate schedules and wide and narrow-band hybrid lighting models. The program focuses on annual energy and dollar savings gained through the hybrid lighting system. An economic model has been incorporated into the model to calculate the break-even capital cost of a hybrid lighting system based on various economic parameters. A user friendly TRNSED (see page 58) interface has been added to increase the usability of the simulation.

Chapter 2 System Components

2.1 Concentrating Collector

The concentrating collector is composed of a concentrator in the form of a circular concave parabolic mirror, and a receiver onto which the radiation is focused. The aperture is the area of the concentrator that can collect sunlight. The geometric concentration ratio is defined as the ratio of the aperture area and the receiver area. The collector gathers the terrestrial radiation and increases the power density of the light by focusing it onto the smaller area of the receiver. Typical materials used for the concentrator have a high average reflectivity of approximately 0.95. Reflection losses, losses due to the secondary element obstruction, and the concentration ratio determine the output of a concentrating collector.

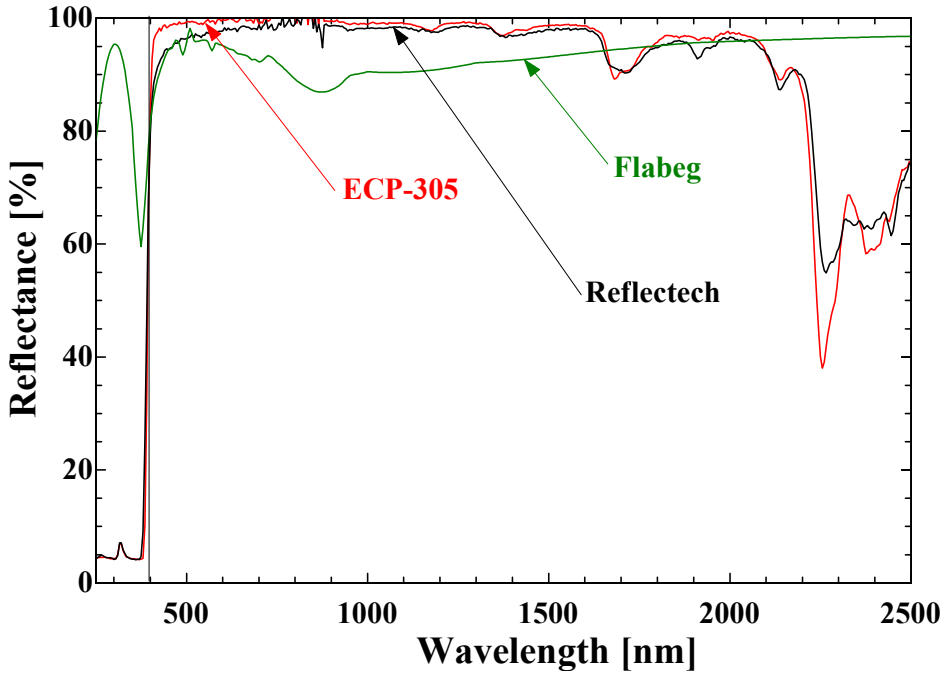

Figure 2.1: Spectral reflectance of concentrator materials

Figure 2.1 shows the spectral characteristics of the three concentrator materials that are being considered for use in the hybrid lighting project. All three materials have a high reflectance over the visible and near infrared spectra up until approximately 2100 nm. Near 2100 nm, the spectral reflectance of all three materials begins to decline. The decreased

reflectance in the long-wavelength region of the spectrum being considered does not have a large impact because approximately 95 % of the power in the spectral distribution is below 2100 nm. Equation 2.1 is used to calculate the average spectral reflectance for each material. Evaluation of Equation 2.1 using air mass one irradiance values and the data from Figure 2.1 resulted in average reflectance values of 0.95, 0.97, and 0.92 for the Reflectech, ECP-305+, and FLABEG materials respectively.

$$\bar{\rho} = \frac{\int_0^\infty G_\lambda \rho_\lambda d\lambda}{\int_0^\infty G_\lambda d\lambda} \tag{2.1}$$

where

$\bar{\rho}$ = average spectral reflectance
ρ_λ = spectral reflectance
G_λ = Irradiance (W/m^2 - nm)
λ = wavelength

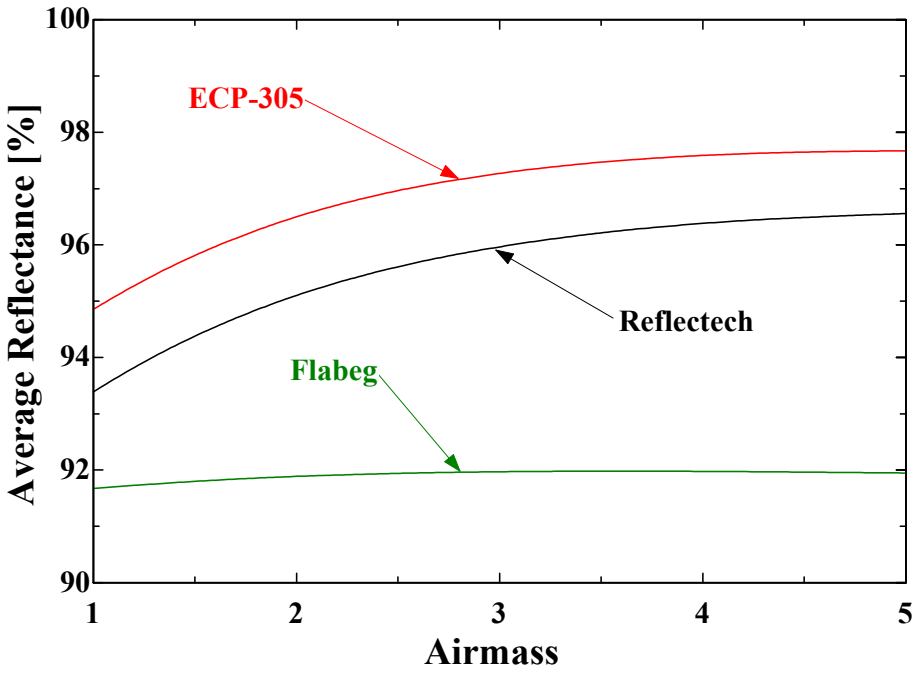

Figure 2.2: Average concentrator reflectance

The irradiance values used in Equation 2.1 will affect the average reflectance values of the concentrator, so the wide-band reflectance will be dependent not only upon irradiance but upon air mass as well. Figure 2.2 shows the wide-band reflectance versus air mass. Notice how the reflectance increases as air mass increases due to decreasing amounts of radiation in the near infrared. Since there is less radiation in the near infrared less is lost due to poor reflectance which leads to a higher average reflectance value. A hybrid lighting model, which included narrow-band spectral data rather than the average or wide-band values, would provide more accurate results by reducing the error associated with the wide-band averaging.

2.2 Secondary Element – Cold Mirror

The secondary element lies near the focal point of the concentrating collector. The exact geometry of the design is not complete, but it is assumed that all of the solar radiation reflected from the dish strikes the secondary element. The secondary element is comprised of an eight faceted "cold" mirror. The "cold" mirror allows infrared energy to be transmitted while the visible energy is reflected. The spectral properties of the cold mirror are not perfect and some of the solar radiation will be lost in the process of being reflected, transmitted, or absorbed. The cold mirror is especially inefficient at the transition between the visible spectrum and infrared spectrum as shown in Figure 2.3. The inefficiency from 650-780 nm is relatively insignificant due to the standard CIE visibility curve, which represents the spectral sensitivity of the human eye. The eye does not see visible light very well at longer visible wavelengths, so the reflectance losses at longer visible wavelengths are not as significant as they appear to be. No spectral data beyond 900 nm were available for the secondary element so the infrared reflectance was assumed to be constant for wavelengths of 900 nm and longer.

The average spectral reflectance and transmittance of the cold mirror was calculated using Equation 2. Initially the calculation was made without weighting the numerator and denominator by the standard CIE visibility curve. Without including the CIE visibility response, the average visible reflectance was 78 %. Including the standard CIE visibility response into the calculation yielded an average visible reflectance of 93 %. Since the hybrid lighting system will be used to displace light visible by the human eye, the higher average reflectance, which includes the CIE visibility factor, represents the average cold mirror reflectance more accurately. From Equation 2.3 and the gray assumption past 900 nm, the average transmittance of infrared energy

was 97 %.

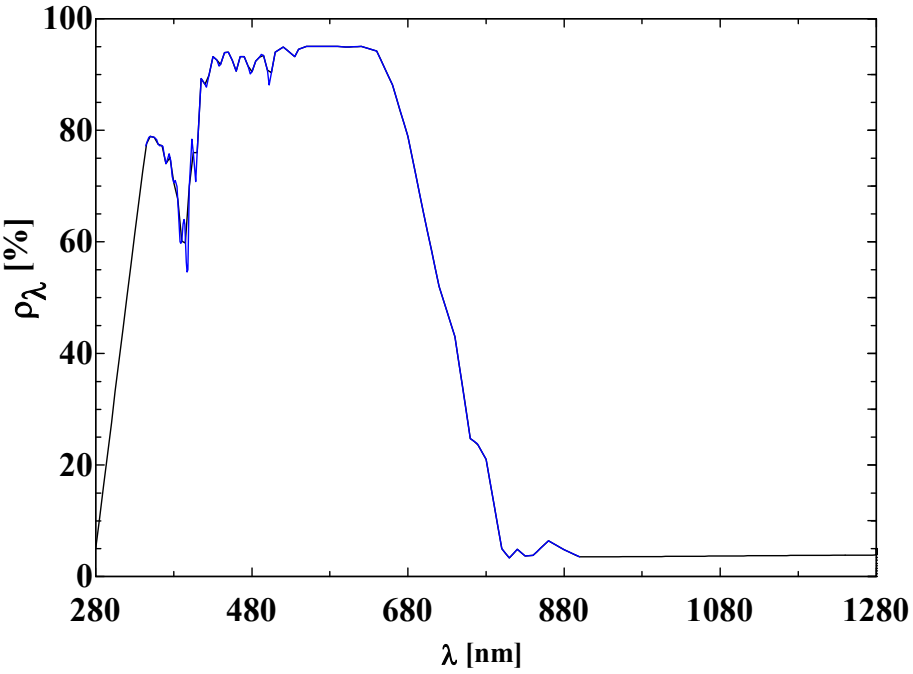

Figure 2.3: Spectral reflectance of secondary element (cold mirror)

$$\bar{\rho}_{visible} = \frac{\int_{380}^{780} G_\lambda v_\lambda \rho_\lambda d\lambda}{\int_{380}^{780} G_\lambda v_\lambda d\lambda} \tag{2.2}$$

$$\bar{\tau}_{\text{infrared}} = \frac{\int_{780}^{2500} G_\lambda (1-\rho_\lambda) d\lambda}{\int_{780}^{2500} G_\lambda d\lambda} \tag{2.3}$$

where

$\bar{\rho}_{visible}$ = average visible reflectance of cold mirror

$\bar{\tau}_{\text{infrared}}$ = average infrared transmittance of cold mirror

ρ_λ = spectral reflectance of cold mirror

υ_λ = 1924 standard CIE visibility curve

The current design of the hybrid lighting system focuses all of the visible light into eight light fibers. In order to ensure that the maximum amount of light enters the fiber, the light needs to enter at an angle as close to perpendicular to the plane of the optical fiber as possible. The cold mirror was designed into eight sections as shown in Figure 2.4, with each section collecting one-eighth of the total visible beam radiation and focusing that visible radiation onto a single fiber. Losses will occur between the collector, the cold mirror, and the entrance to the light fibers, but once the system is aligned correctly the losses should be minimal.

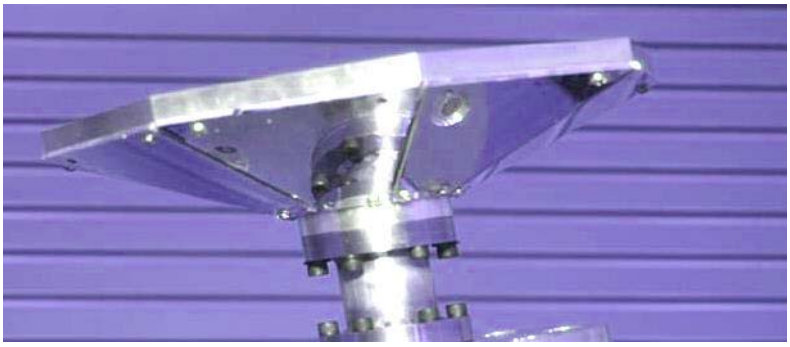

Figure 2.4: Photo of eight faceted cold mirror
(photo courtesy of ORNL, and W.A. Beckman, 2002)

2.3 Thermal Photovoltaic Array

The thermal photovoltaic (TPV) array is a Gallium Antimonide (GaSb) photovoltaic which is sensitive in the near infrared spectrum. The overall benefit of including the TPV array in the system is that energy in the near infrared spectrum, which would otherwise be wasted, can be used to generate electricity. A typical silicon (Si) photovoltaic would not be as effective due to its sensitivity in the visible spectrum. The sensitivity of both types of cells is shown in Figure 2.5. The thermal photovoltaic voltaic array is made up of 100 cells wired in series over an area of approximately 180 cm^2. JX Crystals, the company which developed the TPV array, has flash tested the array and recorded the current and voltage characteristics as shown in Figure 2.6 (Fraas, 2001).

The TPV is sensitive to solar irradiance over the wavelengths from 800 nm to 1500 nm. The wavelength dependent quantum efficiency in Figure 2.5 shows the spectral sensitivity of a GaSb TPV and a silicon based photovoltaic. The quantum efficiency of a photovoltaic defines the ratio of the photons incident upon the surface of the TPV to free electrons created. The

resulting free electrons create the useful current produced by the photovoltaic. For example, if ten photons strike the photovoltaic surface, but only eight electron holes are created then the quantum efficiency of that cell is 80 %. The photovoltaic response shown on the right axis is an indicator of the current output from a silicon photovoltaic based on watts of input radiation. From Figure 2.5 it is clear that a silicon based photovoltaic would not be as effective in a hybrid lighting system as the GaSb TPV cells.

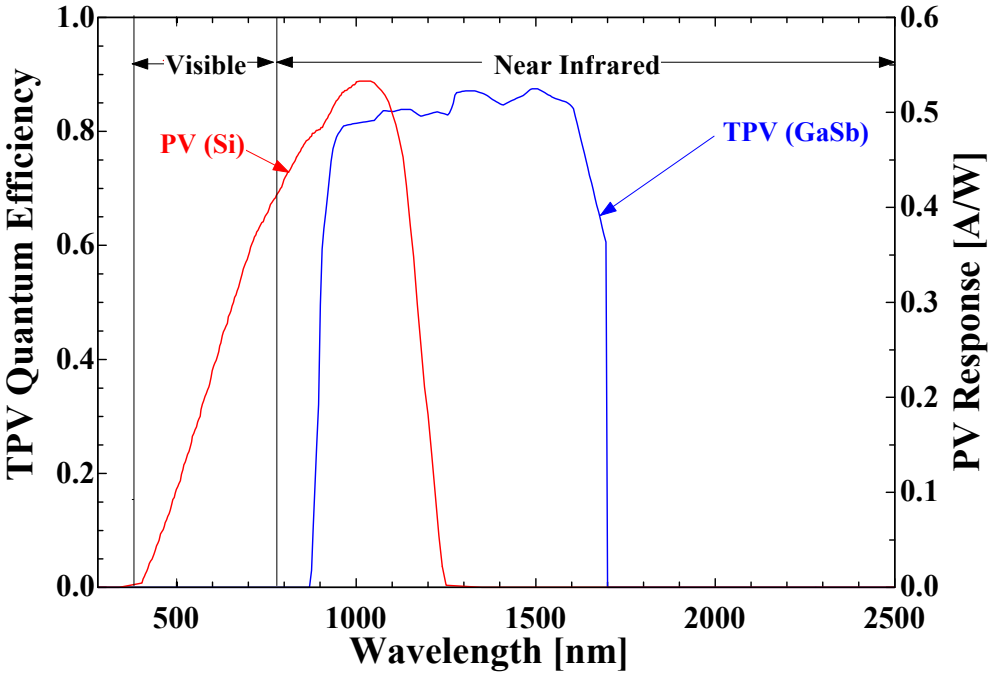

Figure 2.5: Sensitivity of silicone and GaSb photovoltaic cells

To determine the output of the TPV array the amount of photons per second incident upon the surface of the array is calculated. Using the quantum efficiency, the number of free electrons can be calculated. The electron potential can be used to calculate the current produced by the array based on the amount of free electrons. The current and voltage characteristics of the TPV are included in an I-V model which is used to calculate the corresponding output voltage and power. The calculations and equations are explained in detail in Chapter 4.

The voltage and current characteristics of the TPV array are modeled using an equivalent circuit containing a diode, series resistance, and shunt resistance as presented in Duffie and Beckman (Duffie and Beckman, 1991). Cell temperature and solar concentration have an impact on the voltage and current characteristics of the array and are accounted for in the model. The

TPV array will increase in temperature dramatically during operation due to the high concentration of infrared radiation incident upon the array's surface. With increasing temperature, the array voltage drops while the current increases resulting in an overall loss of power from the array. To provide cooling and maintain higher efficiencies, the array will be mounted directly to an air cooled heat sink with forced convection provided by a five watt fan (Fraas, 2001).

The TPV array is also sensitive to the concentration of the incoming solar radiation which is accounted for in the current voltage (I-V) model. The I-V model is fit to the experimental data from JX Crystals as shown in Figure 2.6. Increasing the solar concentration incident upon the TPV array will shift the I-V curve upwards, increasing both the current and voltage. Decreasing the solar concentration will shift the I-V curve downwards with a decrease in both current and voltage. The solar concentration will be determined by the final design geometry of the concentrator dish and the receiver as well as the direct normal solar radiation throughout the day.

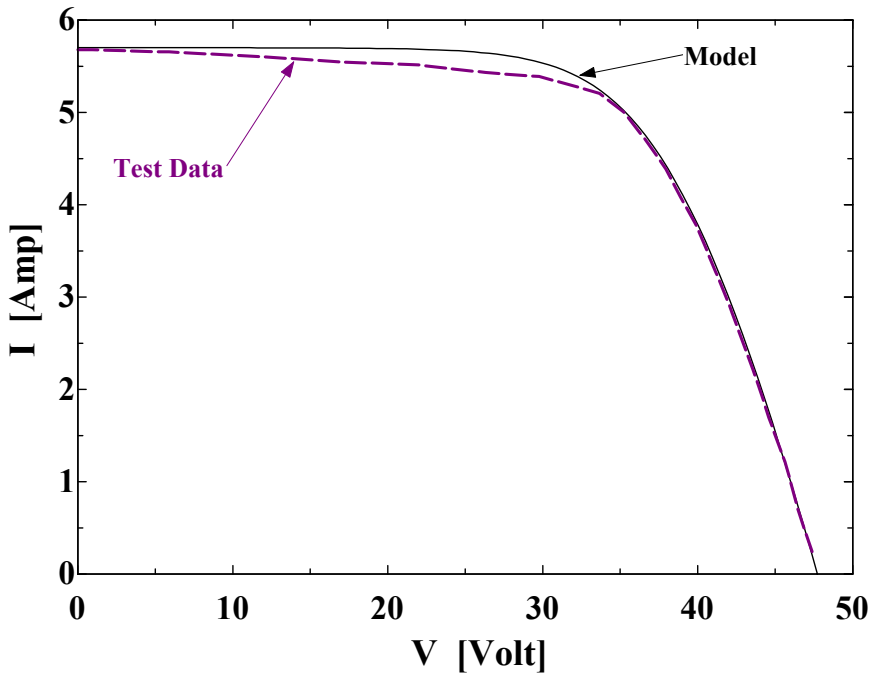

Figure 2.6: Results of TPV prototype testing (Fraas, 2001)

Due to the series configuration of the TPV array, the array performance will be limited by the cell which receives the least amount of radiation. A non-imaging optical device is being developed to provide a uniform level of radiation incident on the surface of the array. Current

simulations performed at the University of Nevada-Reno indicate that a rectangular tube with a gray wall reflectance of 95 % can increase the uniformity of the radiation incident upon the surface of the TPV array (Dye, 2003). The study indicates the flux variation to be 18.7 % (+ 7.9 %, - 10.8 %) when using a rectangular tube approximately 25 inches in length. This is an improvement from a flux variation of 2525 % at the focal point of the concentrator. Additional losses will occur due to geometric differences between the array and the optical device. The model used in the simulations includes a uniform 95 % reflection loss from the walls of the optical device and an additional 20 % loss due to differences in the geometry of the optical device and the TPV array. The negative flux variation limits the output of the array so an additional 10.8 % reduction in incident IR radiation is included to account for the variation predicted by Dye. These additional losses are included as variables in the TRNSED interface so the losses can be easily adjusted as the design improves.

2.4 Light Distribution System

The light transmission system is composed of flexible, large core optical fibers. Visible light reflected from the secondary element is focused into these fibers and transmitted to locations in the building where it is needed. The current material being evaluated is a high luminance light fiber manufactured by 3M. The light fiber is made of polymethacrylate which is flexible and resistant to fatigue, elongation, and vibration. The attenuation losses per foot are shown in Figure 2.7. The fiber attenuation data are very low except for a spike which occurs in the long-wavelength portion of the visible spectrum. Since we are dealing with the visible portion of the spectrum only and the quantity of visible light is important, the standard CIE visibility curve must be included in the calculation. When the attenuation data is weighted by the response of the human eye, the transmission characteristics in the middle of the spectrum (555 nm) become more important, and the spike near 750 nm in the attenuation data is not much of a factor.

The transmission losses through the light fiber were calculated using an exponential decay model. Using the attenuation data in Figure 2.7, the transmission loss over the first foot of fiber can be calculated at each 5 nm bandwidth. From this loss an array of exponential decay coefficients can be calculated and used to determine the transmission losses at different fiber lengths. Equation 2.4 was used to determine the decay coefficients. Since the data from 3M are

percent reduction in attenuation per foot of fiber length, the array of exponential decay coefficients can be calculated for a length of one foot. The attenuation losses are converted to transmission losses by subtracting the attenuation losses from one. The resulting coefficients can be plugged into Equation 2.5 to determine the spectral transmission of the light fiber at various lengths. The average transmission of the light fiber is calculated using Equation 2.6. Since the light fibers are primarily transmitting visible light, the standard CIE visibility curve must be included in the integration in both the numerator and denominator to achieve accurate results.

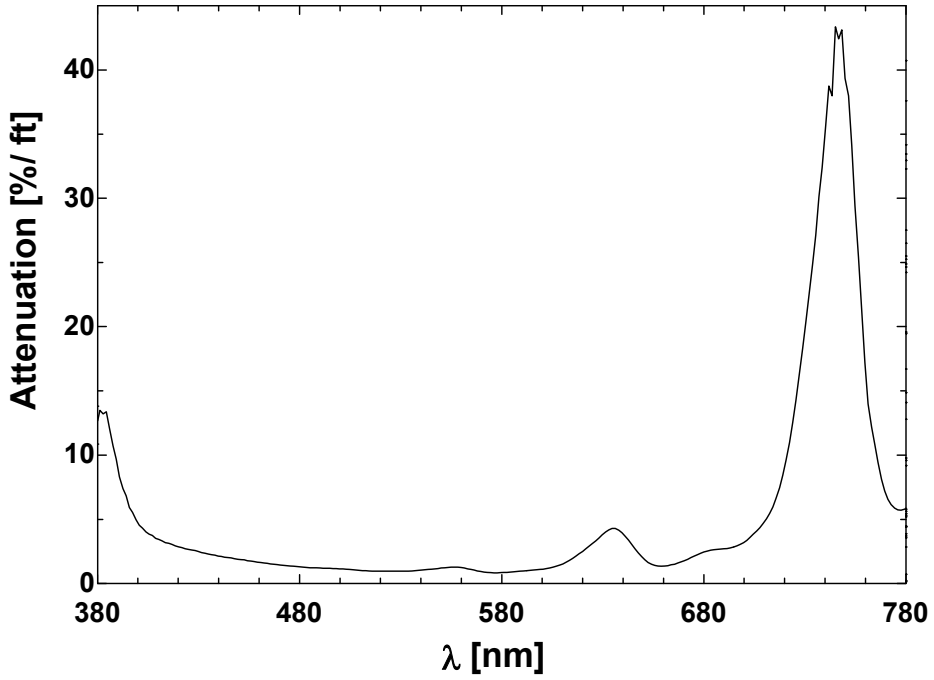

Figure 2.7: Attenuation data of 3M light fiber

The average spectral transmittance of a 7 meter length of light fiber is shown in Figure 2.8. The response of the light fiber is similar to the response of the cold mirror in that the transmittance decreases at longer and shorter wavelengths of the visible spectrum. Again due to sensitivity of the average human eye the decreased transmittance at the upper and lower end of the spectrum is not as important to the overall system efficiency as the fiber transmittance from approximately 500 – 600 nm. The visibility curve included in Figure 2.8 illustrates the eye's sensitivity relative to the transmittance of the light fiber. Using Equation 2.6 to calculate the average transmittance of a 7 meter length of fiber, the result was an average light fiber transmittance of 78 %. Another calculation was performed for a light fiber length of 14 meters.

Figure 2.8 shows the spectral results with the average transmittance of the 14 meter fiber approximately 57 %. The light fiber transmittance is the weakest link of the hybrid lighting system. Increasing the average fiber length severely reduces the light output of the system.

$$A_\lambda = 1 - e^{(-\kappa_\lambda L)} \tag{2.4}$$

$$\tau_\lambda = e^{(-\kappa_\lambda L)} \tag{2.5}$$

$$\bar{\tau}_{\text{light fiber}} = \frac{\int_{380}^{780} G_\lambda \tau_\lambda v_\lambda d\lambda}{\int_{380}^{780} G_\lambda v_\lambda d\lambda} \tag{2.6}$$

where

A_λ = Spectral Attenuation of 3M Light Fiber

K_λ = Exponential Decay Coefficients

L = Overall Light Fiber Length

τ_λ = spectral transmittance of light fiber

v_λ= 1924 standard CIE visibility curve

According to Tekelioglu (Tekelioglu and Wood, 2003) the optical fiber temperature will reach a critical point at the fiber inlet unless some type of IR filtering is used. Tekelioglu evaluated a number of different filtering and cooling methods and concluded that two techniques could be economical and effective. One technique involves the use of an additional IR filter to reflect any IR radiation before it would enter the light fiber. The filter transmittance of 90 % would add significant losses to the light production of the hybrid lighting system. The second technique used fused quartz glass 14 mm thick to filter out any undesirable IR radiation. The fused quartz glass method offered an economical and effective solution to overheating at the fiber entrance. Losses due to the coupling of the quartz and optical fiber were estimated at 3 % (Maxey, 2003) and visible transmission losses through the quartz were estimated at 2 %. The fiber entrance loss is included as an input to the TRNSED interface to allow the user to adjust the magnitude of the entrance losses as the design process continues.

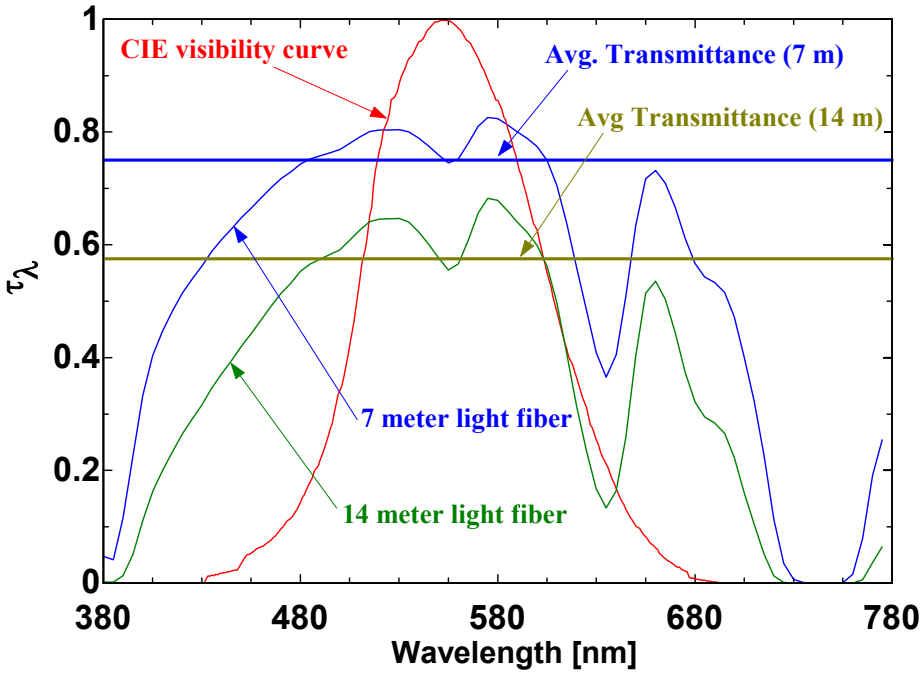

Figure 2.8: Spectral transmittance of light fibers

Another important aspect of the transmission system is the effect the light fiber has upon the color of the light output from the fiber. In a typical installation the light fibers are run through ceilings and walls to get to the appropriate location. The route will undoubtedly contain many bends. Bending the light fiber causes increased attenuation and a shift in the color of the light. Oak Ridge National Laboratory (Earl, 2003a) has developed a chromaticity model to predict the color change of the light depending on the length of light fiber, number of bends, and bend radius. The effect of additional attenuation losses due to bending has not been included in the model. This hybrid lighting model uses the data presented in Figures 2.7 and 2.8 and a uniform entrance loss to model the attenuation losses based on fiber length.

2.5 Luminaires and Control Systems

Control systems will have to be created to allow for electrical lighting when adequate solar radiation is not available. The electrical and natural light sources have to be controlled to provide adequate lighting on cloudy days when there is not enough sunlight. A control system consisting of light sensors coupled with dimmable electronic ballasts can adjust the artificial illumination levels within the building during the presence of natural light. Unfortunately the

efficacy of dimmable fluorescent lighting decreases with decreasing load fraction (NLPIP, 1999). Other control scenarios involve using constant efficacy fluorescent lighting and controlling the illumination by turning the lights off in stages. Problems with the staging control strategy include lighting uniformity and illumination level variation. A control system combining the dimmable fluorescent lighting with a staging control strategy may have the most potential with the least amount of drawbacks.

The hybrid lighting systems have a combination of electrical and natural light sources in each luminaire. Each luminaire needs to be able to produce a uniform source of light using electrical light, natural light, or both. Two designs have been developed that can be integrated into existing or new construction. An end light design 'plugs' the light fiber into a hemispherical diffuser much like typical recessed incandescent lighting. A side light design utilizes a cylindrical diffuser, similar in shape to a fluorescent light bulb, to distribute the light evenly. Illustrations of both designs are shown in Figure 2.9. Both designs are currently being developed to improve the light distribution and efficiency. No technical spectral data are available to predict the efficiency of the different luminaire designs. Preliminary experimental data from ORNL reported a 58.4 % efficiency of the side emitting rod luminaires shown on the left in Figure 2.9 (Earl, *et al*., 2003). It is estimated that nearly 20 % of the losses are due to optical fiber coupling losses which have since been addressed by Maxey (Maxey, *et al*., 2003). Recent unconfirmed reports have indicated that the current design with reduced coupling losses operates at efficiencies near 83 %.

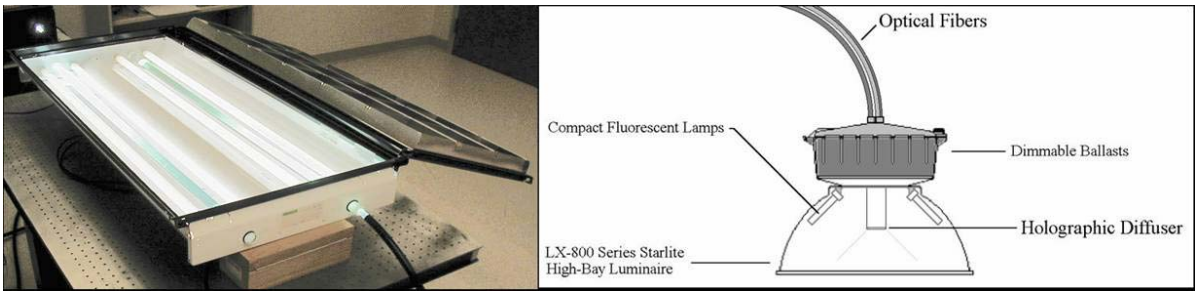

Figure 2.9: Current luminaire designs (photo courtesy of ORNL)

Chapter 3 The Solar Irradiance Model

3.1 SMARTS Version 2.9.1

The Simple Model of the Atmospheric Radiative Transfer of Sunshine (SMARTS) is an atmospheric model that calculates the spectral solar transmittance of a user defined atmosphere under cloudless sky conditions (Gueymard, 2000). The first version of SMARTS was released in 1994. The current version released during the spring of 2002 is version 9.1 which is the version that was used in the TRNSYS simulation. SMARTS is a free, FORTRAN based program which utilizes a DOS interface. Although TRNSYS and SMARTS are both written in the same programming language, SMARTS is not integrated into TRNSYS. SMARTS compares very well to the current standard atmospheric transmission model MODTRAN (Berk, 1989) as shown by (Gueymard, 2000). The inputs into the atmosphere model program include but are not limited to atmospheric pressure, turbidity, precipitable water vapor, and ozone concentration. Among other outputs, the program is capable of predicting the beam, diffuse, and horizontal radiation at the earth's surface for clear sky conditions. A sample input file and a sample output file from a run of SMARTS version 2.9.1 are included in Appendix A. For a complete list of all of the variable input parameters please see the SMARTS2 v9.1 User Reference Manual.

3.2 Typical Meteorological Year 2 Data (TMY2)

TMY2 data are hourly annual solar radiation and meteorological data readily available from the National Renewable Energy Laboratory (NREL). It is important to note that the TMY2 data represents a typical year based upon 30 year weather characteristics. It is unlikely that the data accurately represents any single year, but it is representative of the average weather characteristics over the 30 year time frame. The data files are available for 239 locations throughout the United States and are derived from either measured or modeled data.

3.2.1 TMY2 and SMARTS Data Evaluation

In order to accurately model the atmosphere, the effects of various atmospheric parameters on solar irradiance were evaluated. The SMARTS input variables that are available in the TMY2 data are atmospheric turbidity, water vapor, and atmospheric pressure. These three

parameters were evaluated at different locations representing various climates within the United States. Madison, WI, Denver, CO, and Las Vegas, NV were chosen as locations used to compare the different atmosphere parameters from the TMY2 data files.

A SMARTS reference atmosphere was chosen to compare the three variables. The reference atmosphere parameters were input as shown below:

Site pressure = 1.013 Bar (101.3 kPa)
Site altitude = 0 km (varied by location)
U.S. Standard Default Atmosphere
Precipitable Water Vapor = 2 cm (default value)
U.S. Standard Ozone Concentration
U.S. Standard Gaseous Absorption and Air Pollution Levels
U.S. Standard Volumetric Carbon Dioxide Concentration
Extraterrestrial Spectrum File = "SPCTRM_1.DAT"
Solar Constant= 1367 W/m^2
Aerosol Model = 'S&F Rural'
Turbidity Coefficient = 0.1 (default value)
Albedo = 'green grass' (grngrass.dat)
No Tilted Surface Calculations
Spectral Range = 280 – 2500 nm
Bandwidth = 5 nm
Air Mass = 1.5

The atmospheric pressure data from the TMY2 weather files are shown in Figure 3.1. From the annual TMY2 data it is evident that the atmosphere pressure does not change significantly over the year in a single location, but it does vary by location. The resulting spectral irradiance with varying atmospheric pressures was calculated using SMARTS. All other atmospheric properties were held constant while the pressure was varied from 0.800 – 1.013 bars. Although there was a slight variation in the solar irradiance predicted in the visible spectrum it was evident that the overall spectral variation due to atmospheric pressure effects is negligible.

The next atmospheric parameter which was evaluated was atmospheric turbidity. Atmospheric turbidity is a measure of the amount of aerosols or tiny particles suspended in the atmosphere. High turbidity levels, typically associated with pollution, dust, and warmer weather, will result in reduced solar irradiance due to scattering effects caused by the aerosols. As shown in Figure 3.2, the turbidity values for all three locations varied throughout the year with increasing turbidity in the summer months. The different turbidity constants were entered into the SMARTS model to determine the effect of varying turbidity on the solar spectrum.

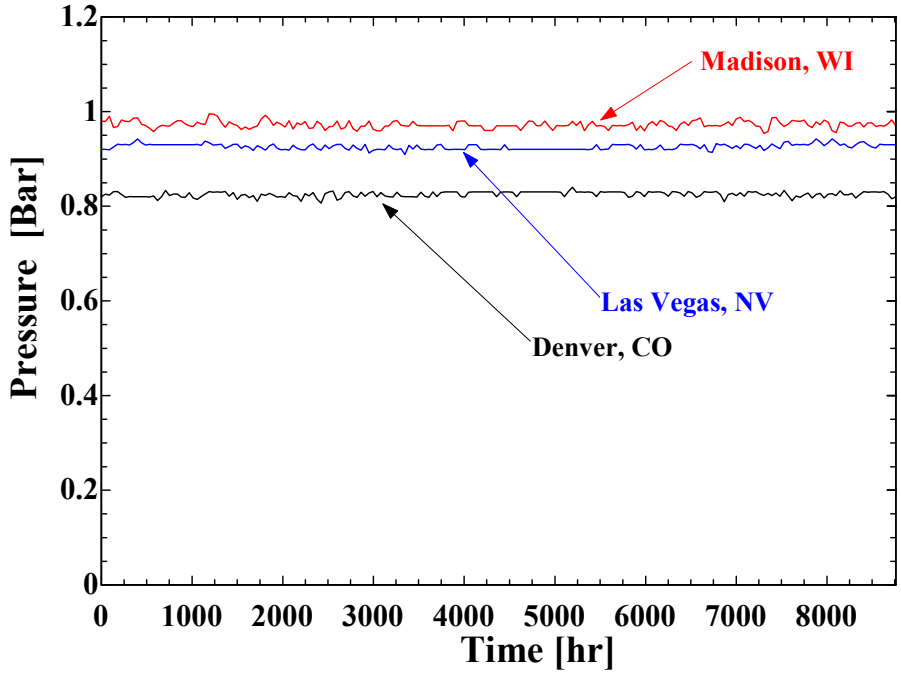

Figure 3.1: Atmospheric pressure

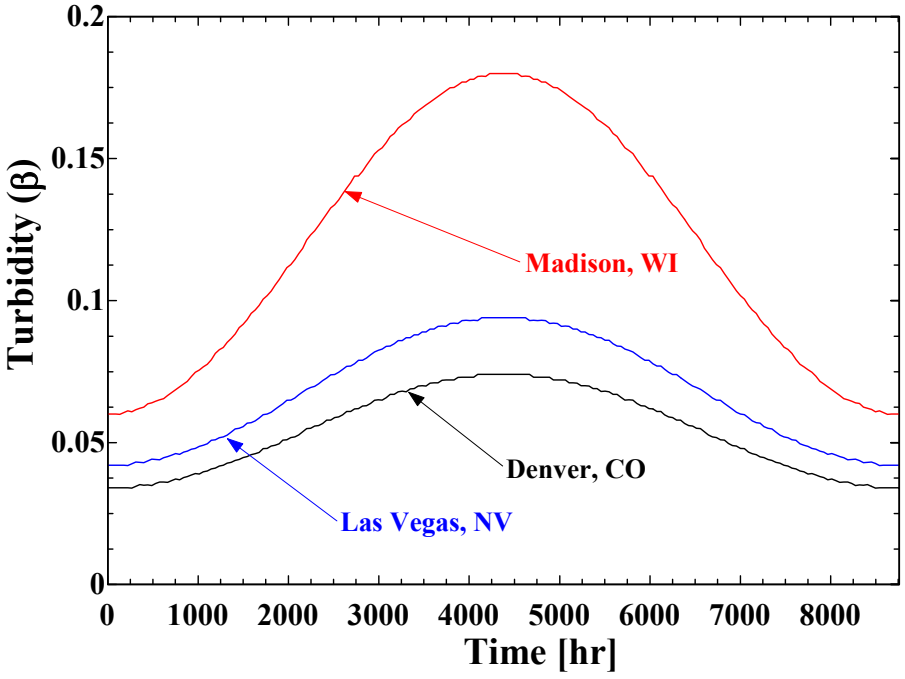

Figure 3.2: Atmospheric turbidity

Figure 3.3 shows the effect of increasing atmospheric turbidity upon the output of SMARTS. The lowest and highest levels illustrate the effect of atmosphere turbidity upon solar irradiance. In Madison, WI where turbidity ranges from approximately 0.08 - 0.18, the solar

irradiance was reduced by nearly a factor of two due to atmospheric turbidity alone. From the information in Figures 3.2 and 3.3, it was concluded that varying atmospheric turbidity has a significant impact upon the solar irradiance transmitted through the atmosphere and that the turbidity effects must be included in the simplified TRNSYS spectral model.

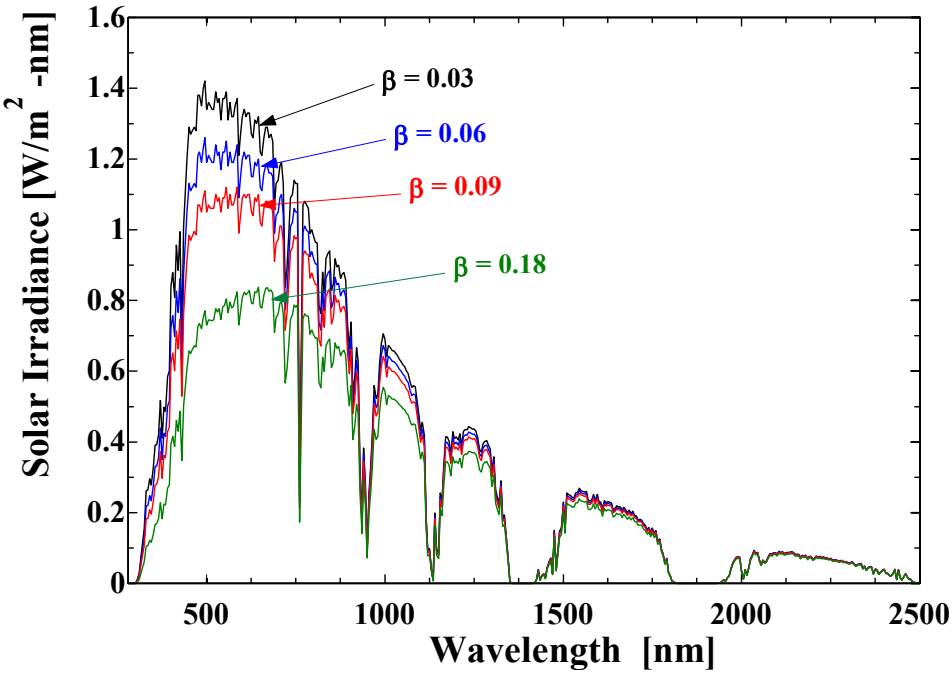

Figure 3.3: SMARTS2v9.1 output, air mass = 1.5, P = 1.013 Bar, w = 2.0 cm, variable atmospheric turbidity

The last atmospheric parameter to be evaluated was precipitable water vapor. Precipitable water vapor can be thought of as the length a column of water would be if all of the water in a column of the atmosphere of the same diameter was condensed. Figure 3.4 shows the annual variation of precipitable water vapor in the atmosphere for Madison, WI and Las Vegas, NV. Although the data contained in Figure 3.4 contain a lot of noise, a general trend with increasing precipitable water vapor in the summer is evident. Figure 3.5 shows the results of a SMARTS evaluation of the precipitable water vapor variation. It should be noted from Figure 3.5 that there is a significant change in solar irradiance over the water absorption bands contained in the infrared spectrum. The nature of the hybrid lighting technology is such that it is most dependent upon the visible energy of the solar spectrum to provide system benefits. Although the infrared energy is used to generate electricity, it was concluded that the variation in

solar irradiance due to precipitable water vapor was not significant enough to be included as a variable in the simplified model.

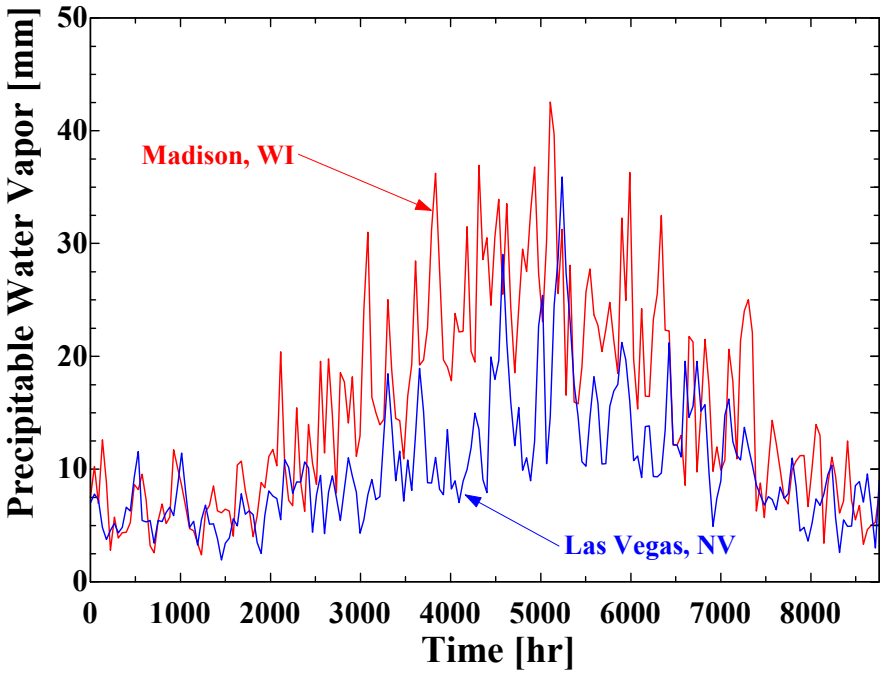

Figure 3.4: Precipitable water vapor

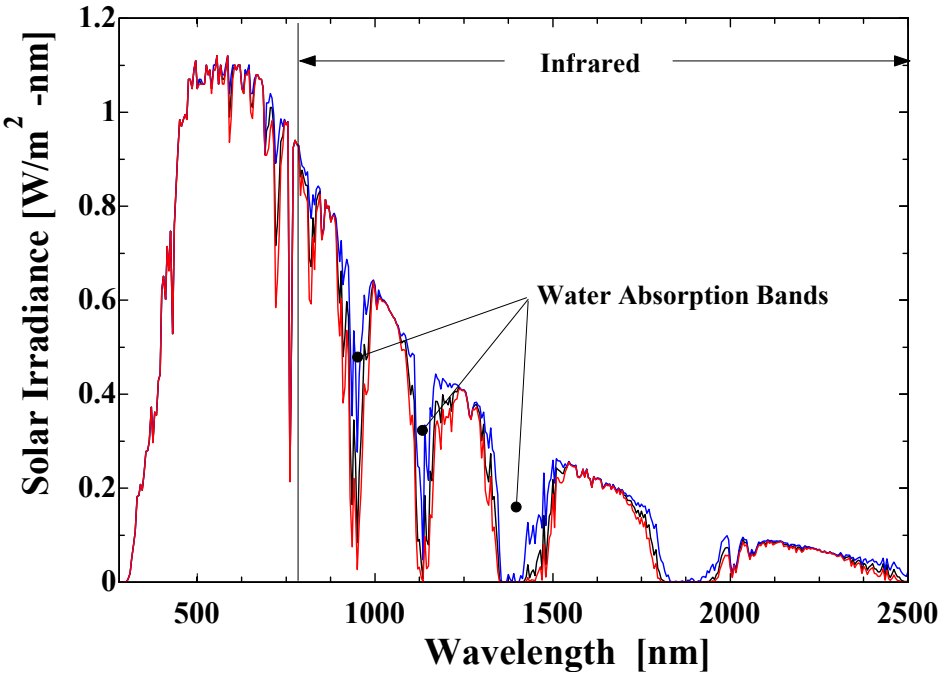

Figure 3.5: SMARTS2v9.1 output, air mass = 1.5, P = 1.013 Bar, β= 0.1, variable precipitable water vapor (w)

3.3 Simplified Atmosphere Model

In order to integrate the functionality of SMARTS into the TRNSYS simulation a simplified atmospheric model was created to maintain the simulation's practicality. If the SMARTS FORTRAN code was included directly into TRNSYS, the annual simulation time would increase substantially and major modifications would have to be performed in both TRNSYS and SMARTS. A simplified model was created to avoid these shortcomings.

From the TMY2 data, it was evident that atmospheric turbidity is the property which has the most impact upon performance of the hybrid lighting system. The model needs to account for hourly variation in the values of turbidity as well as air mass. The highest output resolution SMARTS is capable of is a bandwidth of 5 nm over the spectral range of 280 – 4000 nm. Most of the hybrid lighting component spectral data are constrained to the visible spectrum and if the infrared data were included it only existed out to 2500 nm. Based on these constraints and the fact that more than 95 % of the solar energy occurs below 2500 nm, the simplified model was designed to predict the spectral solar irradiance at 5 nm bandwidths over wavelengths ranging from 280 - 2500 nm.

The simplified model uses an exponential decay function to describe atmosphere transmittance. SMARTS output for horizontal extraterrestrial radiation and horizontal terrestrial radiation is utilized to calculate the decay coefficients. Since the model is affected by two variables, two sets of decay coefficients are calculated. One array of coefficients describes the effect air mass has on transmittance and the other coefficient describes the turbidity effect. Equation 3.1 shows the complete model and Equation 3.2 shows the definition of the turbidity ratio.

Using the SMARTS extraterrestrial spectrum and irradiance data at a single value of air mass and two values of turbidity, both sets of decay coefficients can be calculated. Different values of air mass and turbidity were evaluated to determine which values created the most accurate model. Referring to Figure 3.2, an approximate overall value of turbidity in the United States is 0.1. Based on this observation, the turbidity decay coefficients were fit to turbidity values of 0.1 and 0.2. To evaluate the best value of air mass to use to fit the air mass decay coefficient, information about average air masses in the U.S is needed. Figure 3.6 shows the fluctuation of air mass throughout the day between 20^{o} N latitude and 50^{o} N latitude. Air mass values were calculated on two days representing the longest and shortest days of the year. June

20, being close to the summer solstice, and Dec 20, approximating the winter solstice, represent a maximum and minimum value that air mass reaches throughout the year. The summer solstice produces lower values of air mass than the winter solstice. The values of latitude were chosen to represent the borders of the U.S. 20^o N latitude is approximately the southern most point in the U.S, while 50^o N latitude is approximately the northern most point of the U.S, excluding Alaska. From Figure 3.6, an approximate value of the average annual air mass can be estimated to be between two and three.

$$G_\lambda = G_{\lambda,o} e^{-(\kappa_1 + \kappa_2 R_\beta) AM} \tag{3.1}$$

$$R_\beta = \frac{\beta_{act} - \beta_{low}}{\Delta\beta} \tag{3.2}$$

where

G_λ = Global Horizontal Radiation

$G_{\lambda, o}$ = Extraterrestrial Horizontal Radiation

κ_1 = Air Mass Decay Coefficient

κ_2 = Turbidity Decay Coefficient

R_β = Turbidity Ratio

β_{act} = Actual Turbidity Value

β_{low} = Lower of Two Turbidity Fit Values

Δ_β = Difference Between Turbidity Fit Values

AM = Air Mass

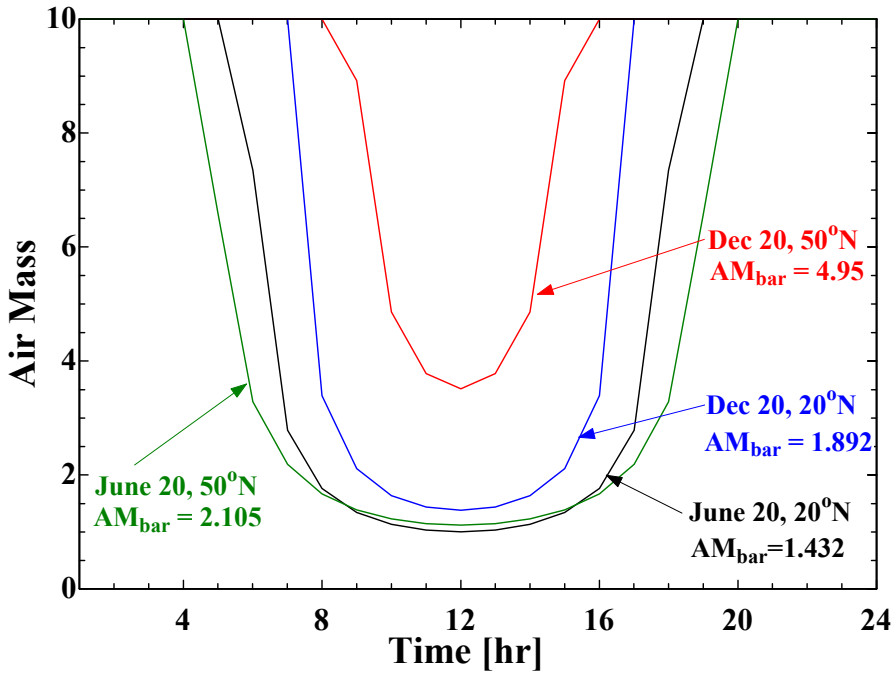

Figure 3.6: Daily air mass variation

3.4 Simplified Atmosphere Model Error Analysis

Using SMARTS irradiance data fit at air mass levels ranging between two and three and turbidity levels of 0.01 and 0.02, the decay coefficients were calculated and the model was evaluated to determine the best fit parameters. Air mass 2.25 produced the best results with minimal error at lower values of air mass and larger errors at higher air mass values. Since a hybrid lighting system is most productive in the southern portion of the United States, where air mass values tend to be lower throughout the year, the results from an air mass fit of 2.25 were acceptable.

Figure 3.7 shows the simplified spectral model error analysis. To calculate the errors, the simplified model results were calculated at air mass values ranging from 1 to 5 and a constant turbidity value of 0.1. The results were integrated over the ultraviolet (280 – 380 nm), visible (380 -780 nm), and infrared (780 – 2500 nm) portions of the spectrum and then compared to the results of the SMARTS model at the same air mass and turbidity values integrated over the same spectral limits. Figure 3.7 shows that the error over the visible spectrum ranges from 0 to 0.5 % and that the error over the infrared band is between +/- 5 %. Both error values increase with increasing air mass. These results are acceptable considering the visible radiation has the largest

effect on the performance of the hybrid lighting system. Although the IR radiation is sent to a thermal photovoltaic (TPV) array, the impact of the error will be negligible considering the low impact of the TPV compared with the overall energy benefits due to the displacement of lighting loads. The accuracy of UV band has little impact upon the performance predictions of the hybrid lighting model.

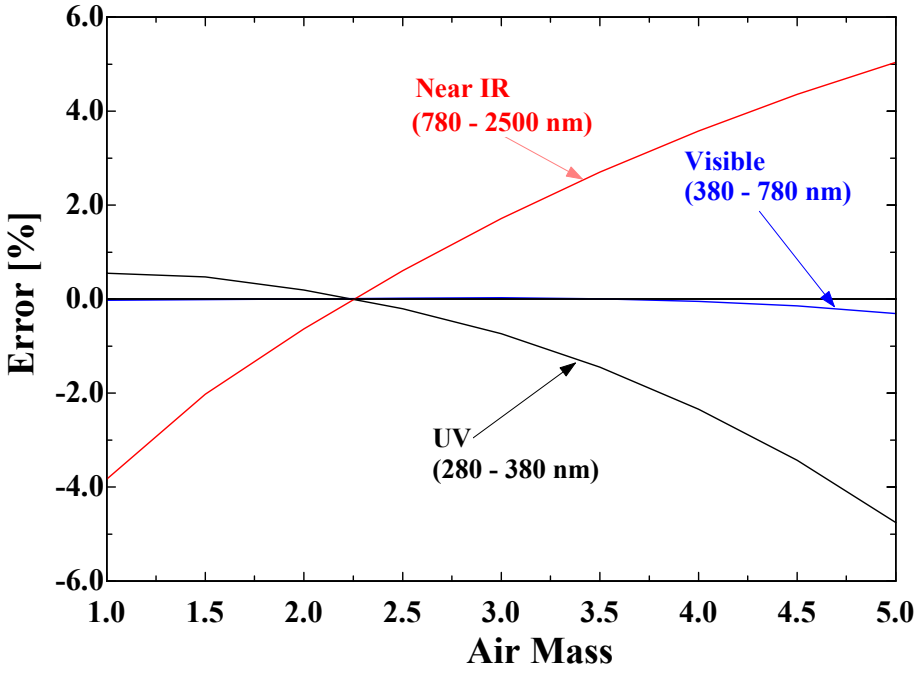

Figure 3.7: Model error, varying air mass fixed turbidity

The model's ability to predict the solar irradiance with varying atmospheric turbidity and air mass was evaluated. The value of turbidity in the model was varied from 0.05 to 0.4 and air mass ranged from 1 to 5. The integrated model results were compared with integrated results from SMARTS for each air mass and turbidity level. The errors between the SMARTS model and the simplified model are shown in Figure 3.8. The model produces the least error at turbidity values of 0.1 with the magnitude of the error increasing with increasing levels of turbidity.

The data in Figures 3.7 and 3.8 show the error observed in the model. The model was fit to the best available data regarding average air mass and turbidity values for the United States. Realizing this, the model is nearly perfect at an air mass value of 2.25 and turbidity level of 0.1.

Errors increase with changing air mass and turbidity, but the error in the visible spectrum remains very small. The error in the infrared spectrum with changing air mass stays within +/- 4 % until the value of air mass exceeds 4.25. At high values of air mass the solar irradiance is greatly reduced and the error does not have a significant impact upon the system performance.

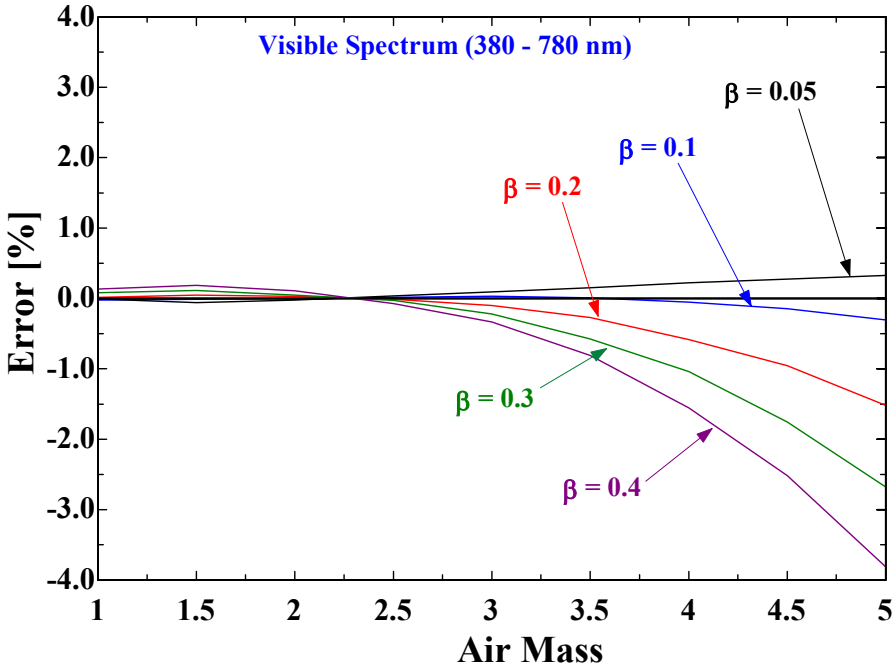

Figure 3.8: Model error, varying air mass & turbidity

The effect of varying turbidity on the simplified atmosphere model is shown in Figure 3.8. Again near air mass 2.25 the model is nearly perfect at all turbidity levels. The model's predictions decrease in accuracy the farther the air mass and turbidity vary from the fit value. The maximum error at an air mass of five and turbidity level of 0.4 is still only 4 % which is acceptable considering the high levels of air mass and low levels of solar irradiance. The error in the infrared spectrum with increasing turbidity and air mass levels slightly decreased over the larger air mass and turbidity values but was not significant enough to be included in this paper. The error in the ultraviolet spectrum with increasing turbidity and air mass levels increased to a maximum error of approximately 12 % at an air mass of five and turbidity level of 0.4, but due to the fact that the hybrid lighting technology does not use any of the ultraviolet radiation, the error values are not included in the analysis.

Chapter 4 The TRNSYS Hybrid Lighting Model

4.1 Introduction

The hybrid lighting system is modeled using TRNSYS (Klein *et al*., 2000). Inside the TRNSYS model, the lighting simulation is separated into visible and infrared components. The current model components include a weather generator, radiation processors, a hybrid lighting model, a building component, building schedules, utility rate schedules, and output components. The results from the simulation predict the annual energy and monetary savings gained from the hybrid lighting system. An economic model has been incorporated into the hybrid lighting model to calculate the break-even capital cost of a hybrid lighting system based on the annual energy savings.

4.2 Weather Data

The simulation has been set up to utilize either TMY2 weather data files or weather data based on the output of the TRNSYS weather generator. The TMY2 data are processed using a type 89 TMY2 data reader in TRNSYS. The simulation uses six of the twenty-four parameters of the TMY2 data including: the direct normal and total horizontal radiation, dry bulb and wet bulb temperatures, relative humidity, and atmospheric turbidity.

If TMY2 data are unavailable, the simulation can be run using the TRNSYS weather generator. The weather generator component, type 54, creates hourly weather data based on monthly average solar radiation, dry bulb temperatures, humidity ratios, and wind speeds.

4.3 Radiation Processor

Two TRNSYS radiation processors, type 16, are used in the model. One radiation processor simulates a two-axis tracking collector while the other radiation processor simulates the radiation that strikes the walls and roof of the building. When TMY2 files are used as the source of radiation and meteorological data, the radiation processor must be adjusted to account for the difference between the local time used in the TMY2 files and solar time. Depending on the location of the simulation, the radiation processor is adjusted to account for the difference between solar time and local time using Equation 4.1 (Duffie and Beckman, pp. 11, 1991).

$$\text{Solar Time - Standard Time} = 4\left(L_{ST} - L_{LOC}\right) + E \tag{4.1}$$

where

L_{ST} = Standard Meridian for the Local Time Zone [Degrees]

L_{LOC} = Longitude of the Location in Question [Degrees West]

E = Equation of time [min]

4.4 The Building Model

The building component is modeled using the TRNSYS type 56 multi-zone building model. Type 56 is designed to provide detailed thermal models of buildings. The model consists of two windowless 2500 m^2 zones. One zone uses standard fluorescent lighting and the other zone uses a hybrid lighting system. Schedules in the two zones simulate the heating, cooling, and ventilation of a typical mixed use environment. Additional gains in the model account for the people, computers, and lights in the building. Cooling in the building is supplied using a chiller and heating loads are met through the combustion of natural gas. Using time-of-day rate schedules, energy costs can be calculated for the two zones of the building model with the difference representing the energy savings due to the hybrid lighting system.

The type 56 model calculates the building UA values based on the building area and wall and roof composition. The walls are based on typical American construction consisting of siding, sheathing, insulation, studs, and wall board. The walls are 17.8 cm (7 inches) thick with a U value of 0.286 W/m^2-K. The roof is modeled using the same construction and the floor is assumed to be adiabatic. The UA value of a building component can be thought of as a measure of the amount of power which can be transmitted through the component in the form of heat for a given temperature difference across the component. For example, a highly insulated wall has a lower UA value that the same wall with less insulation. The total UA value for the building model is composed of the sum of the UA values for the walls, floor, and roof. The building model with four 50 meter long and 4 meter high walls and one 50 by 50 meter roof has a UA value of 943 W/K. The type 56 building model subroutine also accounts for radiative solar gains, thermal mass effects, and the capacitance of the air in the building.

4.4.1 Heating, Cooling, Infiltration, and Ventilation

In addition to the construction of the building, the model also requires inputs for heating, cooling, ventilation, infiltration, and human comfort factors. All heating and cooling set-points were based off of recommendations from ASHRAE (ASHRAE Fundamentals, 2001). The building heating schedule is set at 20°C during occupancy hours. When the building is not occupied the heating temperature is set back to 17°C. Building cooling is set to be active when the building air temperature reaches 26°C. Both heating and cooling schedules are programmed to maintain the building relative humidity between the levels of 30 and 60 %. Ventilation requirements for the building were based off of ASHRAE Standard 62 (ASHRAE, 2001). With a maximum occupancy of 175 people the ventilation was set at 0.60 air changes per hour (ACH) based on a building air volume of 10,000 m^3. Ventilation was setback to 0.17 ACH to account for a smaller evening staff of 50 people. Building infiltration was modeled according to ASHRAE Standard 119-1998. Typical values for building infiltration or leakage for new construction are 0 – 0.4 ACH and 0 – 1.13 ACH in northern and southern climates respectively. For the purpose of this simulation, an infiltration value of 0.4 ACH was used for buildings in Madison, WI and Tucson, AZ.

4.4.2 Gains – People, Equipment, and Lighting

Additional inputs into the building model include gains due to people, computers, and lighting. The building is set up to contain 150 people during the daytime (8 am -5 pm) and 25 people at night. Each person is assumed to be performing light office work which according to International Organization for Standardization (ISO) standard 7730 contributes 150 Watts of heat per person to the building load. Each person also has a computer with color monitor that contributes an additional 230 Watts of heat to the building load. The illumination level in the building is set to 500 Lux (lumens/m^2). According to the 2000 IESNA Lighting Handbook, the efficacy of fluorescent lighting can vary from 10 to 100 lumens/watt (lm/W) (IESNA, 2000). For example, a lamp that has an efficacy of 10 lm/W would produce 10 lumens of light for every watt of electrical power it consumes. The lights used in the building model either have an efficacy of 63 lm/W which corresponds to four foot T-12 bulbs and ballasts or high efficiency T-8 bulbs and ballasts that have an efficacy of 85 lm/W. Eventually, all of the light used in the

zone degrades to heat so the heating gain associated with lighting the building zone with fluorescent lighting is 19.8 kW.

The zone using the hybrid lighting technology has reduced lighting gains due to the higher efficacy of filtered sunlight. Due to the nature of the average human eye and the visible spectrum, the efficacy of filtered solar radiation is approximately 200 lm/W. The solar radiation still degrades to heat over time, but since less energy is creating the same amount of light, less heat is produced. If it were possible to light the building using only hybrid lighting, the gain due to the lighting system would be about one-third the gain due to fluorescent lighting, or 6.25 kW. To combine the fluorescent lighting and hybrid lighting systems, controls, lights sensors, and dimmable fluorescent ballasts will need to be used.

4.4.3 Building Schedules

The building gains and HVAC systems are all run on typical multi-use building environment schedules. The heating schedule is set to be active at 20°C from 5 am to 7 pm seven days a week and is setback to 17°C during the nighttime. The cooling equipment is set to be active whenever zone temperatures rise above the cooling set point of 26°C. The lights are scheduled to be on from 8 am to 5 pm seven days a week with people working in the building at these times. The heating load of the building model in Tucson, AZ on a typical clear day in January is shown in Figure 4.1.

The effects of the timing of the different schedules can be observed in Figure 4.1. The heating load spikes in the morning at 5 am when the heating set point becomes active. At 6 am the ventilation increases bringing in more cold air which increases the heating load. At 8 am the work day begins, people arrive, lights and computers turn on, and the heating load drops. At approximately 8:15 am the sun rises and the hybrid lighting system begins to produce light which reduces the amount of heat produced by the building lighting system. At 8:15 am the effect of the hybrid lighting system size can be observed. The line with the largest heating load represents the largest hybrid lighting system, 15 collectors, while the lowest line represents the smallest system size of 5 collectors, and the middle line represents a system size of 10 collectors. Similar changes in the heating load can be observed towards the end of the day as the building model schedules turn off or setback.

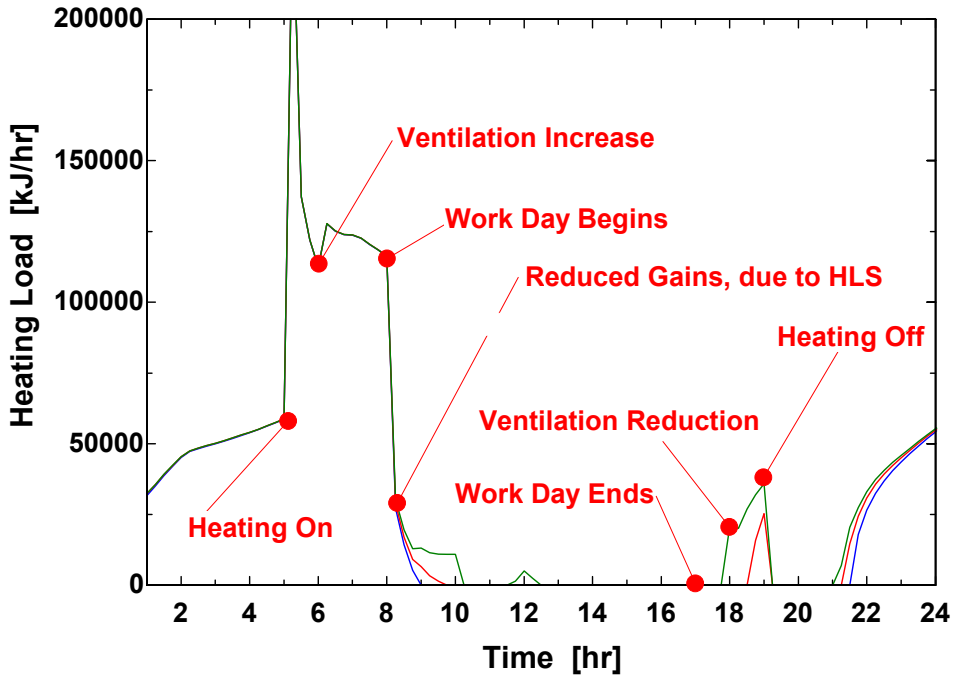

Figure 4.1: Heating load for a typical day in January, Tucson, AZ

The more light that is brought in through a hybrid lighting system results in lower internal building gains and a higher heating load during daylight hours. At 8:15 am in Figure 4.1 the effect of the different sized hybrid lighting systems is evident with the largest system requiring the most heating energy. The change in heating demand from 5 to 10 modules and 10 to 15 modules is not equal as would be expected. The heating load at hours 9 and 18 are much larger for the 15 module system than the 10 module system. On this particular day, a small spike at hour 12 occurs for only the 15 module system as well. When integrated over the year, these effects lead to an incremental heating load that is not linear.

The effect of building capacitance upon heating load can also be observed in Figure 4.1. When the heating controls set back to 17°C at hour 19, the heating load reduces to zero. When the building temperature reduces to the new heating set point the heating demand is activated. Although each building has the same capacitance, the building with the largest hybrid lighting system had the lowest average daytime temperature and cooled to the heating set point the quickest.

4.4.4 Variables

The nature of the type 56 building model interface Prebid allows the user of the simulation to alter most of the components of the building model. Potentially all of the gains, schedules, and temperature set points can be changed by the simulation user. The TRNSED interface currently does not allow the simulation user to alter the building size or construction, but the current simulation does allow the user to alter the lighting schedule, building lighting efficacy, and lighting level.

4.5 Utility Rate Schedules

The utility rate schedules use current Pacific Gas & Electric (PG&E), Madison Gas & Electric (MG&E), Southern Electric, Hawaiian Electric Company (HECO), Tucson Electric, Seattle City & Light, and Sierra Pacific Power rates. Other rate schedules can be defined in the TRNSED user interface as needed. All electricity rate schedules use small to medium sized time-of-use commercial rates. Natural gas costs were based on the 2001 average commercial price of natural gas for each state (DOE, 2003). All simulations were run using rates from each local utility.

The rates are input into a variety of forcing functions which divide the year into winter, summer, weekdays, weekends, and holidays. Using the forcing functions, a complete electricity rate schedule can be input into the program. Figure 4.2 shows the forcing function representing weekday PG&E electricity rates. As depicted in Figure 4.2 daily rate schedules are divided into on-peak, off peak, and shoulder rates during the summer, and on-peak and off-peak rates during the winter. Rates from each utility follow the same pattern as the PG&E rates shown in Figure 4.2. Energy rates and times do vary by location as shown in Table 4.1.

In addition to the energy charges each pricing schedule includes a daily distribution charge as well as a monthly demand charge. Daily distribution and monthly peak demand charges are divided up evenly between the lighting and cooling loads throughout the day. The monthly demand charge is based on an estimated 100 kW peak demand which is held constant for each location simulated. The monthly demand charge cost is evenly distributed across hourly energy charges. Table 4.1 shows the various distribution, demand, and energy charges for each utility schedule included in the model. The last column of Table 4.1 contains the annual average cost of electricity from each utility. According to the rates schedules in Table 4.1, electricity

from HECO in Honolulu, HI is the most expensive at $ 0.184/kWh while electricity from Southern Electric in Atlanta, GA is the least expensive at $ 0.062/kWh.

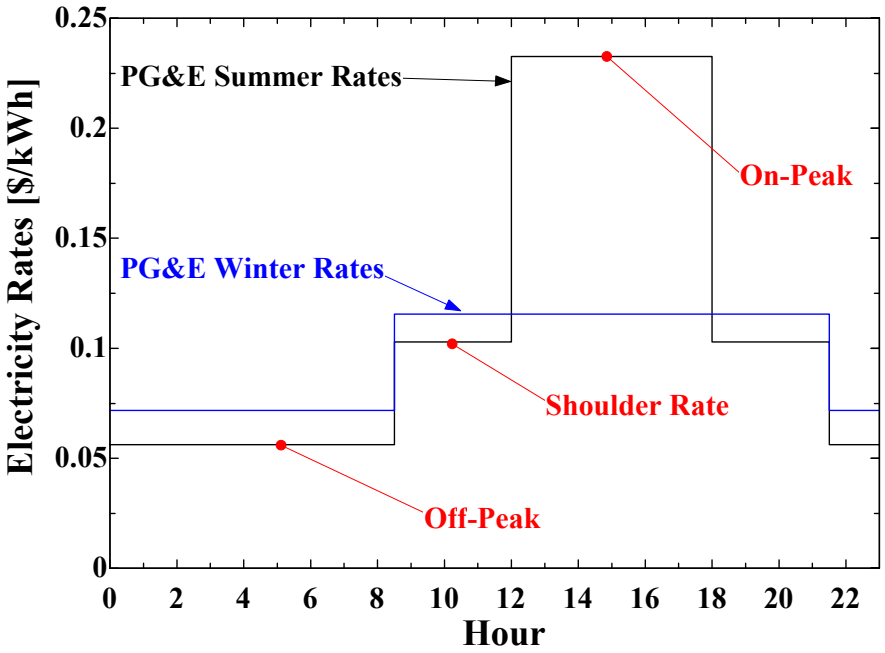

Figure 4.2: PG&E's current weekday time-of-use electricity rates

Utility	Season	On-Peak Energy Rate ($/kWh)	Off Peak Energy Rate ($/kWh)	Shoulder Rate ($/kWh)	On-Peak Time (Shoulder Time)	Daily Distribution Charge [$/day]	Monthly Demand Charge [$/kW]	Natural Gas Prices ($/kW)	Average Electricity Rate ($/kWh)
MG&E	summer	0.0636	0.03066	-	10am-9pm	1.0355	8.65	0.0247	0.0822
	winter	0.0567	0.03066	-	10am-9pm	1.0355	8.65	0.0247	
PG&E	summer	0.23258	0.05618	0.10288	Noon-6pm (8:30am-noon, 6pm-9:30 pm)	0.48953	-	0.02925	0.0937
	winter	0.11562	0.07169	-	8:30am - 9:30 pm	0.48953	-	0.02925	-
Southern Electric	summer	0.102	0.01802	0.04808	2pm-7pm (noon-2pm, 7pm-9pm)	5.592	6.5	0.02843	0.062
	winter	0.01802	0.01802	-	-	5.592	6.5	0.02843	-
Sierra Pacific	summer	0.09177	0.0515	-	10am-8pm	6.5	5.33	0.0259	0.0966
	winter	0.0715	0.0515	-	7am-10pm	6.5	5.33	0.0259	-
Tucson Electric	summer	0.222943	0.067853	0.140551	1pm-6pm (6pm-8pm)	6.78	-	0.02648	0.0898
	winter	0.15024	0.053312	-	7am-11am	6.78	-	0.02648	-
Seatlle City & Light	summer	0.0586	0.0586	-	-	0	1.03	0.02798	0.0635
	winter	0.0586	0.0586	-	-	0	1.03	0.02798	-
Hawaiian Electric	summer	0.16545	0.14545	-	7am-9pm	2	5.75	0.05723	0.184
	winter	0.16545	0.14545	-	7am-9pm	2	5.75	0.05723	-

Table 4.1: Utility rates

4.6 The Hybrid Lighting Model

The hybrid lighting simulation was developed to be able to utilize either 'real' spectral data or average spectral data when the real data is unavailable. The TRNSYS model consists of one new subroutine, type 292. Type 292 contains all of the programming for both the narrow-band and wide-band models.

4.6.1 The Wide-Band Model

The wide-band model simulates a hybrid lighting system using average spectral properties of the components of the system. The four components include the concentrator, secondary element, thermal photovoltaic cell, and the distribution components. The model predicts the potential savings of a hybrid lighting system in terms of both energy and dollars.

4.6.1.1 The Concentrator and Secondary Element

The wide-band model reads the direct normal radiation from the TRNSYS radiation processor and applies losses to account for inefficiencies in both the collector dish and the secondary element. Since there are three materials being evaluated for the concentrator dish, the model includes the ability to choose the desired material and then automatically uses the correct average spectral reflectance. The model also allows the user to enter the concentrator reflectance manually. The average spectral reflectance of the various materials is listed below:

Reflectech - 95 %
ECP-305 – 97 %
FLABEG – 92 %

TRNSYS passes the reflected beam solar radiation to the secondary element within the type 292 subroutine. The secondary element acts as a device which splits the solar radiation into the visible and infrared components. The visible solar radiation is reflected by the secondary element while the near infrared solar radiation is transmitted through the cold mirror. The average spectral reflectance of the cold mirror material is 93 % over the visible spectrum, and the average spectral transmittance of the cold mirror over the near infrared spectrum is 97 %. After applying these efficiency factors to the beam radiation reflected from the concentrator, the resulting visible radiation is sent to the light distribution system while the infrared energy is sent to the thermal photovoltaic cell.

According to data from SMARTS, the visible spectrum contains 47 % of the total spectral power and the near infrared spectrum contains 51 % of the total spectral power. These numbers are based upon calculations performed at an air mass value of 1.5 and reference atmosphere conditions as described in Chapter 3. The near infrared and visible spectral fractions vary with changing air mass values. The values stated above are used as an approximate value and the user of the simulation does have the ability to alter the values of the spectral fraction as needed.

4.6.1.2 The Light Distribution System

The distribution system model simulates the losses from the light fibers as light enters the light fibers and is transmitted throughout the building. Based on the geometry of the secondary element, alignment issues, and extra filtering needs at the beginning of the light fiber, a portion of the light which leaves the secondary element is lost. These losses are included in a light fiber entrance reflectance factor of 95 %.

The distribution losses as light travels throughout the building are calculated using attenuation data and the losses are based on the length of each individual light fiber. For the 3M LF120 end light fiber, which is to be used in the hybrid lighting systems, the average transmittance of visible radiation over a 7 meter length is 78 %.

The final factor which is applied to the light output is the luminaire efficiency. Although there currently is no spectral data available for the luminaire, scientists at Oak Ridge National Laboratory have estimated the overall luminaire efficiency to be approximately 83 %. The resulting output from the distribution model is the visible light from a hybrid lighting system. Using this output, the benefit of the hybrid lighting system can be calculated in terms of energy or monetary units.

4.6.1.3 The Thermal Photovoltaic Cell

The solar radiation in the near infrared spectrum is transmitted through the secondary element and focused onto a thermal photovoltaic (TPV) array. The wide-band model uses a default average efficiency of 16 % based upon the near infrared energy incident upon the array. The default value of 16 % was calculated using irradiance values from the SMARTS reference atmosphere as described in Chapter 3 at an air mass value of one and the quantum efficiency of

the GaSb thermal photovoltaic cells. The efficiency value agrees well with the efficiencies measured by JX Crystals (Fraas, 2002).

4.6.1.4 The Output Module

Output subroutines were created within type 292 to integrate the building model and the hybrid lighting components. Using parameters from the building model including the lamp efficacy, building illumination level, and lighting schedule, the output module calculates the baseline, or standard, lighting load. Using the same parameters but also including the daylight from the hybrid lighting system the module calculates the reduced lighting load.

The baseline and hybrid lighting loads are fed back into the type 56 building model. The building model adjusts the internal gains due to the lighting in both zones and calculates the appropriate change in sensible internal loads. The internal gain of the baseline zone is derived from the efficacy of the lighting fixture used in the zone.

4.6.2 The Narrow-Band Model

The narrow-band model simulates a hybrid lighting system using spectral properties recorded at 5 nm bandwidths. The model utilizes spectral data for the three concentrator materials, the secondary element, the TPV, the optical fibers, and the human eye. No spectral data is currently available for the luminaires. Type 292 reads the component spectral data from preprocessed data files. The solar irradiance model embedded within the type 292 subroutine predicts the spectral distribution of direct normal solar radiation at 5 nm bandwidths. The component spectral data are applied to the solar spectral distribution at 5 nm increments.

4.6.2.1 The Concentrator and Secondary Element

The narrow-band model reads the spectral properties of the three concentrator materials being evaluated and the secondary element and assigns the data to four 445 component arrays representing the wavelength range from 280 – 2500 nm at 5 nm intervals. The concentrator reflectance is directly applied to the solar spectral distribution. The reflectance or transmittance of the cold mirror is applied to the solar radiation reflected from the concentrator, and the remaining energy is transmitted to either the light distribution system or the TPV array.

4.6.2.2 The Light Distribution System

When the narrow-band model is specified, the type 292 module also reads in optical fiber attenuation data and standard human eye visibility data at 5 nm intervals. From the attenuation data, the subroutine calculates an array of optical decay coefficients and the spectral transmittance of the optical fiber based on the average fiber length as discussed in Chapter 2. The optical fiber transmittance is applied to the solar radiation incident upon the entrance of the fiber. An entrance reflectance factor of 95 % is included to account for losses as the light enters the fiber. The reflectance factor can be changed through the user interface.

At this point the light exits the light fiber and is distributed to the room through the luminaires. Since not all of the light leaving the luminaire can be seen be the human eye, the average human eye sensitivity data is applied to light leaving the luminaire. At 555 nm the eye can process light perfectly meaning that the eye can convert 1 watt of energy into 683 lumens of illuminance. The efficiency of the human eye decreases significantly before and after 555 nm which is accounted for by the sensitivity curve.

4.6.2.3 The TPV Model

The TPV array in the narrow-band hybrid lighting simulation is modeled in two parts. The first section of the model calculates the free electrons created in a single cell of the array as a function of the quantum efficiency of the Gallium Antimonide (GaSb) semi-conductor material and the energy of the photons incident upon the TPV. The second part of the model uses an I-V curve fit to experimental data from JX Crystals. The I-V model is used to calculate the electrical power output from the array.

The number of photons incident upon the TPV array is calculated using Equation 4.2. The amount of incident photons is a function of the solar radiation at the specified wavelength, Planck's constant (h), the speed of light in a vacuum (c), the wavelength, and the useful concentrator area. The current calculated in Equation 4.2 is a function of the GaSb quantum efficiency, the incident photons, and charge of an electron. The quantum efficiency describes the free electrons created from each photon incident upon the array; therefore the free electrons of the TPV can be calculated by applying the quantum efficiency to the number of incident photons. The charge of the free electrons is calculated by multiplying the number of free electrons by the

electron charge. This entire product is integrated from 280 to 2500 nm and the resulting value is the current, in amps, produced by the TPV array.

$$\text{Photons}_{\lambda}\left[\frac{1}{\text{s-nm}}\right] = \frac{G_{\lambda}\lambda\ C_{AREA}}{hc} \tag{4.2}$$

where

G_{λ} = Solar Irradiance Transmitted through Cold Mirror at 5 nm bandwidths [W/m^2-nm]

λ = wavelength [m]

C_{AREA}= Concentrator Area [m^2]

h = Planck's constant [6.626196e-34 J-s]

c = speed of light [2.9979250e8 m/s]

$$\text{Current}\left[\frac{\text{amps}}{\text{m}^2}\right] = \int_{280}^{2500} Photons_{\lambda}\ \eta_{QE,\lambda}\ e\ d\lambda \tag{4.3}$$

where

$\eta_{QE,\lambda}$ = Quantum Efficiency

e = electron charge [1.620917e-19 Coulombs]

To simplify the FORTRAN programming, some algebra was performed upon Equations 4.2 and 4.3 reducing all of the constants down to one. The resulting equation for calculating the TPV array current, Equation 4.4, is a function of the useful concentrator area, the quantum efficiency, and the wavelength. All of the constants included in Equations 4.2 and 4.3 reduced to the constant 1240 [W-s/Coulomb] which assumes that all wavelengths are in nanometers. Since the array is composed of 100 cells in series a factor of 1/100 was necessary to calculate the current produced by the array. The FORTRAN code uses trapezoidal integration over 5 nm bandwidths.

$$\text{Current} = \left(C_{Area}\middle/1240\right)(0.01)\int_{280}^{2500} G_{\lambda}\ \eta_{QE,\lambda}\ \lambda\ d\lambda \tag{4.4}$$

4.6.2.4 I-V Model

An I-V model of the GaSb array was created using a diode and series resistance model as outlined by (Duffie and Beckman, 1991). The characteristics of the array were taken from measurements made by JX Crystals (Fraas, 2001). The value of the band gap of the GaSb material was adjusted to make the model fit the measured data from JX Crystals. Information regarding the reference irradiance used in the flash test and cell temperature to produce the reference I-V curve in Figure 4.3 was not available.

Figure 4.3 shows the I-V curve of the model compared to the test data as well as the effect of cell temperature on the I-V model. Figure 4.3 shows that the model agrees fairly well with the test data. The majority of error in the model occurred when the voltage was lower than the voltage at the maximum power point (MPP). The model assumes that the load is configured to run at MPP so that the errors at voltages less than the MPP are not a factor in the TPV model's performance. Figure 4.3 also depicts how cell temperature affects the output of the array. From the figure it is clear that higher cell temperatures lead to lower output from the array. Constants used in the I-V Model include measured values from the actual prototype array at JX Crystals as well as data from the literature. JX Crystals measured the following parameters (Fraas, 2001):

Open Circuit Voltage, V_{OC} = 47.72 [V]
Short Circuit Current, I_{SC} = 5.7 [V]
Current at Maximum Power Point, I_{MAX} = 5.13 [A]
Voltage at Maximum Power Point, V_{MAX} = 34.52 [V]

Measured values for the temperature coefficients of the short circuit current, μ_{SC}, and open circuit voltage, μ_{OC}, were taken from a study performed by Lin and Burger (1995). In the study, the output of a gallium antimonide photovoltaic cell was measured under variable cell operating temperatures and fixed illumination. Both of the temperature coefficients were directly measured from the results. The coefficients did vary slightly with temperature but Lin and Burger (1995) recommended that the following values should be used:

Temperature Coefficient of the Short Circuit Current, μ_{SC}, = 0.00031 [A/°C]
Temperature Coefficient of the Open Circuit Voltage, μ_{OC}, = -0.001205 [V/°C]

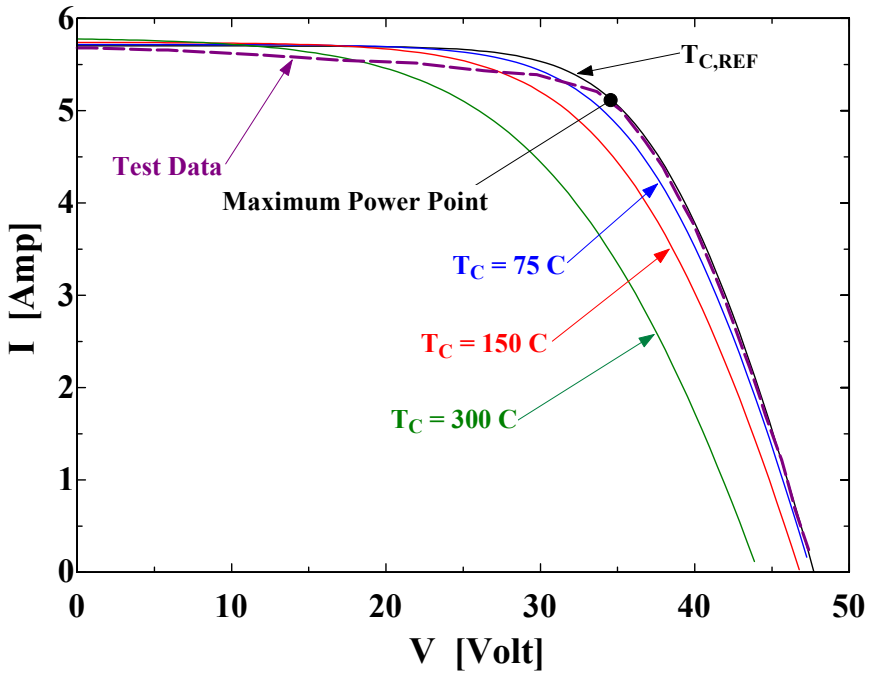

Figure 4.3: GaSb, I-V model

In the literature describing the array testing performed by JX Crystals (Fraas, 2001), the reference cell temperature, cell band gap, and reference cell irradiance were not provided. Lin and Burger (1995) reported a GaSb band gap of 0.69 eV. To make our I-V model fit the measured data from JX Crystals the band gap of the model was adjusted to 0.382 eV. The reference cell temperature was chosen to be 25°C and the reference cell irradiance was estimated to be 850 W/m^2. The reference cell irradiance approximates the direct normal solar irradiance at an air mass value of one. All three parameters result in a model that performs in agreement with the GaSb prototype test data from JX Crystals.

The I-V model is based on an equivalent circuit containing a diode and series resistance as outlined by Duffie and Beckman (1991). Equation 4.5 describes the equivalent circuit including variables for the light current, I_L, the diode reverse saturation current, I_O, the voltage, V, the current, I, the series resistance, R_S, and a curve fitting parameter, a. Under short circuit conditions when V=0, Equation 4.5 reduces to Equation 4.6. The short circuit current is equal to the light current. Under open circuit conditions when I=0, Equation 4.5 reduces to Equation 4.7. Substituting Equations 4.6 and 4.7 into 4.5 at measured maximum power conditions gives a relationship between R_S and a as shown in Equation 4.8.

The first step in programming the model was to determine the reference conditions of the light current, $I_{L,REF}$, the curve fitting parameter, a_{REF}, and the diode reverse saturation current, $I_{O,REF}$. The equations for these reference conditions are listed below in Equations 4.9 - 4.11.

$$I = I_L - I_O \left[\exp^{\left(\frac{V + IR_S}{a} \right)} - 1 \right] \tag{4.5}$$

$$I_{SC} = I_L \tag{4.6}$$

$$I_O = I_L \exp\left(\frac{-V_{OC}}{a} \right) \tag{4.7}$$

$$R_S = \frac{a \ln\left(1 - \frac{I_{MAX}}{I_L} \right) - V_{MAX} + V_{OC}}{I_{MAX}} \tag{4.8}$$

$$I_{L,REF} = I_{SC} \tag{4.9}$$

$$a_{REF} = \frac{\mu_{V,OC} T_{C,REF} - V_{OC} + \varepsilon N_S}{\frac{\mu_{I,SC} T_{C,REF}}{I_{L,REF}} - 3} \tag{4.10}$$

$$I_{O,REF} = I_{L,REF} \exp\left(\frac{-V_{OC}}{a_{REF}} \right) \tag{4.11}$$

where

$T_{C,REF}$ = Reference Cell Temperature [^{O}C]

ε = band gap of GaSb [eV]

Using the results from Equations 4.9 – 4.11 to calculate the reference conditions, the model can now calculate the array parameters at operating conditions. The model presented by Duffie and Beckman (1991) assumes that the series resistance is independent of temperature as shown in Equation 4.12. The following equations, Equations 4.13 – 4.15, are used to calculate the light current, diode reverse saturation current, and the curve fitting parameter all at operating conditions.

$$R_S = R_{S,REF} \tag{4.12}$$

$$I_L = \left(\frac{G_T}{G_{T,REF}}\right)\left(I_{L,REF} + \mu_{I,SC}\left(T_C - T_{C,REF}\right)\right) \tag{4.13}$$

$$I_O = I_{O,REF}\left(\frac{T_C}{T_{C,REF}}\right)^3 \exp\left(\frac{\varepsilon N_S}{a_{REF}}\left(1 - \frac{T_{C,REF}}{T_C}\right)\right) \tag{4.14}$$

$$a = \left(\frac{T_C}{T_{C,REF}}\right) a_{REF} \tag{4.15}$$

Noting that, at short circuit conditions, all of the current flowing through the array is due to the photons incident upon the array, the light current calculated from Equation 4.4 can be set equal to the short circuit current, I_{SC}. Assuming the load and array are designed to operate at maximum power point the output voltage of the array has been set equal to $V_{MAX,}$ or the maximum power point voltage. The output power is calculated from Ohm's law shown in Equation 4.16. The JX Crystals array is intended to be mounted on an air cooled heat sink and fan that consumes five watts of power (Fraas, 2001).

$$P = V \bullet I \tag{4.16}$$

4.7 Lighting Controls

Four different control strategies were evaluated for use in the hybrid lighting model. The first strategy included constant efficacy lighting with no losses assessed for dimming the lights. The second control strategy involved operating the lights at full power, but turning them off in stages to reduce the lighting level. This strategy allowed the lights to operate at high efficacies but raised concerns about the uniformity of the light in the space. The third scenario used photo sensors and dimmable fluorescent ballasts and lamps. At approximately 20 % of the maximum light output, the dimmable lighting system cannot produce light effectively (NLPIP, 1999). The lighting limitation below 20 % load led to an over and under-illuminating design region depending upon whether the lights are left on or turned off at the 20 % load level. The fourth strategy combined staging the lights and the dimmable fluorescent systems. This last strategy would maintain the desired illumination level while allowing the dimmable light fixtures to operate at higher efficacies.

The control strategies were evaluated through simulations performed in Tucson, AZ. The simulations used the narrow-band hybrid lighting model, TMY2 weather data, and the previously described building model. All variables affecting the hybrid lighting system were assigned the default values described earlier. Figure 4.4 shows the output from the first two control scenarios. The ideal case represents a perfect dimmable lighting system with no losses associated with part load lighting. With the ideal control strategy, the lighting load reduces linearly with each additional module until the building begins to saturate with light at approximately 12 modules. After saturation, the load reduction per additional module is reduced.

The second control system in Figure 4.4 is the staging controls. By dividing the lights into equal stages, the lights can be maintained at full operational levels and turned off or on to reduce or increase the lighting load as needed. In a two stage system the lights are divided into two groups. Both groups remain on until the hybrid lighting system provides 50 % of the lighting load. At this point one stage, or in this case, half, of the lights are turned off while the remaining lights stay on. The remaining half of the lights stay on until the entire load is met by the hybrid lighting system. Staging systems with more than two stages are designed in the same manner with each stage designed to meet an equal fraction of the lighting load. Figure 4.4 shows how the staging controls would operate with increasing system size. The hybrid lighting system has no effect in a two stage control strategy until the system can provide 50 % of the lighting load. In Tucson, AZ, up until 4 modules, a hybrid lighting system is not capable of meeting half the lighting load. From four to eight modules the hybrid lighting system is meeting 50 % load increasingly often resulting in a decrease in lighting load. From 8 to 12 modules, the system begins to meet the 50 % load almost all of the time and begins to meet 100 % load more often resulting in decreased lighting loads. Between 12 and 14 modules, the building becomes saturated with light; with the hybrid lighting system providing all of the needed lighting most of the year. The difference between the staging load and the ideal case is the remaining cloudy or partly cloudy days that have a hard time meeting 50 % or 100 % of the building's lighting needs.

From Figure 4.4 it is clear that increasing the number of stages produces a better control system that does approach the ideal case. A potential problem with this control system would be the light uniformity with increasing stages. Two stages could be contained within one four bulb luminaire, each stage consisting of two bulbs. Four stages would consist of two four bulb luminaires; six stages would consist of three four bulb luminaires, and so on. Using more than

four stages may introduce unsatisfactory illumination uniformity and would have to be investigated further.

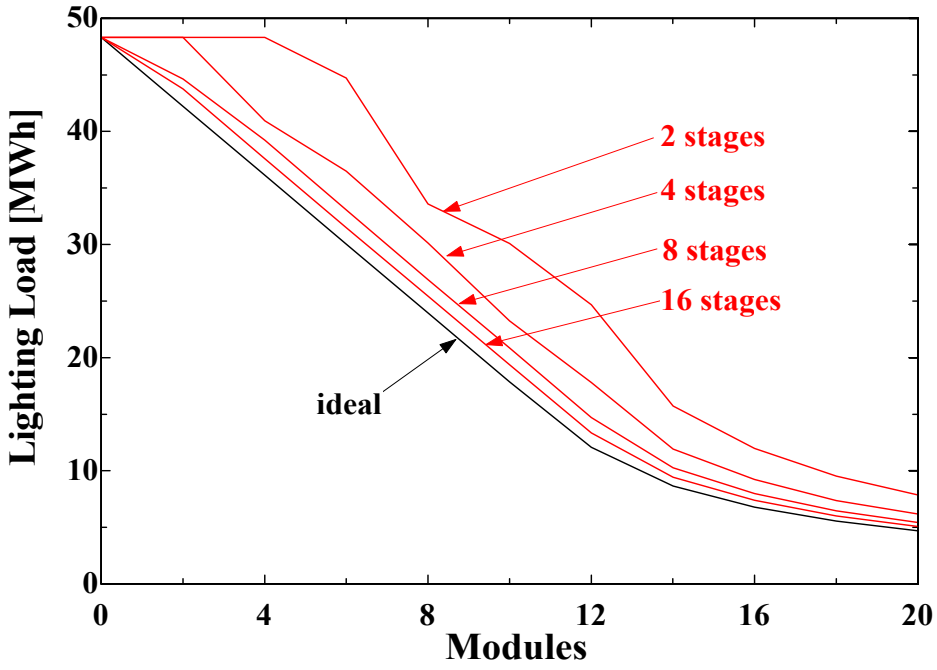

Figure 4.4: Controls, ideal and staging

Unfortunately an ideal dimmable fluorescent system does not exist. Figure 4.5 shows the results of a study of the efficacy of available dimmable fluorescent systems under part load (NLPIP, 1999). From Figure 4.5 it is clear that the dimmable fluorescent systems operate most effectively at their rated loads. At lower light outputs the efficacy of the fluorescent system decreases and approaches that of an incandescent lamp. At a 20 % light fraction or less, the fluorescent system does not effectively produce any lumens.

The ideal control system, the dimmable fluorescent system with losses, and the dimmable fluorescent system with losses and staging are shown in Figure 4.6. The lighting load of the dimmable fluorescent system increases with respect to the ideal case due to higher lamp inefficiencies with decreasing rated load fractions. At about 8 modules, the hybrid lighting system begins to meet 80 % of the lighting load some of the year. At this load level the curve splits depending upon whether the lights are left on, over-illuminating the space, or whether the lights are turned off and the space is under-illuminated. It is important to note that the space will only be under or over-illuminated when the hybrid lighting system is providing between

80 -100 % of the lighting load. After 12 modules the system begins to meet all of the building lighting needs some days of the year and the lighting load decreases. The under-illuminated curve approaches the ideal curve, but the over-illuminated curve does not because any day of the year that the hybrid lighting system is meeting between 80 -100 % of the lighting load, the fluorescent lighting system remains partially on.

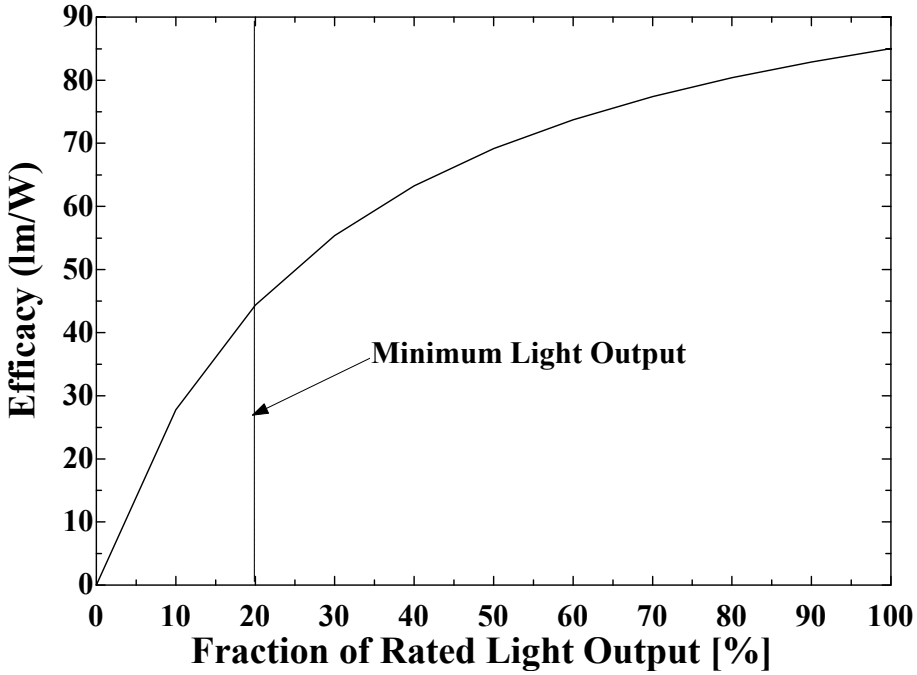

Figure 4.5: Performance of an 85 lm/W dimmable fluorescent lighting system.

The last control strategy, a dimmable fluorescent system with staging, allows the lamps to maintain higher efficacies while still meeting the desired lighting levels. The difference due to staging can be observed from Figure 4.6. From 2 to 4 modules, the lighting load of the dimmable ballast system increases with respect to the ideal load. At two modules, the hybrid lighting system begins to meet 75 % of the load, which with a 4 stage system, causes the efficacy of the fluorescents to increase because they are operating at higher light fractions. The efficacy of the fluorescent lamps in the dimmable fluorescent system without staging continues to decrease resulting in less efficient operation and higher lighting loads.

The choice of control system will be largely dependent upon the building and its occupants. The staging control scenario is not very effective until the lighting system begins to be divided into approximately 8 stages. Up until the eighth stage the losses due to the control

system are over 15 % of the total lighting load reduction using ideal controls. More research into an appropriate staging size could resolve potential light uniformity problems due to the staging controls. The dimmable fluorescent system is effective when the hybrid lighting system is designed to meet nearly all of the building's lighting needs, but this control system is inefficient when the hybrid lighting system is producing between 50 -100 % of the building lighting load. In addition, the dimmable fluorescent system cannot meet loads under 20 % of the rated design load resulting in the need to over or under-illuminate the building during certain conditions. A dimmable fluorescent system with staging combines the best of both control scenarios resulting in an efficient but most likely expensive control system.

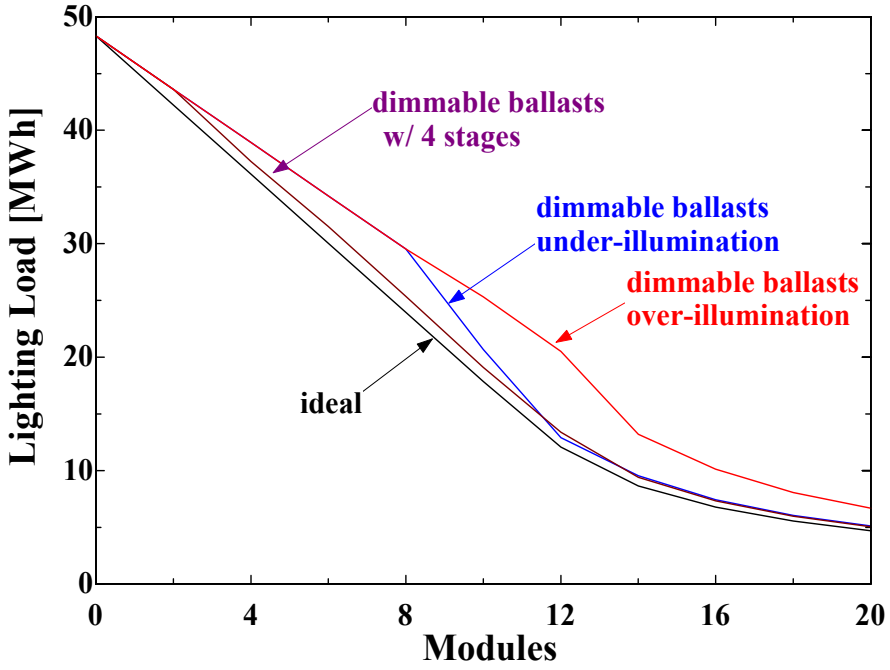

Figure 4.6: Controls, ideal and realistic dimmable fluorescent systems

4.8 P_1, P_2 Economic Model

The hybrid lighting model uses the P_1, P_2 economic method (Duffie and Beckman, 1991) to calculate the break-even capital cost of a hybrid lighting system. The break-even capital cost was chosen due to the nature of the economic indicator. At this point in the design stage, realistic component prices are not available for determining economic parameters such as years to payback, life cycle savings, or return on investment. Instead the break-even capital cost was

calculated to be used as a price target where the energy savings predicted by the TRNSYS model will economically compensate for the system components.

The P_1, P_2 economic method condenses 14 economic parameters into two which simplifies any additional economic analyses. P_1 is the ratio of the life cycle cost of fuel to the first year fuel costs, and P_2 is the ratio of equipment life cycle owning cost to initial equipment cost. The parameters P_1 and P_2 can be used in Equation 4.17 to calculate the life cycle savings (LCS) of a piece of equipment.

$$\text{LCS} = P_1\ (\textit{First Year Fuel Costs}) - P_2\ (\textit{Initial Equipment Cost}) \tag{4.17}$$

The parameter P_1 takes into account the discount rate, fuel inflation rate, number of years of analysis, income tax levels, and if the subject is income or non-income producing. To understand how the parameters affect the value of P_1 it helps to remember the definition described above while viewing Equation 4.18. Increasing the years of analysis or fuel inflation rates result in an increased life cycle cost of fuel and consequently a higher P_1 value. Increasing the discount rate decreases the value of P_1 because in effect the life cycle cost of fuel is decreasing.

$$\text{P}_1 = (1 - C\bar{t})\left(\frac{1}{(dis - \text{inf}_f)}\right)\left(1 - \left[\frac{(1+\text{inf}_f)}{(1+dis)}\right]^{\wedge n}\right) \tag{4.18}$$

P_2 is the more complex of the two parameters since it simplifies the following 13 economic parameters into one number:

Years of Analysis (*n*)
Discount Rate (*dis*)
General Inflation Rate (*inf*)
Initial Down Payment (*Down*)
Mortgage Rate (*m*)
Years of Loan (Y_L)
Years of Depreciation (Y_D)
Incoming Producing (C=1), or Non-Income Producing (C=0)
Income Tax Rate (*t bar*)
Ratio of First Year Miscellaneous Costs to Initial Cost (M_s)

Ratio of Resale Value at the End of the Analysis to Initial Cost (R_v)
Ratio of Initial Valuation to Initial Cost (Val)
Property Tax Rate (PR_{tx})

The definition of P_2, quantifies the effect of these economic parameters upon the economic analysis. Any economic parameter that increases the life cycle equipment cost increases the value of P_2. Increasing mortgage rates, inflation rates, years of depreciation, initial down payment, or miscellaneous costs result in an increased value of P_2. Increasing the discount rates or the length of loan terms will result in a decreased value of P_2.

Setting the LCS to zero Equation 4.17 can be re-arranged to give Equation 4.19, the break-even capital cost in terms of the ratio P_1 to P_2 and the annual energy savings in dollars from a hybrid lighting system. Figure 4.7 shows the general trends of the P_1, P_2 ratio with changing years of analysis, general inflation rates, and fuel inflation rates. A discount rate of 6 %, a fuel inflation rate of 2 %, a general interest rate of 3 %, result in a P_1, P_2 ratio of 6.1 based on a 10 year analysis period. Increasing the analysis period or fuel inflation rate would result in a higher P_1, P_2 ratio. Appendix B contains additional plots showing the effects of various economic parameters upon the P_1, P_2 ratio.

$$\text{Break Even Capital Cost} = \frac{P_1}{P_2} \text{ (First Year Fuel Costs)} \tag{4.19}$$

Figure 4.8 shows the annual savings of a hybrid lighting system in Honolulu, HI with and without the TPV array, with low efficacy fluorescent lighting, and with a high efficient luminaire design. Using a P_1, P_2 ratio of 6.1, a benchmark break-even capital cost is $2946 per module based on high efficacy (85 lm/W) fluorescent lighting. The difference between the benchmark and the curve representing a different technology is the change in annual savings due to that different technology. Applying the P_1, P_2 ratio to the difference provides the break-even capital costs for adding or developing the technology. For example, in Honolulu the TPV array saves $17 a year. Applying the P_1, P_2 ratio results in a break-even capital cost for the TPV array of $104. The luminaire efficiency improvement from 83 % to 95 % contributes an additional annual savings of $68 per module resulting in an additional system break-even capital cost of $415. Using the simulation in conjunction with the P_1, P_2 ratio allows the system designers to evaluate the capital cost of components before any design work has begun.

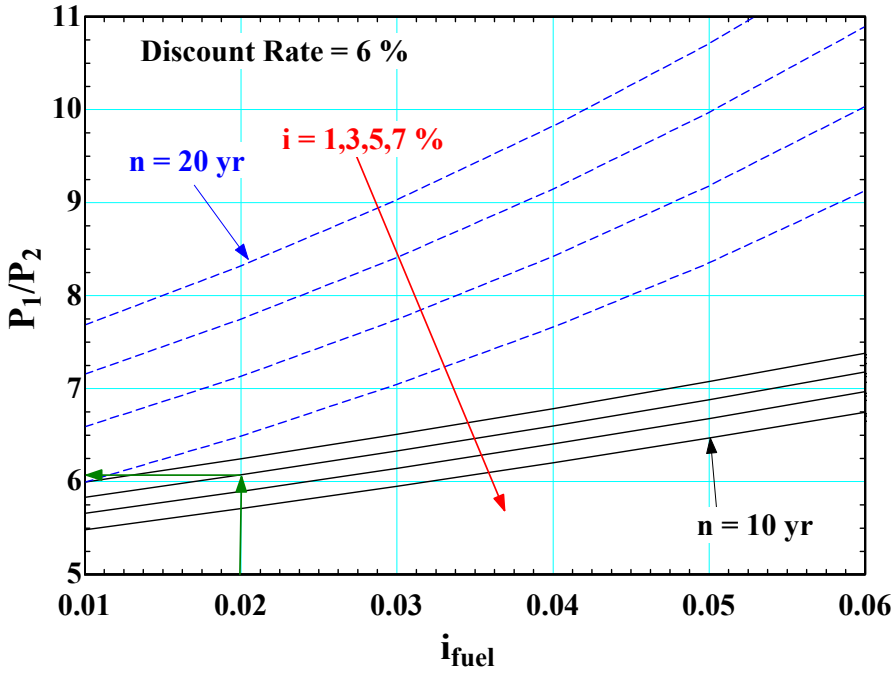

Figure 4.7: P_1 ,P_2 ratio

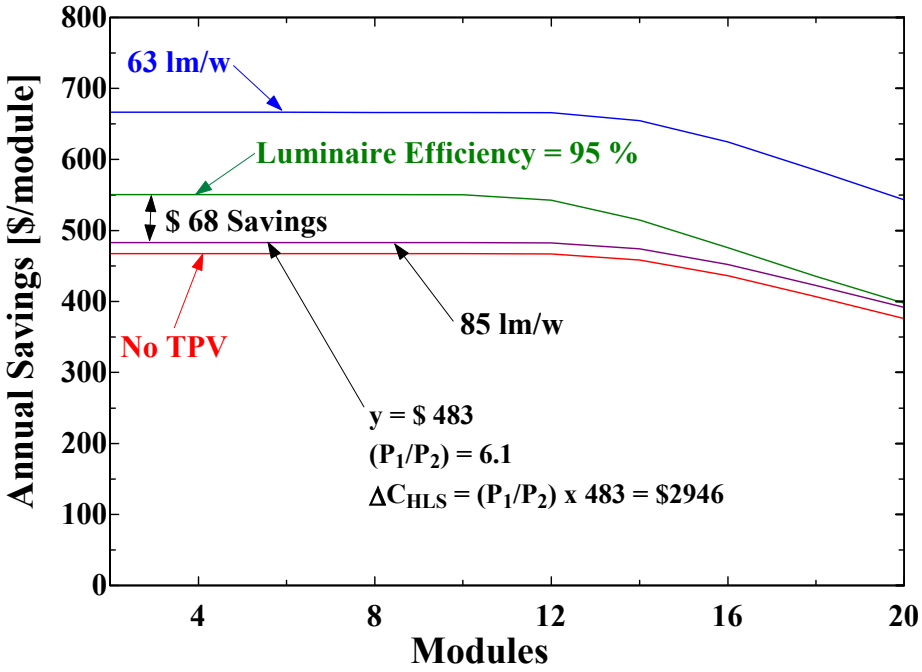

Figure 4.8: An example of break-even capital costs

4.9 The TRNSED User Interface

A user interface has been created using TRNSED and is partially shown in Figure 4.9. The TRNSED interface allows the user to modify different input and output parameters of the system to suit their particular needs without having to interface with the underlying FORTRAN code. For more detailed information about TRNSED variables, the TRNSED interface, and a full view of the interface see Appendix C.

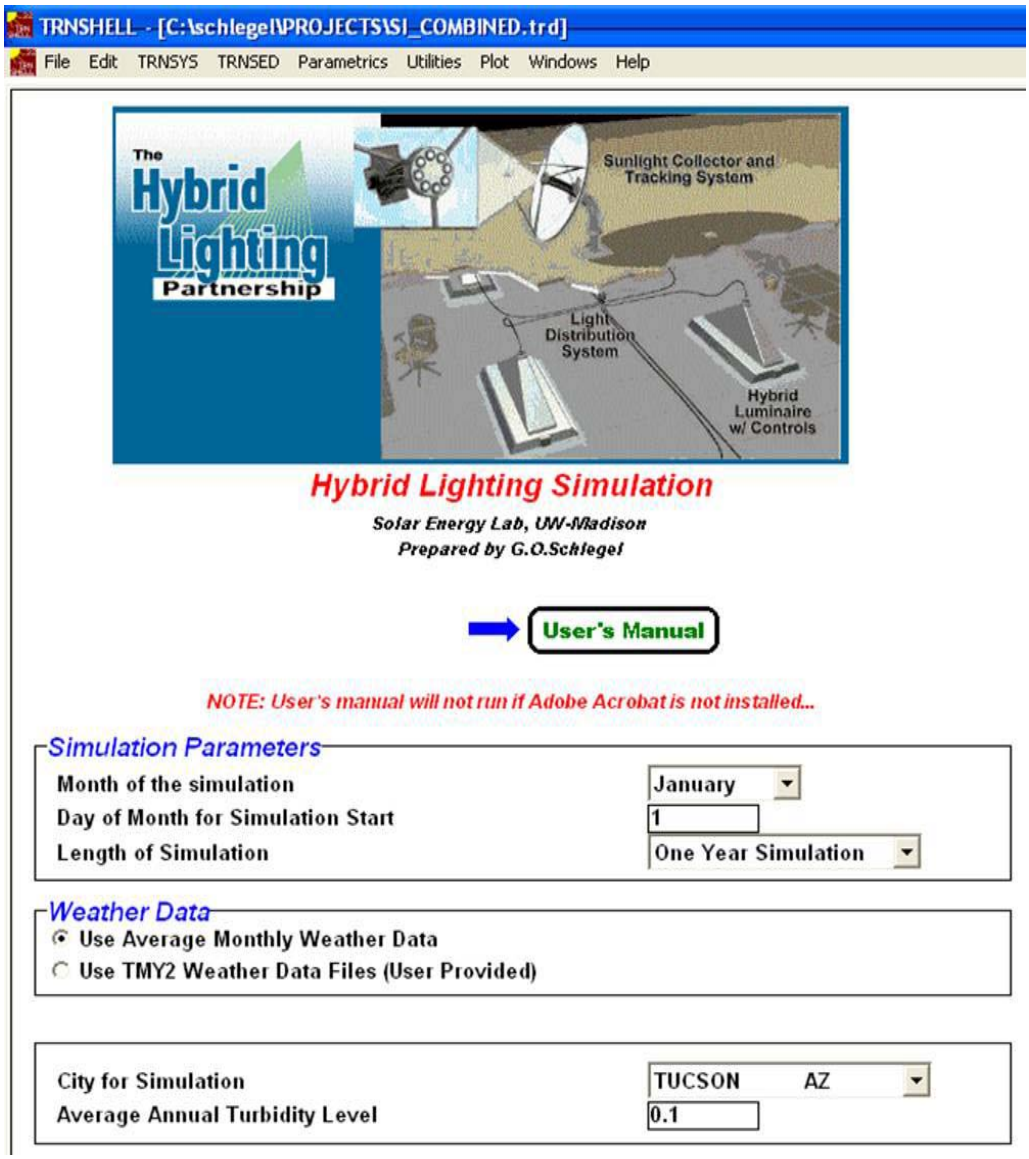

Figure 4.9: Hybrid lighting TRNSED interface

Chapter 5 Simulation Results

5.1 Introduction

Annual simulations were run to evaluate a hybrid lighting system in six different locations in the United States. The six locations were chosen to provide a representation of different climate regions in the U.S. Reno, NV and Tucson, AZ, were the locations used to represent mountain and desert climates. Seattle, WA, was chosen to show the effectiveness of the technology in the Pacific Northwest. Madison, WI was chosen to represent the Midwestern United States, and Atlanta, GA was used to represent the Eastern U.S. An additional simulation was run for Honolulu, HI due to the large amount of sunshine and high electricity prices in Hawaii. The results of the simulation include lighting, heating, and cooling load estimates for the building model with and without the hybrid lighting system. From the difference in energy loads and the generation from the TPV array, the annual energy savings due to the hybrid lighting system can be calculated. Using the annual energy savings and the P_1, P_2 economic methodology, the break-even capital cost of a hybrid lighting system can be determined for a particular location. Break-even capital cost can be used both as a design goal for the development team as well as a metric to measure where the technology will be most effective.

5.2 Model Comparisons, Wide-Band Model vs. Narrow-Band Model

Simulations were performed using the two different hybrid lighting models to determine the difference between the simulation results for the wide and narrow-band models. The building model described in Chapter 4 was used with a 5 module hybrid lighting system. Each module has an active collector area of 1.7 m^2 corresponding to a concentrator 1.5 meters in diameter with a secondary element 0.25 meters in diameter. For the narrow-band model run, the concentrator material used was the ECP-305, 5 % optical fiber entrance losses were included, and the average length of an optical fiber was 7 meters.

The wide-band model simulation used the default average values for all of the spectral component properties which included a concentrator reflectance of 97 %, secondary element reflectance of 93 %, secondary element transmittance of 73 %, optical fiber attenuation for the first foot of fiber length of 1.3 %, TPV efficiency of 16 % over the IR spectrum, an IR spectrum

fraction of 0.51, and a visible spectrum fraction of 0.47. For both the narrow and wide-band simulations, the building was kept at a lighting level of 500 lux from 8 am to 5 pm seven days a week. The auxiliary lighting in the building consisted of T-8 fluorescent lamps with an efficacy of 85 lm/W.

The electrical lighting loads predicted by both the narrow-band and wide-band hybrid lighting simulations are shown in Figure 5.1. The lighting load predicted by the wide-band model is slightly higher than the load predicted by the narrow-band model. The difference between the two models is due to errors introduced through averaging the hybrid lighting component spectral properties. By using small bandwidths, the narrow-band model minimizes these errors and is more accurate but consequentially uses more computational time. The wide-band model predicts nearly a 10 % smaller lighting load reduction due to the errors associated in averaging across the larger bandwidths. The results in the remainder of this chapter were compiled using TMY2 meteorological data and the narrow-band hybrid lighting model.

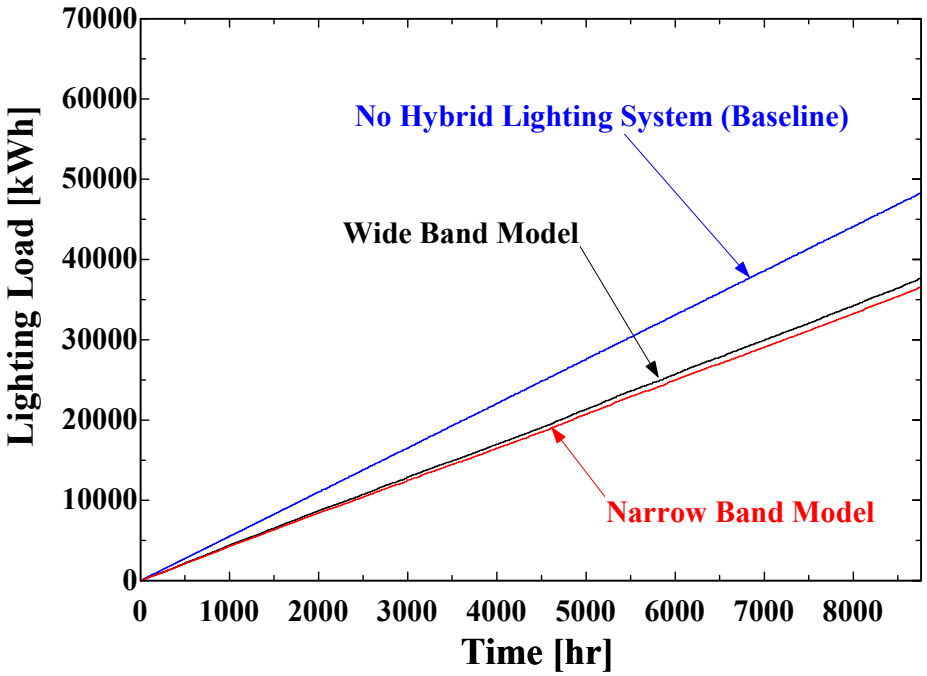

Figure 5.1: Narrow and wide-band lighting load predictions

5.3 Simulation Results

Simulations were run in six different locations using the previously described type 56 building model, the narrow-band hybrid lighting model, and TMY2 weather data. The concentrator consisted of the ECP-305 material with an active area of 1.7 m^2. The optical fibers averaged 7 meters in length and a 5 % fiber entrance loss was included to account for additional IR filtering. Illuminance levels in the building were set to 500 lux from 8 am to 5 pm 7 days a week, and the luminaire efficiency was assumed to be 83 %. Simulations were performed using both high efficacy and low efficacy lighting to show the effect of building lighting upon the hybrid lighting system performance.

5.3.1 Lighting

The lighting loads of the building with increasing hybrid lighting system size are shown in Figures 5.2 and 5.3. The shape of each curve in both figures is very similar with a linearly decreasing lighting load until the lighting system begins to saturate. At the saturation point, the hybrid lighting system produces more light than is needed on some days and thus displaces less energy per additional system. As would be expected, the system in Tucson, AZ performed the best and the system in Seattle, WA showed the worst performance. Although the system in Hawaii is closer to the equator the high amounts of moisture in the Hawaiian climate lead to smaller amounts of annual beam radiation than dry climates like Reno, NV and Tucson, AZ.

The system in Hawaii saturated at higher number of systems than the other locations because the lower latitude resulted in daylight hours more in phase with the building lighting hours. The fluorescent lighting in the building is operational from 8 am to 5 pm. In Hawaii the sun always rises by 8 am and sets after 5 pm, but in Reno for 2-3 months of the year the sun sets before 5 pm. During this time the hybrid lighting system cannot be used in Reno but it still can be used in Hawaii. The longer useful daylight hours in Hawaii lead to a larger system saturation size than a system in Reno.

The baseline lighting efficacy in Figure 5.2 was set to 85 lm/W while the fluorescent lighting used in the simulations of Figure 5.3 had a lower efficacy of 63 lm/W. As would be expected the lighting load with no hybrid lighting modules is higher when using a low efficient light bulb as shown in Figure 5.3. When the number of hybrid lighting systems is increased the energy savings is greater for the set of simulations using the low efficient lighting. Although this

makes the hybrid lighting systems seem more attractive it is more reasonable to assume that hybrid lighting systems will be accompanied by high efficiency fluorescent lighting systems.

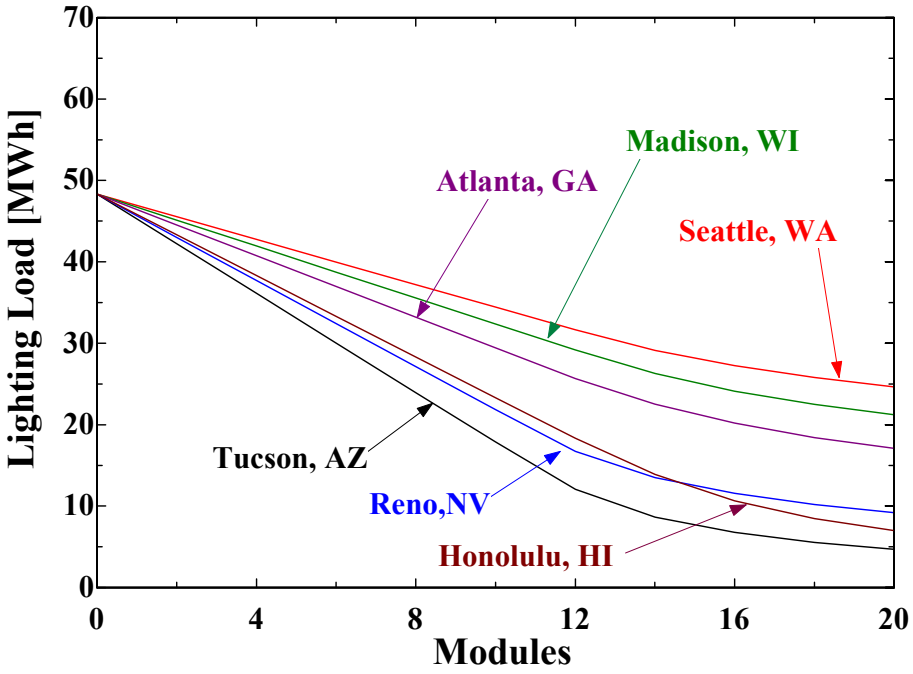

Figure 5.2: Lighting load, lamp efficacy = 85 lm/W

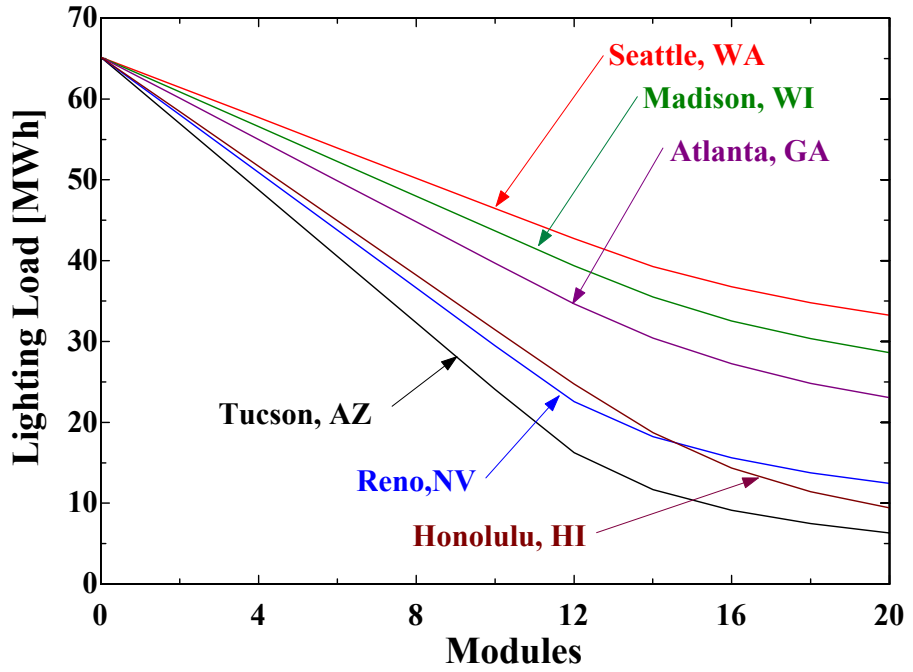

Figure 5.3: Lighting load, lamp efficacy = 63 lm/W

Simulations were performed to determine the effects of a control system on system performance. The best available control system using 85 lm/W electronic dimmable ballasts, photo sensors, and a 4 stage control strategy was implemented in the model. Simulations using identical physical parameters from the previous runs were performed and the results are included in Figure 5.4. A comparison of Figures 5.3 and 5.4 indicates that a well designed control system has very little impact upon system performance. For the six locations simulated, the losses due to the controls were responsible for approximately a 5 % increase in lighting load per system module. A poorly designed control system could result in higher lighting loads and decreased benefits from the hybrid lighting system. The curves in Figure 5.4 are not as smooth as the previous two figures notably at a system size of 2 modules. At 2 modules the hybrid lighting systems begin to meet 70 - 80 % of the lighting load of the building depending upon location. With 2 to 4 modules in a 4 stage system, the efficacy of the dimmable fluorescents begins to increase because they are operating at higher light fractions, which results in a larger reduction in lighting load. Similar results due to the control system were seen in the building heating and cooling loads. Cooling energy savings decreased by roughly 5 % for all locations while changes in heating energy savings were negligible.

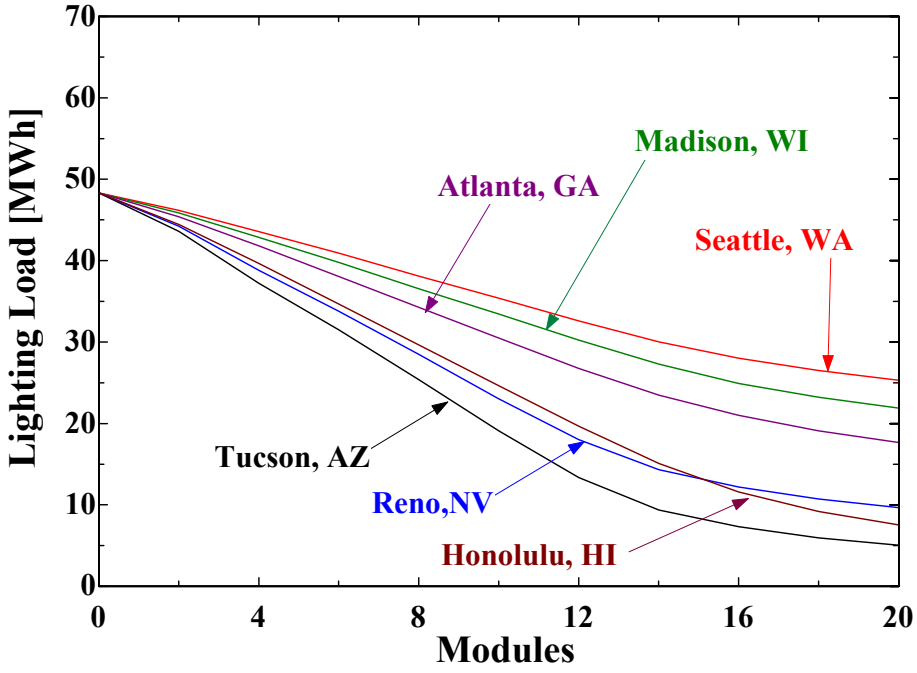

Figure 5.4: Lighting load, 85 lm/W, dimmable ballasts, 4 stage controls

5.3.2 Cooling

The annual cooling loads for the building model simulated in the various locations are shown in Figures 5.5 and 5.6. Warmer climates such as Honolulu and Tucson tended to have higher annual cooling loads than cooler climates in Seattle and Reno. Madison which has the coldest climate of the selected locations surprisingly has a higher cooling load than Reno or Seattle due to the latent cooling load in the summer. In all of the locations, the cooling load decreased with increasing hybrid lighting modules and then began to increase again as excess light was introduced into the building.

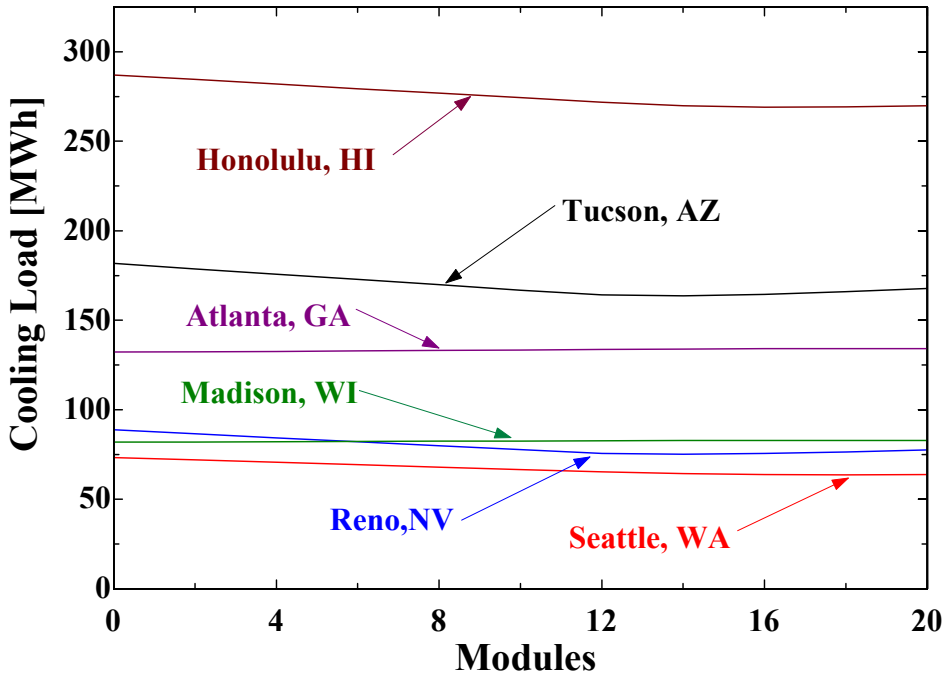

Figure 5.5: Lamp efficacy = 85 lm/W

The effect of the different fluorescent lighting systems can be discerned in Figures 5.5 and 5.6. The more efficient lamps use less energy to produce the same amount of light. Since all of the energy used to produce the light will eventually degrade to heat, using the higher efficacy lamps should result in a lower cooling load. Comparing Figures 5.5 and 5.6, the overall cooling loads of Figure 5.6 are higher than the loads shown in Figure 5.5 as expected.

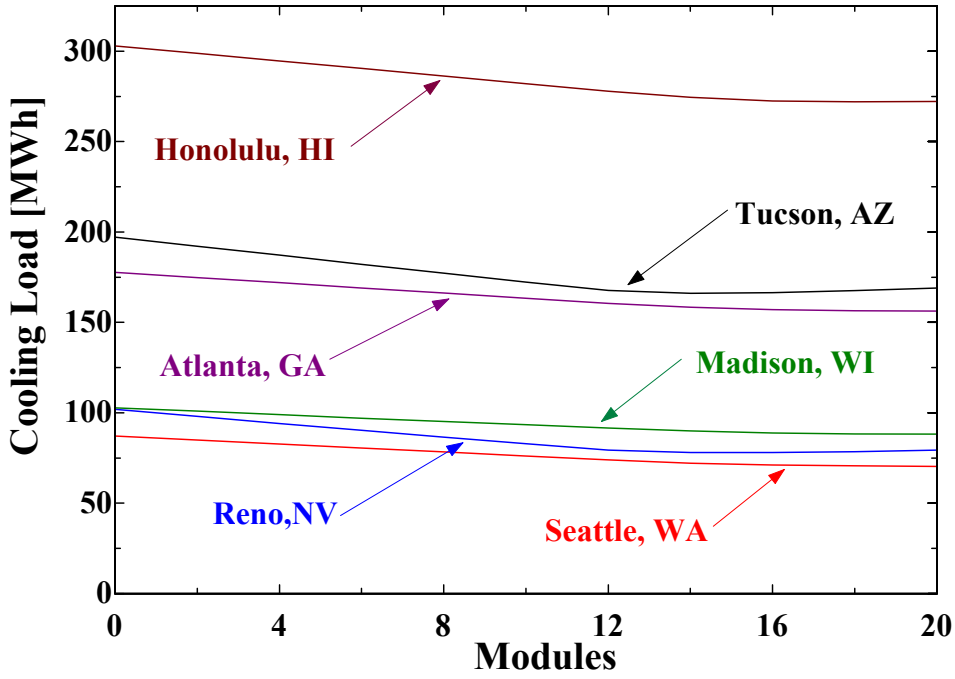

Figure 5.6: Lamp efficacy = 63 lm/W

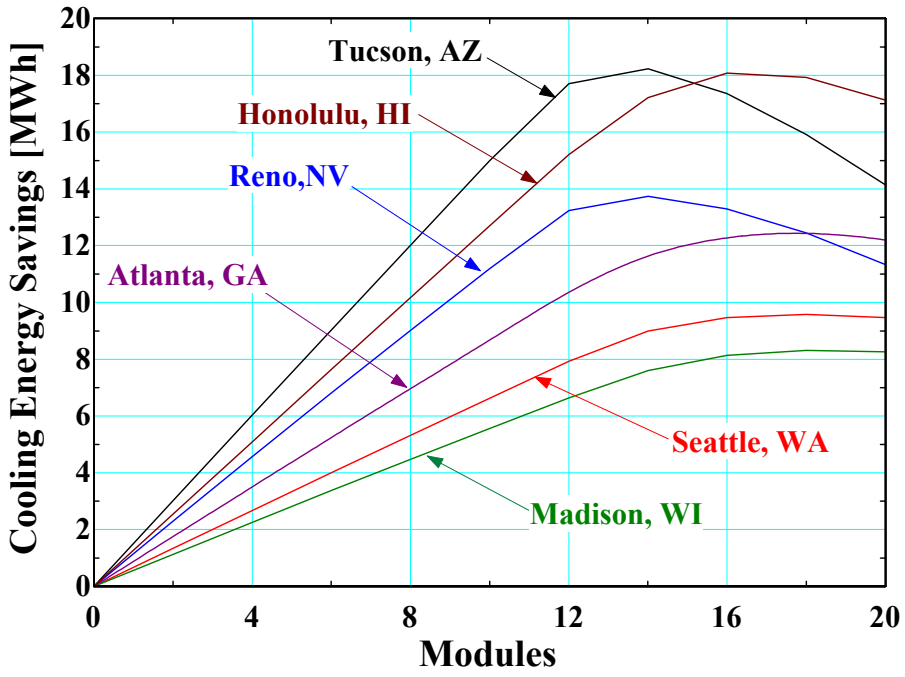

Figure 5.7: Lamp efficacy = 85 lm/W

Since filtered natural light has an efficacy of approximately 200 lm/W, increasing the amount of natural light that displaces artificial light in the building should result in a reduced

cooling load. Figure 5.7 shows the change in cooling load with additional hybrid lighting modules for the simulation using 85 lm/W fluorescent lamps. As with the lighting load, the cooling load decreases linearly with additional systems until the building begins to saturate. As the building saturates, more light is brought into the building than is needed. This extra light, which eventually turns into heat, causes the cooling load to increase after the saturation point. From Figure 5.7 it is clear that sunny locations like Tucson, AZ, Reno, NV, and Honolulu, HI which already benefit from an abundance of natural daylight also have large reductions in cooling load making them ideal places for a hybrid lighting system.

5.3.3 Heating

The heating loads of the building model with increasing number of hybrid lighting modules are shown in Figure 5.8. As expected, the locations with colder climates have a higher heating load than the areas with warmer climates. All locations need some type of heating except for Hawaii where the heating load is very small. Figure 5.8 shows the heating load with a building using 85 lm/W fluorescent lamps. An additional figure showing the heating load using a low efficacy bulb was not included because the results were very similar. The change in lighting gains has less of an effect on the heating load because the majority of the heating load occurs at night when the lights are off. This result is in contrast to the cooling load which typically occurs during the day when building gains and ambient temperatures are highest.

Due to the range of heating loads in the various locations, Figure 5.9 was included to show the effect of increasing numbers of hybrid lighting systems upon the building heating load. The buildings in Madison, WI and Atlanta, GA behave as would be expected with a linear increase in heating load with increasing number of hybrid lighting systems. The unexpected decrease in heating load in Seattle and Tucson is due to the low annual heating demands which are dominated by night-time heating. The hybrid lighting system is only effective during daylight hours and most of the heating in these locations occurs just before sunrise. From further analysis it was found that the change in heating load was directly due to the hybrid lighting system's impact upon the cooling load during the day. The decreased cooling load from the hybrid lighting system resulted in a higher average zone temperature. As heating becomes necessary the higher zone temperature due to the hybrid lighting system results in a lower heating load.

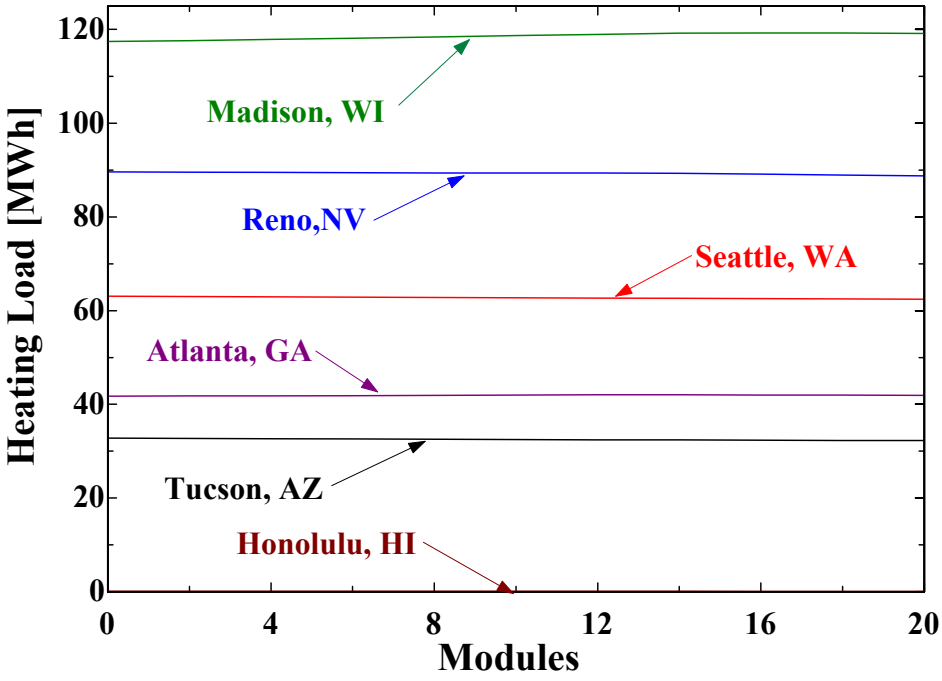

Figure 5.8: Heating load, lamp efficacy = 85 lm/W

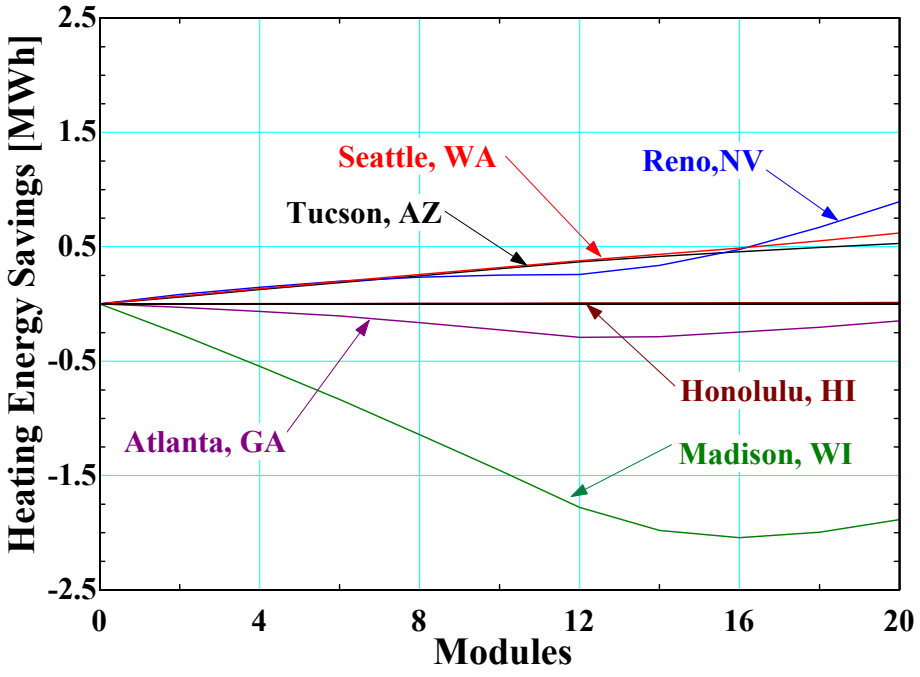

Figure 5.9: Change in heating load, lamp efficacy = 85 lm/W

The climate in Reno results in both heating and cooling during the same day for much of the year. Up until about 6 systems the building in Reno experiences a decreased heating load

much like Tucson and Seattle. From 6 to 14 systems the heating load begins to increase slightly due to an increased heating load during the day caused by the hybrid lighting system. At approximately 12- 14 systems the building begins to saturate with light and the heating load decreases due to the heat associated with the excess light.

5.3.4 TPV

The electricity produced by the TPV array is shown in Figure 5.10. The electricity produced by the array is directly proportional to system size and annual beam radiation. The array in Tucson, AZ receives the most beam radiation and produces the most electricity while the array in Seattle, WA receives the least amount of beam radiation and produces the least amount of electricity.

The revenue produced by the TPV array, shown in Figure 5.11, is a function of the annual energy production as well as the local utility's rate of electricity. All energy produced by the array is assumed to be sold back to the utility at the rate the utility charges less metering, distribution, and demand fees. Electricity in Hawaii is the most expensive at an average cost of $0.184/kWh while the average cost of electricity in Atlanta is only $0.062/kWh.

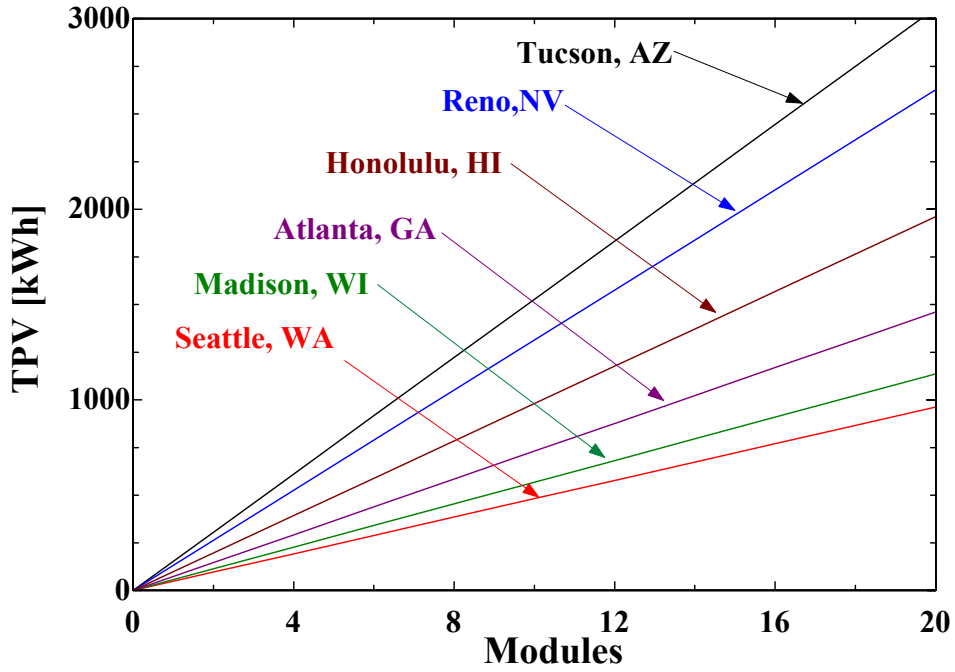

Figure 5.10: Annual TPV energy production

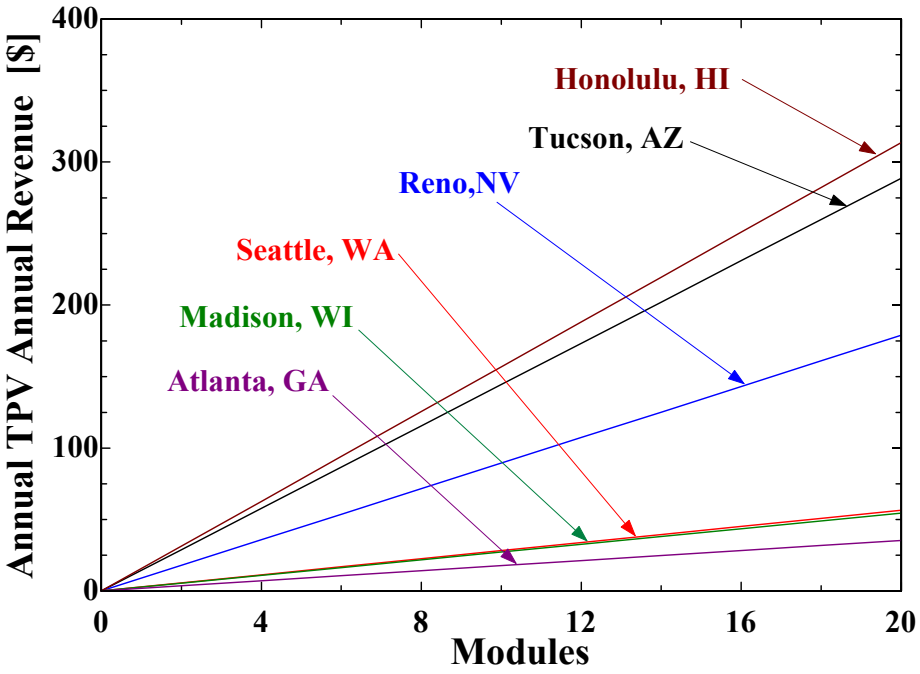

Figure 5.11: Annual TPV revenue

5.3.5 Annual Savings

The annual savings of each system is a total of the reduction in lighting and cooling loads, the heating load impact, and the additional energy from the TPV array. The energy savings is converted into dollars using rate schedules from utilities near the simulated locations. Time-of-use commercial rates were used for electricity costs and natural gas costs were based off of fixed commercial rates. Figure 5.12 shows the annual savings for the hybrid lighting systems in the locations simulated.

Due to the high cost of energy, a hybrid lighting system saved the most money in Honolulu, while inexpensive energy in Atlanta resulted in low savings for the systems located there. The annual savings curves exhibit similar shapes with a constant energy savings per additional module until each system begins to saturate the building with light. As saturation occurs the cost benefit of the hybrid lighting technology decreases.

The dimmable fluorescent control system with staging affected the annual savings as shown in Figure 5.13. The maximum annual savings occurs just as the systems begin to saturate at a system size of 12 - 14 modules. The difference between the shape of the curves in Figure 5.12 and Figure 5.13 is due to the efficiency of dimmable ballasts at part load. The curves in Figure 5.12 use the assumption that the fluorescent lighting systems can be operated at part load

without any losses. In Figure 5.13 the fluorescent lighting operates at a lower efficiency due to losses from the dimmable lights and controls. The annual savings peaks when the hybrid lighting system can meet nearly the entire building lighting load.

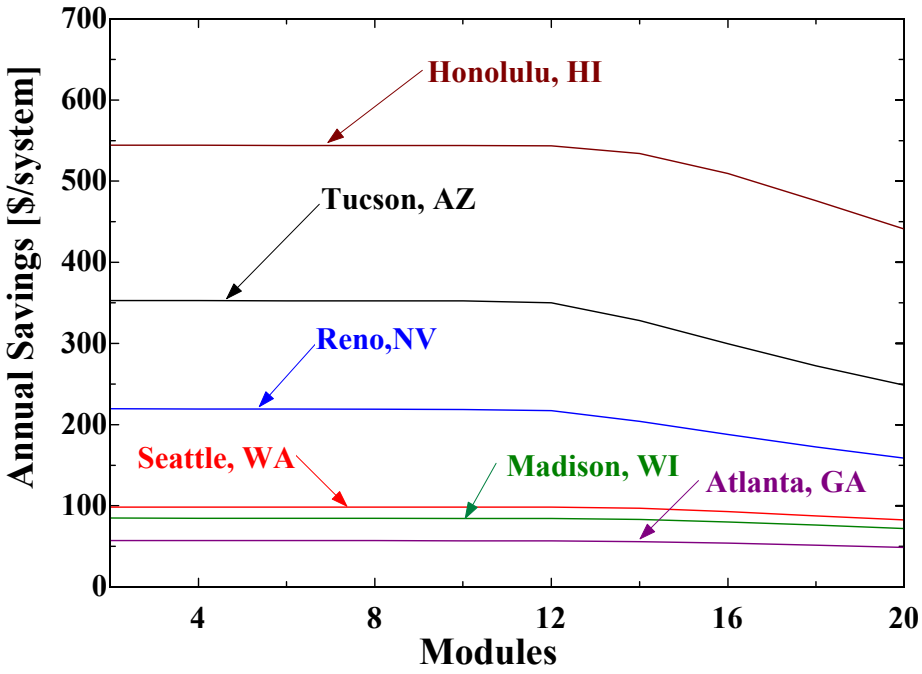

Figure 5.12: Annual savings, 85 lm/W

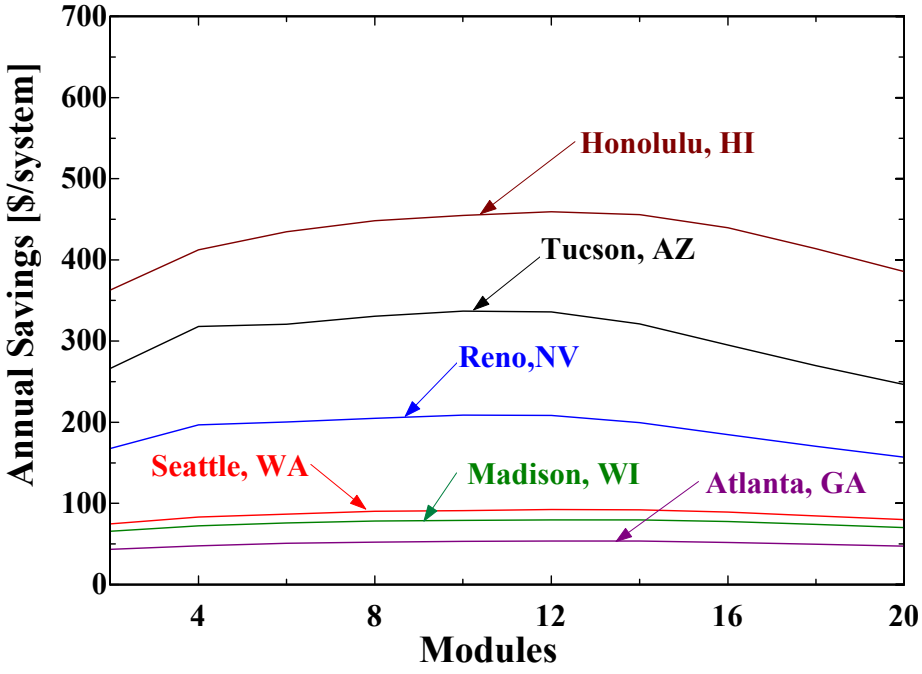

Figure 5.13: Annual savings using a control system

Using Honolulu, HI as an example, Figure 5.14 shows how simulations can be used as a tool to evaluate different components of the hybrid lighting system and building model. The upper most line shows the effect of fluorescent lamp efficacy on annual savings. By increasing the efficiency of the fluorescent lamp from 63 lm/W to 85 lm/W, the peak annual energy savings drops from $667 to $483. This result shows the importance of establishing the correct baseline building technology. The value that the TPV array adds to the total system can be calculated by removing its contribution to the annual savings. The difference between the two curves is the money saved due to the TPV. Assuming that research time and money could be used to increase the luminaire efficiency from 83 % to 95 %, the increased efficiency would lead to $68 saved each year. Similar arguments can be made regarding the value associated with different control systems. Applying an economic analysis to the annual savings can produce a break-even figure for the cost of the TPV, the more efficient luminaire, or a control system.

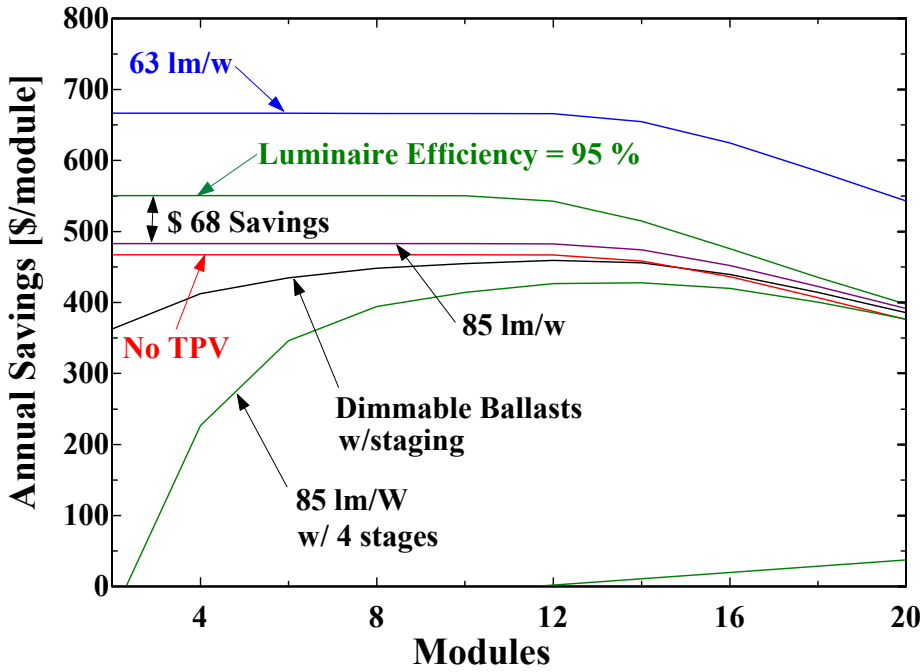

Figure 5.14: Annual savings, Honolulu, HI

5.4 Economic Analysis

Using a P_1/P_2 ratio (see Section 4.8) based on current economic conditions, the break-even capital cost of a complete hybrid lighting system can be calculated using the annual savings

predicted by the TRNSYS model. Table 5.1 shows the break-even capital costs (BECC) of a hybrid lighting system for the various locations simulated. The break-even capital costs are calculated based on the maximum annual savings for each system over a 10, 20, or 30 year analysis period. For a 10 year analysis period Honolulu, HI and Tucson, AZ offer the highest break-even capital costs of and $2800 and $2050. In Madison, WI and Atlanta, GA the break-even capital costs were much less due to inexpensive electricity and lower amounts sunshine.

Table 5.1: Break Even Capital Costs

Location	Annual Savings [$/module]	Analysis Period [yrs]	P_1/P_2	BECC [$/module]
Honolulu, HI	$459	10	6.1	$2,800
		20	7.7	$3,534
		30	8.5	$3,902
Tucson, AZ	$336	10	6.1	$2,050
		20	7.7	$2,587
		30	8.5	$2,856
Reno, NV	$210	10	6.1	$1,281
		20	7.7	$1,617
		30	8.5	$1,785
Seatlle, WA	$93	10	6.1	$567
		20	7.7	$716
		30	8.5	$791
Madison, WI	$80	10	6.1	$488
		20	7.7	$616
		30	8.5	$680
Atlanta, GA	$53	10	6.1	$323
		20	7.7	$408
		30	8.5	$451

Table 5.2 contains a further economic break-down of the hybrid lighting system in Honolulu. Applying the P_1, P_2, economic analysis to the annual savings shown in Figure 5.14, the BECC can be calculated for different hybrid lighting system technologies. From this analysis the incremental BECC of the various technologies can be established and analyzed. For instance, a hybrid lighting system that is displacing light from low efficacy fluorescent lighting (63 lm/W) has a BECC in Honolulu of $4069 compared to the BECC of $2946 for a system that

displaces light from high efficiency bulbs and ballasts. The difference, $1123, is the BECC cost associated with increasing the efficacy of the building's lighting system, not a cost benefit due to the hybrid lighting system. Another example is the BECC of different control systems. The incremental BECC between dimmable fluorescents with 4 stage controls and constant efficacy fluorescents with 4 stage controls is $189 for a 10 year analysis period. If the constant efficacy ballasts and bulbs could be replaced with dimming technology for $189/module or less, the change in controls would be a sound economic decision. The BECC can be used in this manner to evaluate new developments or design cost issues based upon system energy benefits predicted by the TRNSYS hybrid lighting model.

Table 5.2: Break Even Capital Costs, Honolulu, HI

Simulation Type	Annual Savings [$/module]	Analysis Period [yrs]	P_1/P_2	BECC [$/module]
Low Efficacy Lighting (63 lm/W)	$667	10	6.1	$4,069
		20	7.7	$5,136
		30	8.5	$5,670
95 % Luminaire Efficiency	$551	10	6.1	$3,361
		20	7.7	$4,243
		30	8.5	$4,684
85 lm/W fluorescents, ideal controls	$483	10	6.1	$2,946
		20	7.7	$3,719
		30	8.5	$4,106
85 lm/W fluorescents, ideal controls, no TPV	$466	10	6.1	$2,843
		20	7.7	$3,588
		30	8.5	$3,961
85 lm/W dimmable fluorescents,4 stage controls	$459	10	6.1	$2,800
		20	7.7	$3,534
		30	8.5	$3,902
85 lm/W fluorescents,4 stage controls	$428	10	6.1	$2,611
		20	7.7	$3,296
		30	8.5	$3,638

5.5 Summary

Simulations were performed in six locations throughout the U.S. Based on the results of these simulations, hybrid lighting was found to be most effective in Honolulu, HI. Although a location like Tucson, AZ actually receives more sunshine annually, the benefits of the technology are strongly driven by the cost of electricity. Honolulu has both high electricity costs and lots of sun.

Using Figure 5.14 and Table 5.2 as guides, various break-even capital costs and annual savings can be determined. The most striking figure is the annual savings due to the TPV array. In Honolulu, HI, where the system performs best, the annual savings due to the TPV are $17 or a ten year BECC of $103.70. The components which comprise the TPV assembly include the TPV array, the cooling fan, the non-imaging optics, and the mechanical infrastructure. All of these items would have to be manufactured and sold for $103.70 or less to achieve a ten year payback. Dimmable fluorescents with four stage controls results in a 10 year BECC of $2800, and the same system with constant efficacy lamps results in a BECC of $2611 or a $189 difference. The dimmable fluorescent ballasts and bulbs have a BECC of $189. Other BECC figures from the analysis are $1123 to upgrade from low efficacy to high efficacy lighting and $415 to upgrade the efficiency of the luminaires.

Using this analysis method allows the designer to determine what components of the hybrid lighting system are cost effective. With a BECC of $103.70, the TPV assembly is not a cost effective component especially considering the high volume cost target of the TPV array is $100 (Fraas, 2001). Current prices of standard T-8 bulbs and ballasts at a local retail store are $2 and $38. Each module would require at least 8 ballasts and 16 bulbs for a total cost of $336. The cost of the ballasts and bulbs are well under the BECC of upgrading from low efficacy T-12 lighting to high efficacy T-8 lighting insuring the lighting upgrade will pay back in less than ten years.

Chapter 6 Other Solar Lighting Technologies

6.1 Introduction

The analysis of Chapter 5 showed that locations like Tucson, AZ and Honolulu, HI were optimal locations for using the hybrid lighting technology. Break-even capital costs for systems in those locations were $2050 and $2800 respectively, based on a P_1, P_2 ratio of 6.1 and a 10 year payback period. This chapter looks at alternatives to hybrid lighting and presents comparisons based on annual energy savings, annual dollar savings, and break-even capital costs.

6.2 Lighting with Photovoltaics

A technology competing with hybrid lighting is photovoltaics. A photovoltaic (PV) array can generate electricity that would be used to displace the electrical lighting load. Unlike hybrid lighting, a photovoltaic array does not affect the building thermal loads. The electricity generated by the array is integrated into the building's current electrical system and used to displace the lighting loads. Any excess electricity generated by the array is sold back to the grid at local energy rates.

The analysis is based on the premium performance crystalline photovoltaic cells available from BP Solar (BP 5170). Each panel of the array generates 170 W of electricity based on illumination of 1 kW/m^2 (BP Solar, 2003). Each panel has a total area of 1.25 m^2 and a corresponding panel efficiency of 13.6 %. The PV array is wired to a grid connected inverter, BP Solar GCI 1200. The inverter operates with a minimum efficiency of 90 %. No batteries are used in this system as all excess energy is sold back to the utility. Total system efficiency including the inverter is 12.25 %.

PV lighting systems were evaluated in Tucson, AZ and Honolulu, HI where hybrid lighting was most effective. For simplicity of comparison, the PV system was split into modules, each module having an area of 1.7 m^2 which corresponds to the active collector area of the hybrid lighting modules. Simulations were performed in TRNSYS using TMY2 meteorological data. The building model was identical to the model used in the hybrid lighting simulations including 85 lm/W, T-8 fluorescent lighting. The PV array was simulated both as a fixed array and as a two-axis tracking array.

Figure 6.1 shows the building lighting energy savings in Tucson, AZ and Honolulu, HI. For both locations the curves exhibit a linear increase in energy savings with increasing system size. Using a two-axis tracking system increased the energy savings in both locations. A saturation effect with decreasing incremental savings as observed in the hybrid lighting simulations is expected at a system size of approximately 40 - 60 modules.

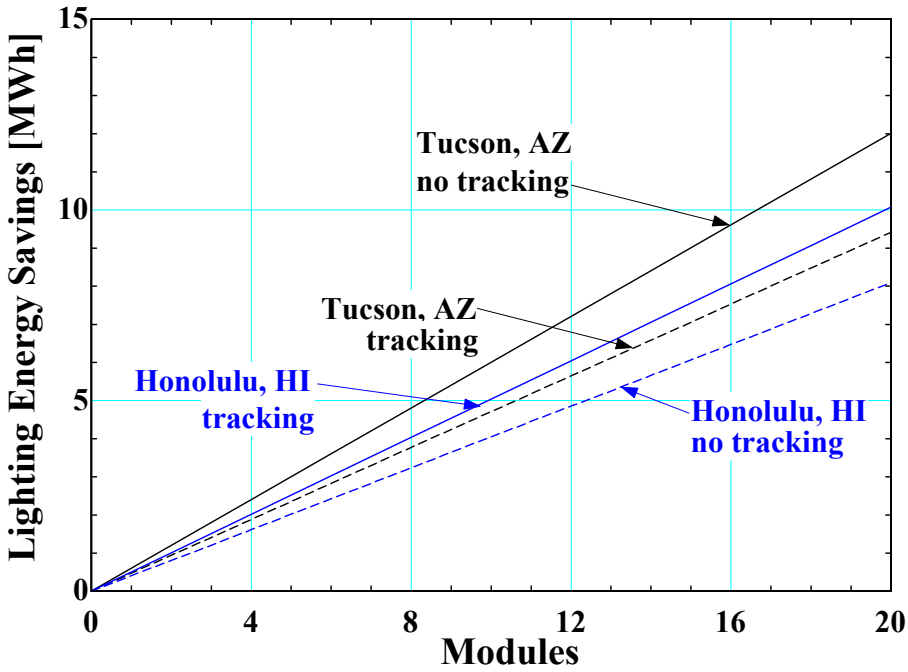

Figure 6.1: Lighting load with PV generated electricity in Tucson, AZ and Honolulu, HI

Figure 6.2 shows the annual savings in dollars for the PV lighting systems. Due to high energy costs, the annual savings for a PV system in Honolulu is greater than a system in Tucson although the PV system in Tucson produces more energy. Using a P_1, P_2 ratio of 6.1 (see Section 4.8), the break-even capital cost (BECC) of the two-axis tracking PV array in Honolulu is $575/module. A PV array in Honolulu that does not track has a BECC of $418/module. The BECC of the corresponding tracking system is the difference or $157/module. Each module of the array has a capacity of 230 W making the BECC per watt of displaced electricity to be $1.82 for a non-tracking system and $2.50 for a tracking system.

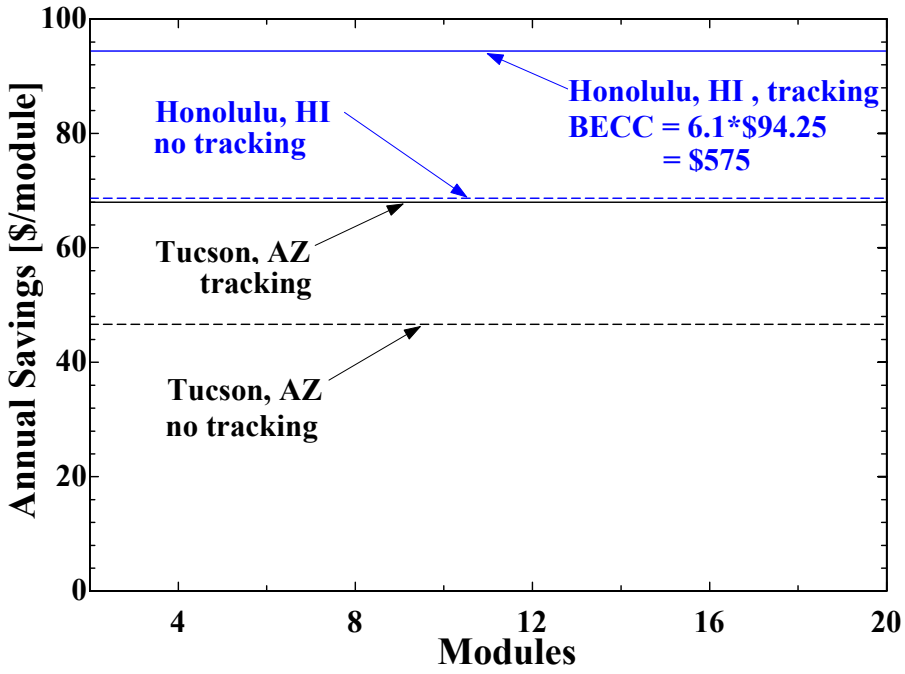

Figure 6.2: Annual savings PV lighting Tucson, AZ, Honolulu, HI

6.3 Toplighting

Conventional skylights, or toplighting, represent another alternative daylighting technology. Horizontal skylights spaced evenly on the roof of the building allow sunlight to illuminate the building throughout the day. The skylights modeled in this comparison are based on data from ASHRAE (ASHRAE Fundamentals, 2001). The light from the skylights is combined with the same lighting systems and control strategies used in the hybrid lighting simulations. The simulation results include the energy and monetary savings due to the reduced lighting load as well as thermal impacts due to the addition of the skylights.

Each skylight is comprised of a domed surface, a light well, and a diffusion filter at the bottom of the well. The domed surface consists of a clear double glazing with an overall transmittance of 0.72. The light well is 1 meter deep, 1 meter wide, and 1.7 meters long matching the dimensions of the skylight. Some light is lost as it is transmitted through the light well. Based on the geometry of the light well and a light wall reflectance of 80 %, IESNA recommends using a light well efficiency factor of 0.7 (IESNA, 2000). The translucent filter at the bottom of the light well produces a uniform source of diffuse light with a transmittance of 0.53. With a dome transmittance of 0.72, a well efficiency of 0.8, and a diffuser transmittance of

0.53, the overall system efficiency based on the horizontal irradiance on the surface of the skylight dome is 0.27. The overall U-value of the skylight including the frame is 5.8 W/m^2-K based on a clear double glazing skylight (ASHRAE Fundamentals, 2001) and available window data in PreBid. The area of each skylight module is 1.7 m^2.

Throughout the day the solar radiation incident upon the skylight is transmitted through the skylight dome, into the light well, and onto the working space. The illuminance is calculated based on Equation 6.1. TMY2 data files were used to provide the total horizontal irradiance. The average efficacy of sunlight was assumed to be 100 lm/W (see Figure 1.6).

$$E_i = G_{total,\,hor}\,\tau_{skylight}\,Efficacy_{sunlight}\,N\,Area_{skylight}\,\eta_{Light\ Well}\,\tau_{diffuser} \tag{6.1}$$

where

E_i = Illuminance (lumens)

$G_{total,\,hor}$ = Total Horizontal Irradiance (W/m^2)

$\tau_{skylight}$ = Skylight Transmittance

$Efficacy_{sunlight}$ = Average Efficacy of Sunlight (lm/ W)

N = Number of Skylight Modules

$Area_{skylight}$ = Area of Skylight Module (m^2)

$\eta_{Light\ Well}$ = Light Well Efficiency Factor

$\tau_{diffuser}$ = Diffuser Transmittance

Simulations were performed in Tucson, AZ and Honolulu, HI using the TRNSYS type 56 building model with skylights instead of the hybrid lighting system. All other variables in the model remained constant including building schedules, rate schedules, and building size. The 85 lm/W, dimmable, fluorescent lighting system was controlled using photo sensors and a four stage control system. The total area of the toplighting system was increased initially from 0 – 20 modules. Due to the relatively low skylight transmittance the maximum number of modules was increased to 60 in order to observe the point of optimal system size. The building lighting and thermal loads associated with toplighting were modeled and the annual savings using local utility rates were calculated.

Figure 6.3 shows the lighting energy savings due to toplighting in Honolulu, HI and Tucson, AZ. From the figure, the energy savings associated with the skylights is linear with increasing systems until the building begins to receive too much light. The fluctuation in the energy savings curve is due to the lighting controls. The small 'dip' at about 10 modules is due to the skylights providing nearly 75 % of the lighting load for a large portion of the year. At a load fraction directly before a stage is turned off, the fluorescent lighting system is the most inefficient. After the 75 % load fraction is met, the lighting system becomes more efficient since it is operating closer to its rated load.

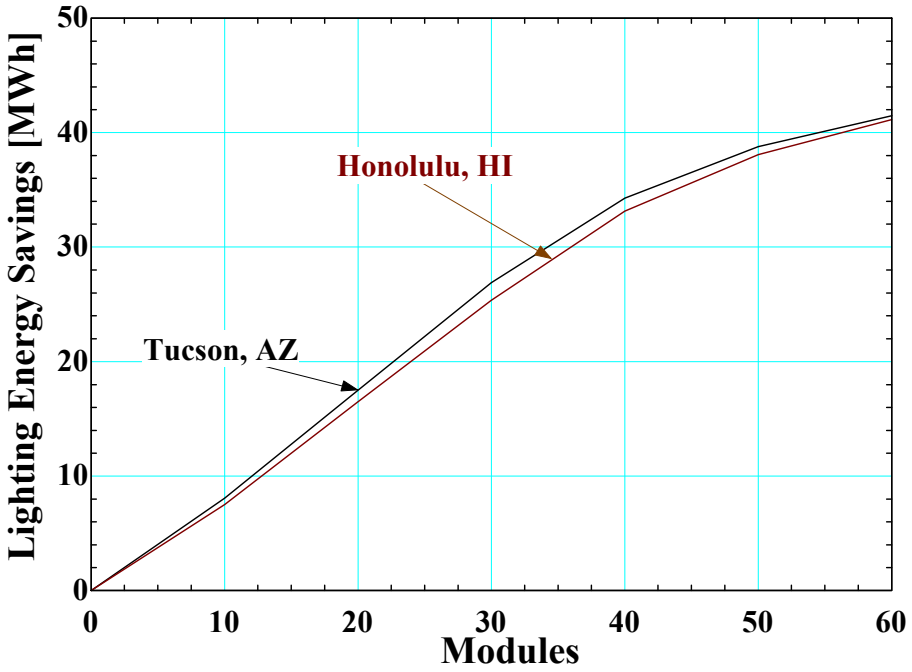

Figure 6.3: Lighting energy savings with skylights

The major disadvantage of toplighting is the thermal loads associated with skylights. Figure 6.4 shows the effect of increasing the toplighting system size upon the cooling load. The negative cooling energy savings indicates an additional cost. The additional cooling cost increases nearly linearly with increasing system size until the building becomes saturated with light. At this point, approximately 40 modules, the rate of change of cooling costs increase due to the heat associated with the extra light from the skylights.

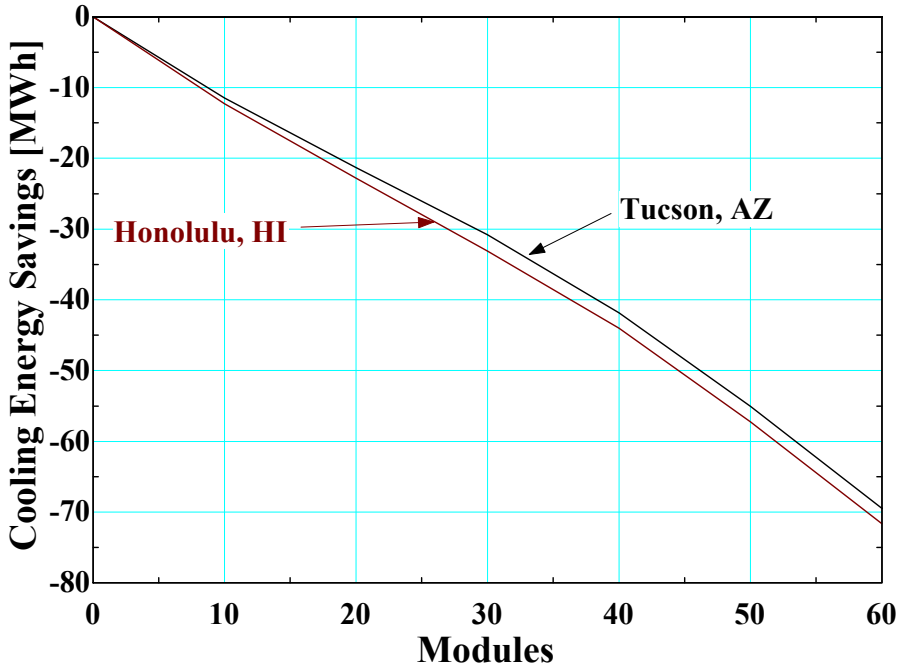

Figure 6.4: Cooling energy savings with skylights

The U-value of the skylights also leads to higher heating loads as shown in Figure 6.5. In Tucson, AZ, temperatures can drop significantly at night, and the low thermal insulation of the skylights leads to losses through the roof at night. Mild night-time temperatures in Honolulu resulted in less of a heating load impact.

The annual savings of the toplighting systems in both locations are shown in Figure 6.6. The savings in Honolulu, HI are greater due to a smaller heating penalty associated with the skylights. As shown in Figure 6.6, the annual savings peak around 30 systems. From 10 to 30 systems the incremental annual savings per module is increasing due to inefficiencies in the lighting control system. After 30 systems excess light begins to be brought into the space, and the additional cooling penalty outweighs any benefit associated with savings due to lighting.

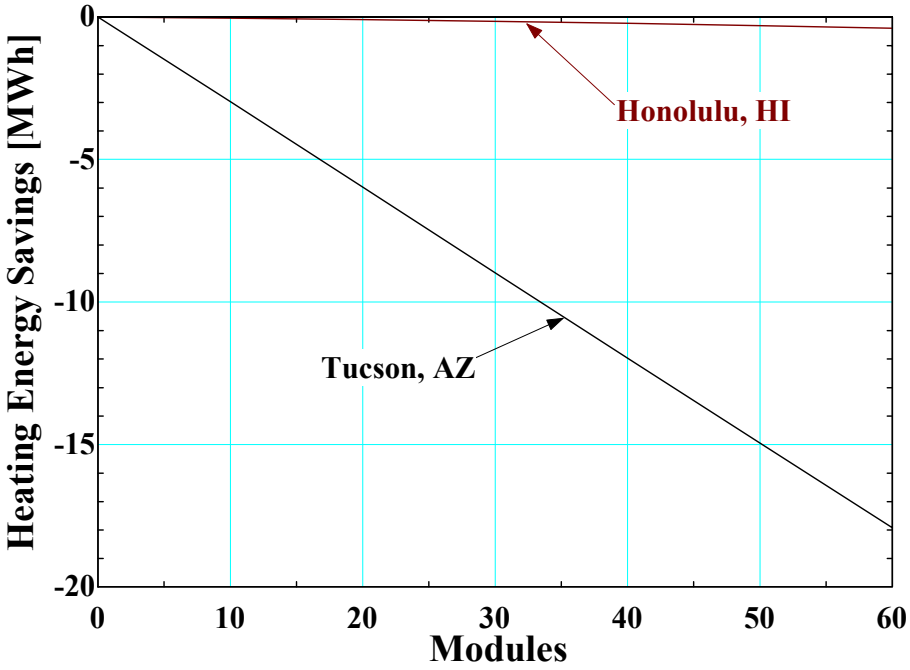

Figure 6.5: Heating energy savings with skylights

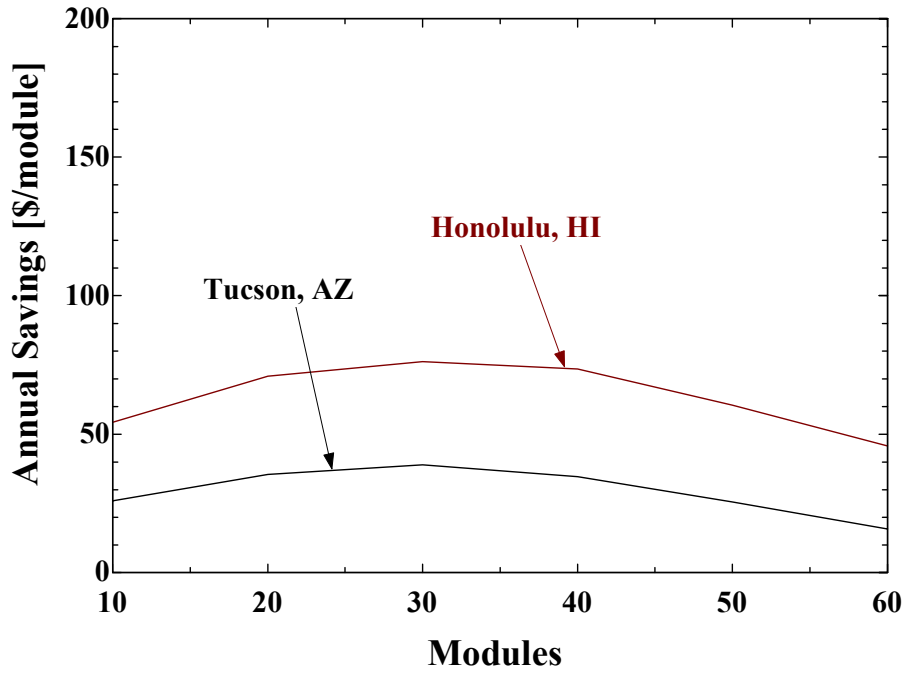

Figure 6.6: Annual savings with skylights

6.4 Summary

Using the maximum benefit associated with the competing technologies the break-even capital cost (BECC) per system module of each daylighting technology is listed in Table 6.1. The results are based on the simulations performed in Hawaii to show a best-case scenario for all of the technologies. The module size for each technology was held constant so that a clear comparison could be made.

Table 6.1: Technology Comparison in Honolulu, HI

Technology	Annual Savings [$/module]	P_1/P_2	BECC [$/module]
Hybrid Lighting	$459	6.1 7.7 8.5	$2,800 $3,534 $3,902
PV Lighting Two-Axis Tracking	$94	6.1 7.7 8.5	$573 $724 $799
PV Lighting No Tracking	$69	6.1 7.7 8.5	$421 $531 $587
Skylights	$76	6.1 7.7 8.5	$464 $585 $646

Photovoltaic lighting technology with two-axis tracking produced a benefit of $94/module. Based on a 1.7 m^2, 230 W module, the BECC of a complete PV module, including two-axis tracking, is approximately $2.50/W. The BECC of a fixed PV module is $1.83/W. Current commercially available photovoltaics cost in the range of $3-5/W not including the two-axis tracking system, mounting equipment, or inverters (Muhs, 2000a). Currently photovoltaic lighting is not an economically sound investment.

Toplighting, a more direct comparison with hybrid lighting, resulted in an annual savings of $76/module. The numbers in Table 6.1 are based upon a toplighting system size of 30 modules or roughly 2 % of the building roof area. The BECC of the 30 module system is

$464/module based on a 10 year analysis. The Means catalog provides a cost estimate of $17.85/ft^2 for a plastic, double glazed dome skylight including installation costs (Means, 1995). The cost of 1.7 m^2 skylight based on the Means data is approximately $340/module. Based on these prices, the toplighting system will payback in less than 10 years, but it should be considered that the Means prices do not include any construction costs associated with the light well or costs associated with the controls.

Hybrid lighting systems will payback after 10 years if each module can be manufactured and installed for $2800 or less. A hybrid lighting system module includes a concentrating collector, a secondary element, a TPV array and optics, the optical fibers, the luminaries, the controls, and installation costs. Clearly the hybrid lighting designers will find it challenging to be able to produce cost effective systems. Based on the numbers of Table 6.1 toplighting systems could be an economical alternative and major competitor with hybrid lighting. The capital cost of a toplighting module is significantly less than the BECC over the 10 year analysis period, but this cost shown in Table 6.1 does not include additional construction and control costs. Assuming that these additional expenses would cost less than $124/module may be optimistic, but toplighting systems do seem to be a very attractive alternative lighting technology.

Another factor that must be considered in these systems is the value of natural light. Studies have indicated the benefits of natural light include personal well-being and productivity (Fay, 2003). If natural light can be attributed to a small improvement in an office workers productivity a monetary value can be assigned to the natural light and the BECC of both the skylights and the hybrid lighting system will improve.

Chapter 7 Conclusions and Recommendations

7.1 Summary

This thesis studies a new building lighting technology that separates the solar spectrum and uses the visible portion to light buildings and the infrared portion to generate electricity. The technology is currently under development by a design team comprised of members of industry and academia and led by Oak Ridge National Laboratory. The purpose of this particular study is to evaluate the feasibility of the technology and to create a flexible, simulation tool that other members of the design group can utilize.

The hybrid lighting technology consists of a two-axis, concentrating collector that gathers direct normal solar radiation throughout the day. The direct normal solar radiation is reflected onto a secondary element which divides the solar radiation into the visible and infrared spectrums. The visible light is reflected off of the secondary element and focused into large core optical fibers which transport the light into a space where it is needed. The infrared energy is transmitted through the secondary element and focused onto a photovoltaic array which uses the energy to generate electricity. There are two major benefits from hybrid lighting. The first benefit is the reduction in electricity needed to light the building, and the second benefit is a reduced cooling load due to the high efficacy of natural light.

A model of a hybrid lighting system was created in TRNSYS. The model consists of two major components; the building component and the hybrid lighting component. The TRNSYS type 56 building component was configured to simulate a large multi-use environment which could potentially represent a retail or office space. The hybrid lighting component uses the incoming beam radiation and spectral properties of the hybrid lighting system to determine the light and electricity benefits produced. The light 'produced' by the hybrid lighting component is fed back into the building model to calculate the impacts the hybrid lighting technology has upon building loads.

An economic model was implemented into the TRNSYS simulation based on the P_1, P_2 methodology. Utility rate schedules convert the hybrid lighting impacts upon the building lighting, heating, and cooling loads into dollars. Using the P_1, P_2 economic model in conjunction with the energy savings predicted by TRNSYS results in a break-even capital cost for the hybrid

lighting technology based on economic parameters, hybrid lighting properties, and the location specified in the simulation.

7.2 Conclusions

Based on annual TRNSYS simulations, the best hybrid lighting system performance was seen in Honolulu, HI with Tucson, AZ being the best location within the continental United States. Using the predicted annual savings, the break-even capital cost of hybrid lighting modules operating in those locations are $2800 and $2050. These costs represent the total cost of an installed hybrid lighting module which include these major components:

concentrating collector (active collecting area of 1.7 m^2)
two-axis tracking equipment
secondary element
TPV assembly
optical fibers (~56 meters)
luminaires (8)
controls

To manufacture, ship, and install a hybrid lighting module for less than $2800 will be extremely challenging for the design team.

Using the TRNSED simulation tool, a cost-benefit analysis was performed on various components of the system. Under best-case conditions in Honolulu, HI, the TPV array contributed $17 to the overall annual savings of a hybrid lighting module. The 10 year, break-even capital cost associated with that savings is $104, thus the entire TPV assembly including the array, the non-imaging optics, the cooling apparatus, and the mechanical infrastructure would all have to cost $104 or less to achieve a 10 year payback. The TPV assembly does contribute additional value to the project by potentially allowing each module to operate without connections to an electrical supply as well as the marketing appeal associated with new technology and ‘using the entire spectrum’. Unfortunately the TPV concept does not provide near enough benefits to outweigh the potential component costs.

A cost benefit analysis was performed upon potential control strategies that will be used to combine the hybrid and auxiliary lighting systems. The analysis that was performed looked at a simple four stage control strategy using constant output fluorescent lighting and another control system using the same four stage control strategy but with dimmable fluorescent lighting. Again under best-case conditions in Honolulu, HI, the control system with dimmable lighting resulted

in an annual savings $189 more than the control system without the dimmable lighting. Although costs of the new bulbs and ballasts are greater than the annual savings, the correct design decision in this scenario is not clear. A certain amount of value provided by the lighting system is associated with the level of quality light produced by the system. A lighting system that produces noticeable fluctuations in illumination throughout the day will have a smaller value to the building's occupants than the system that can maintain a uniform building illuminance. These factors must be taken into account on a building by building basis when deciding what levels of light fluctuation are permissible.

A study was performed to compare hybrid lighting with photovoltaic lighting and toplighting. Photovoltaic lighting was not a very cost effective building lighting technology with current costs approximately double the break-even capital cost, but toplighting did provide economic benefits to cover the capital costs over a ten year analysis period. Although the energy benefits of a skylight module were about one-sixth the energy benefits from an equivalently sized hybrid lighting module, low capital costs, new glass coating technologies, and a simple design make toplighting a viable solar lighting technology.

One major item missing from this analysis is the monetary benefit that can be associated with natural daylight. If the presence of natural light could be attributed to one less sick day a year, a slight improvement in employee productivity, or a higher probability that people would visit your store, then the break-even capital costs of a hybrid lighting system would increase tremendously. For instance, if the average employee with a salary of $30,000/year is responsible for $60,000 of revenue each year, and this employee's productivity increases by just 1 % annually due to daylighting, then the additional revenue that the natural light indirectly provides would be $600 per employee per year. Assume that this occurs in an office environment like the office modeled, with about 150 employees, and the annual savings and additional revenues due to the daylighting increase to $90,000. If the physiological benefits of natural light could be included in the overall benefits received from a hybrid lighting system, the break-even capital cost of the technology would increase making it easier to economically justify.

7.3 Recommendations and Future Work

The next logical step after this thesis is to perform a detailed cost analysis of the hybrid lighting technology. The analysis could include compiling a thorough bill of materials with detailed high volume cost targets. When this analysis is completed, a more definitive decision can be made on the feasibility of the hybrid lighting technology.

Future work can focus on improving the functionality of the hybrid lighting model. The model needs to include a more detailed model of the optical fibers that will account for fiber routing and bends. The bends will have a significant impact on the total attenuation of the fiber as well as the color temperature of the light leaving the fiber. A large part of this work would be integrating the chromaticity model developed at Oak Ridge National Laboratory into the TRNSYS hybrid lighting model.

Integrating certain functionalities of the PreBid building description program into TRNSED would create a more flexible hybrid lighting model and a more robust software package in general. A weakness of the hybrid lighting model lies in a limitation of the TRNSED interface to alter the physical construction and dimensions of the building model. A more flexible model would allow the user to manipulate the simulated building to their needs.

Although controls were briefly evaluated in Chapter 5, it is clear that the control design of a hybrid lighting system plays a critical role in system performance. Many factors contribute to the cost and performance of a control system including the photo sensors, switching or staging strategies, and auxiliary lighting systems. In addition to this thesis, additional work could focus on determining acceptable illumination variances of the workplace and the illumination variance due to different control scenarios.

The commercial building sector is only one potential market that could be tapped by hybrid lighting systems. The retail sector, in particular large discount stores, would be another market for hybrid lighting. The store hours and building construction lend itself to the technology and are in fact very similar to building modeled in this thesis. The large discount retail chains could absorb some of the initial costs of the technology, while benefiting not only from the energy savings and natural light in their stores, but from the ‘green’, environmentally friendly image associated with solar technology. Future studies could focus on not only the commercial sector but perhaps a case study of a large discount store as well.

The hybrid lighting model described in this thesis used a simple building model without any windows or other daylighting technologies. Additional work could look at hybrid lighting systems placed on more complex structures. In addition to comparisons with toplighting, studies need to be performed to show how hybrid lighting will work in a building already receiving natural light through windows, skylights, roof monitors, or something similar. An interesting study would be to evaluate hybrid lighting systems in combination with current daylighting techniques in a multi-story building. Perhaps hybrid lighting technology will work best when combined with other daylighting techniques.

Appendix A – SMARTS2v9.1 Input and Output Files

Input File

```
'7_15_02(Atmospher_Comparison)'     !Card 1 Comment
1                        !Card 2 ISPR
1013 0.0                 !Card 2a Pressure & altitude
1                        !Card 3 IATMOS
'USSA'                   !Card 3a Atmosphere
0                        !Card 4 IH2O
2                        !Card 4a W
1                        !Card 5 IO3
1                        !Card 6 IGAS
370.0                    !Card 7 qCO2
1                        !Card 7a ISPCTR
'S&F_RURAL'              !Card 8 Aeros
1                        !Card 9 ITURB
0.1                      !Card 9a Beta
12                       !Card 10 IALBDX
0                        !Card 10b ITILT
280 4000 1.0 1367.0      !Card 11 Input wavelengths; solar spectrum
2                        !Card 12 IPRT
280 2500 5               !Card12a Print limits
3                        !Card12b # Variables to Print
1 2 4                    !Card12c Variable codes
0                        !Card 13 ICIRC
0                        !Card 14 ISCAN
2                        !Card 15 ILLUM
0                        !Card 16 IUV
2                        !Card 17 IMASS
2.25                     !Card 17a Air mass
```

Output Summary File

```
******************  SMARTS2, version 2.9.1  *******************

 Simple Model of the Atmospheric Radiative Transfer of Sunshine
                    Chris A. Gueymard, May 2002

    This model is documented in FSEC Report PF-270-95
 and in a Solar Energy paper, vol. 71, No.5, 325-346 (2001)

 NOTE: These references describe v. 2.8 or earlier!!!
 See the User's Manual for details on recent changes...

*************************************************************

       Reference for this run: 7_15_02(Atmospher_Comparison)

-------------------------------------------------------------

* ATMOSPHERE : USSA   AEROSOL TYPE: S&F_RURAL
```

```
* INPUTS:
     Pressure (mb) = 1013.00   Altitude (km) =  0.000
     Relative Humidity (%) = 45.45   Precipitable Water (cm) = 2.0000
     Ozone (atm-cm) = 0.3438 or 343.8 Dobson Units
   AEROSOLS:  Optical Depth at 500 nm = 0.2698   Angstrom's Beta = 0.1000
Schuepp's B = 0.1172
     Visual Range (km) =  34.2   Visibility (km) =  26.2
     Alpha1 = 0.9401  Alpha2 = 1.4319   Mean Angstrom's Alpha = 1.1860

* TEMPERATURES:
     Ground Level = 288.2 K
     Sea Level = 288.2 K
     Ozone (effective) = 225.4 K
     NO2 (effective) = 225.4 K

**WARNING! Ground reflectance data for GRASS
 extend only from 0.3000 to 1.1900 µm,
 whereas the wavelength limits for this run are 0.2800 and 4.0000 µm.
 Consequently, reflectance is fixed at 0.031 below 0.3000 µm and at 0.127
above 1.1900 µm.

The following spectral variables will be output to file: SMARTS2.EXT

 * Extraterr_spectrum
 * Dir._normal_irrad.
 * Global_horiz_irrad

  Spectral ZONAL albedo data: GRASS
   with a reflection process: NON_LAMBERTIAN

=======================

* SOLAR POSITION (deg.):
    Zenith Angle (apparent) = 63.715  Azimuth (from North) =  180.00

  RELATIVE OPTICAL MASSES:
  - Rayleigh =  2.250
  - Water Vapor =  2.257
  - Ozone =  2.238
  - NO2 =  2.243
  - Aerosols =  2.256

 CO2 Mixing Ratio (ppmv):  370.0

 Total column abundances for all gases except H2O (atm-cm) and
normal/standard conditions:

   BrO        CH2O       CH4        ClNO3      CO         CO2        HNO2
HNO3       NH3

0.2500E-05 0.3000E-03 0.1284E+01 0.1200E-03 0.8744E-01 0.2970E+03 0.1000E-03
0.3811E-03 0.1300E-03

   NO         NO2        NO3        N2         N2O        O2         O3
O4         SO2
```

```
0.3210E-03 0.2044E-03 0.5000E-04 0.3718E+01 0.2384E+00 0.1678E+06 0.3438E+00
0.1678E+06 0.1070E-03

*  *  *  *  *  *  *  *  *  *  *  *  *  *  *  *  *  *  *  *  *  *  *  *  *

 * SPECTRUM:
  Total (0-100 µm) Extraterrestrial Irradiance used here = 1367.00 W/m2
  (i.e., 1.0000 times the selected solar constant, 1367.00 W/m2, due to the
actual Sun-Earth distance.)
  Source for selected solar spectrum: SMARTS_Gueymard

Wavelength Range =  280.0 to 4000.0 nm ;   Number of Wavelengths =  2002

*** BROADBAND IRRADIANCES (W/m2):

* DIRECT BEAM AT NORMAL INCIDENCE:
  Extraterrestrial = 1347.94   Terrestrial =  598.58   Atmospheric
Transmittance = 0.4441

* FOR THE HORIZONTAL PLANE:
  Direct Beam =  265.07   Diffuse = 121.18   Global =  386.25
  Diffuse irradiance components:
  Rayleigh scattering =  35.78   Aerosol scattering =  79.88   Backscattering
=   5.52

*** ILLUMINANCES (klux) obtained with the Vlambda curve from CIE 1988:
 E.T. = 133.86  BEAM NORMAL =  57.03 DIFFUSE =   16.80 GLOBAL =   42.05
GLOBAL TILT =   42.05

*** LUMINOUS EFFICACY (lm/W):
 E.T. =  97.92  BEAM =  95.271 DIFFUSE = 138.622   GLOBAL = 108.872   GLOBAL
TILT = 108.872
```

Appendix B – P_1, P_2 Ratio

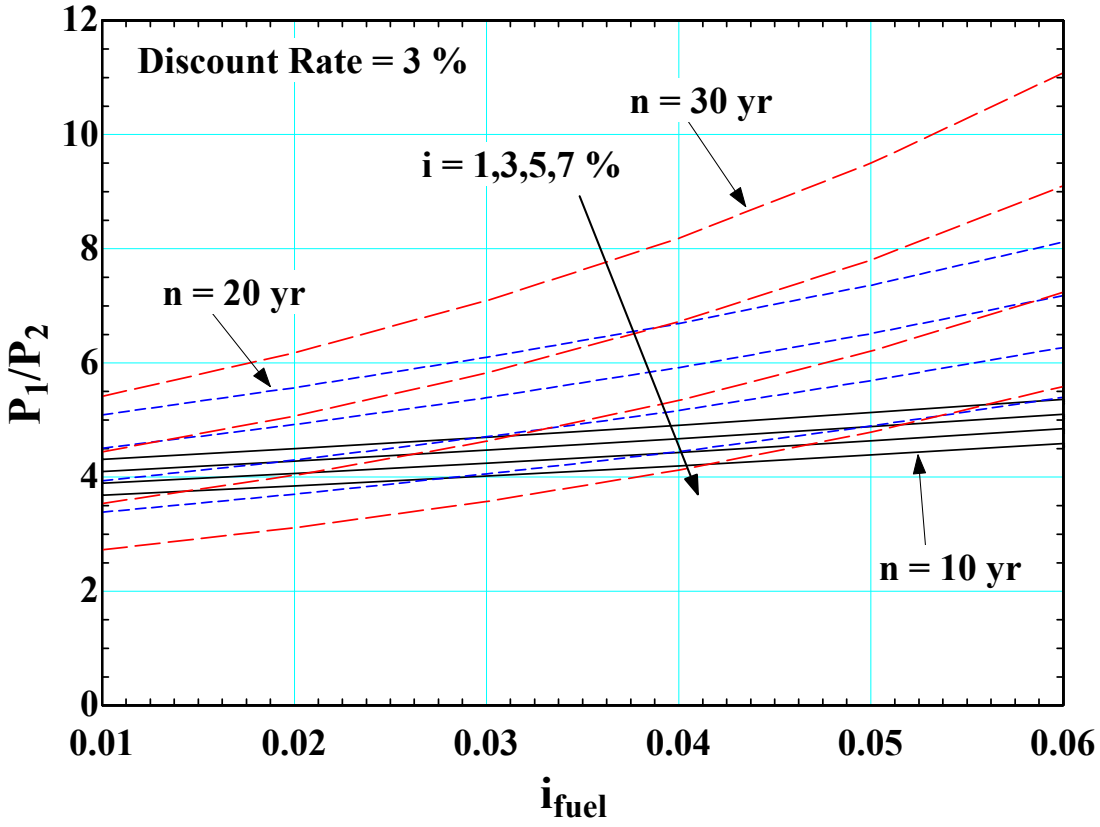

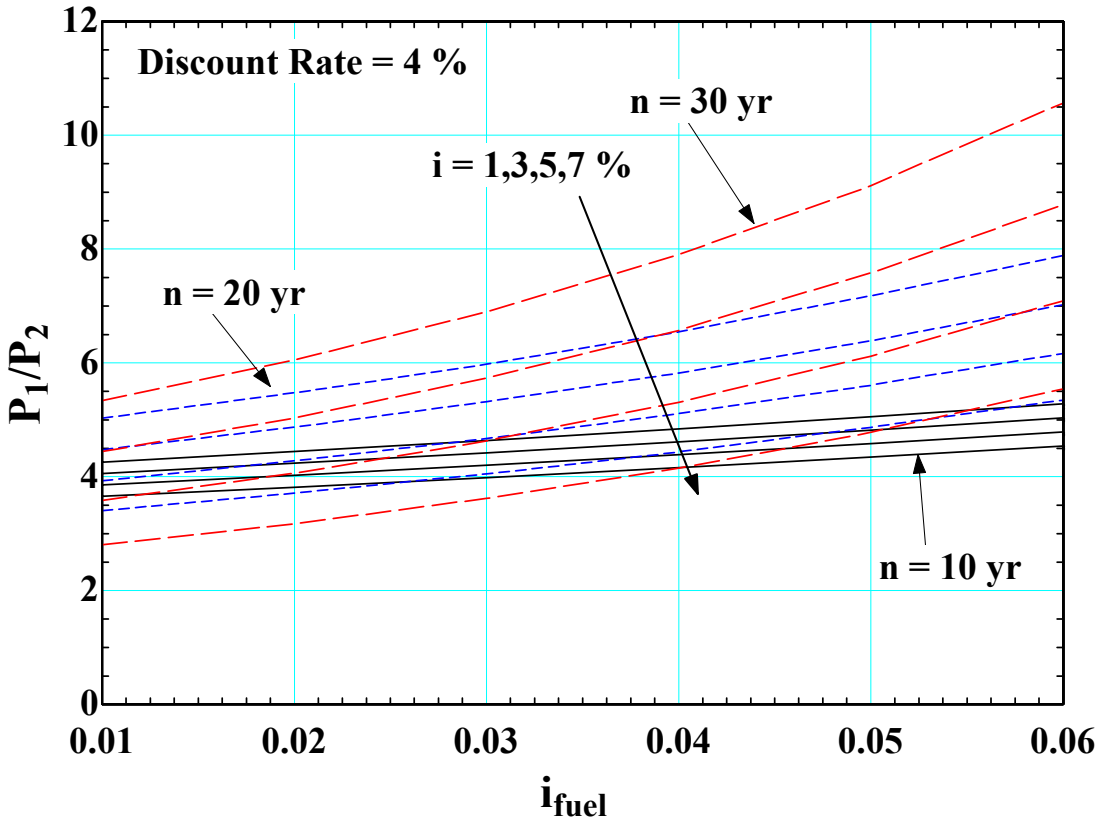

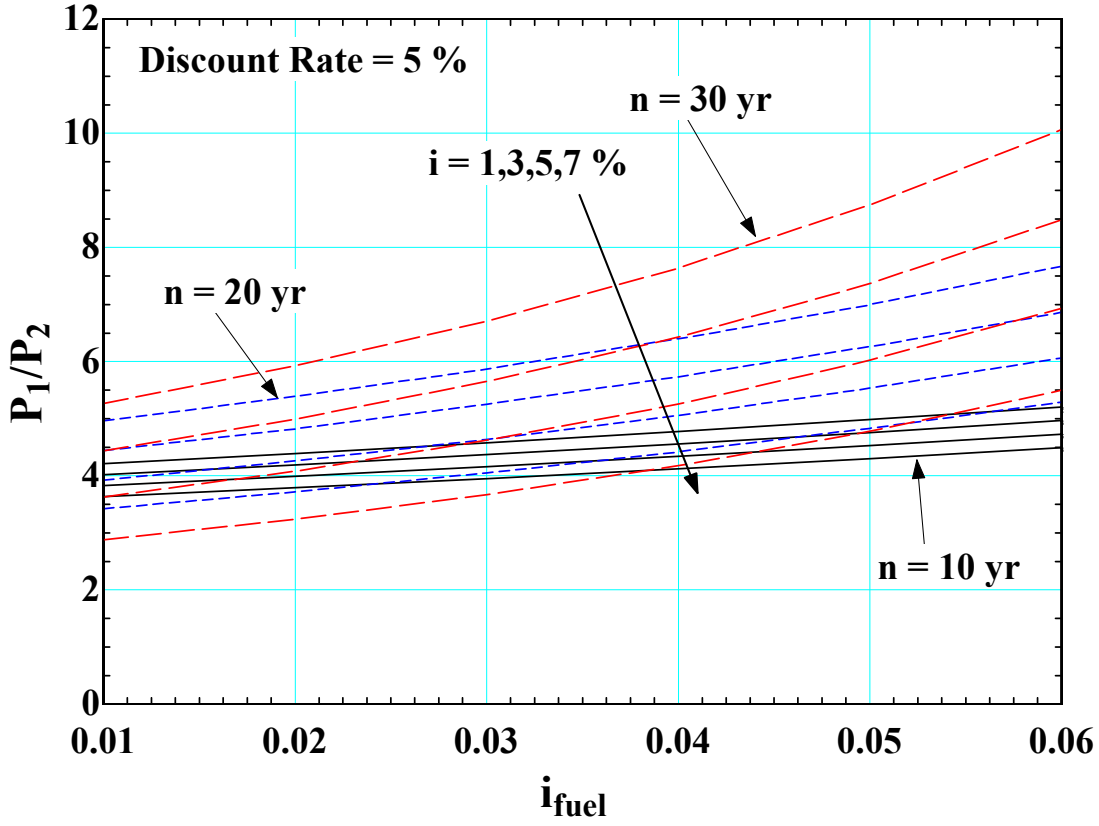
Discount Rate = 5 %
n = 30 yr
i = 1,3,5,7 %
n = 20 yr
n = 10 yr
P1/P2
ifuel
0
2
4
6
8
10
12
0.01
0.02
0.03
0.04
0.05
0.06

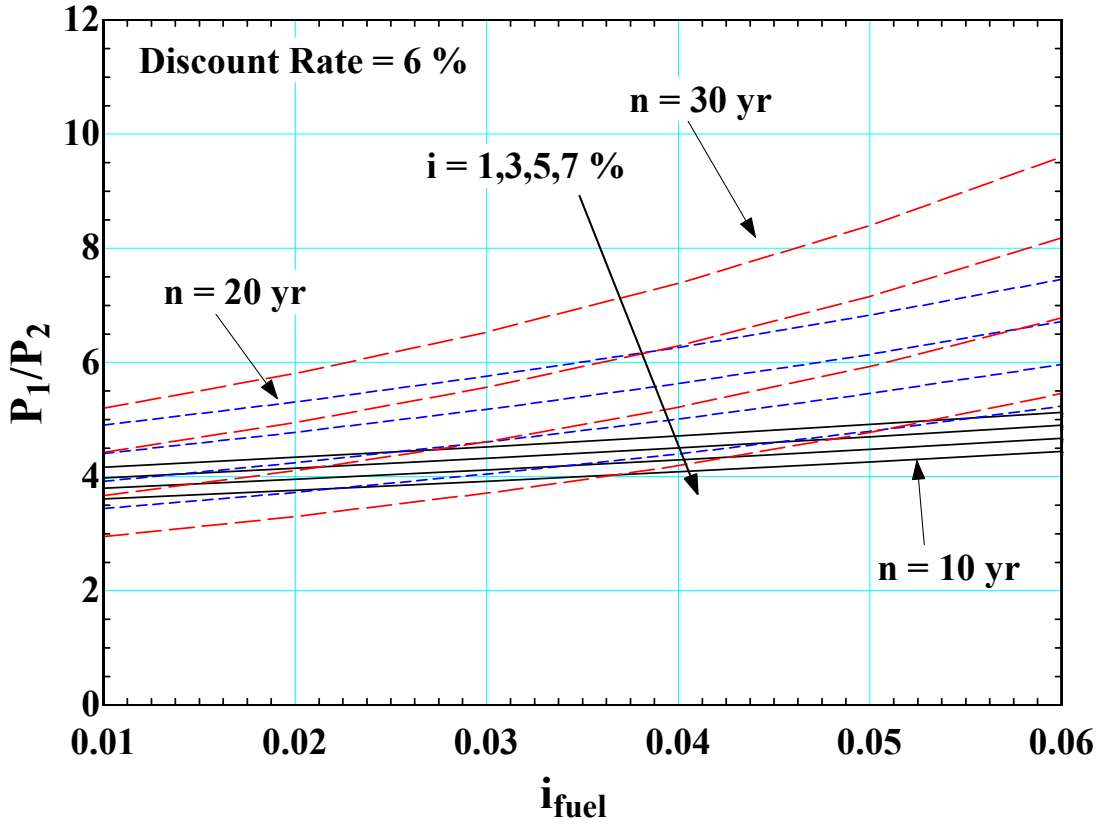
Discount Rate = 6 %
n = 30 yr
i = 1,3,5,7 %
n = 20 yr
n = 10 yr
P1/P2
ifuel
0
2
4
6
8
10
12
0.01
0.02
0.03
0.04
0.05
0.06

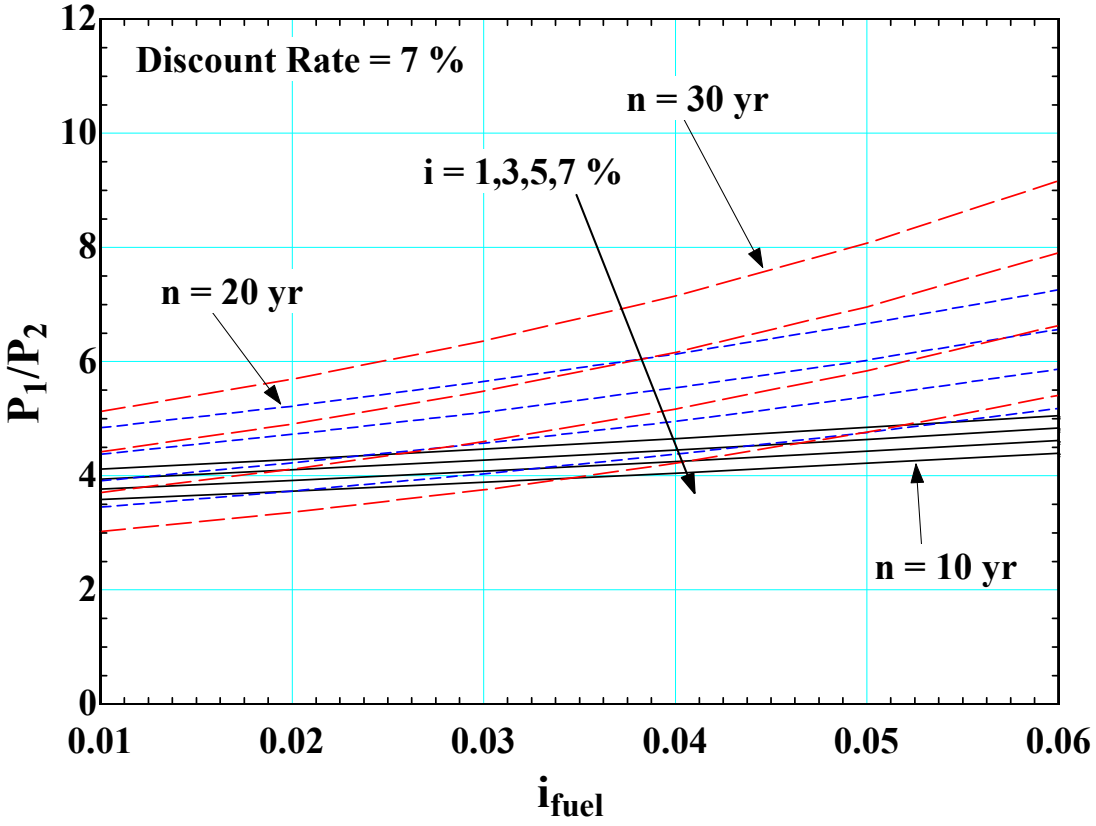
Discount Rate = 7 %
n = 30 yr
i = 1,3,5,7 %
n = 20 yr
n = 10 yr
P1/P2
ifuel
0
2
4
6
8
10
12
0.01
0.02
0.03
0.04
0.05
0.06

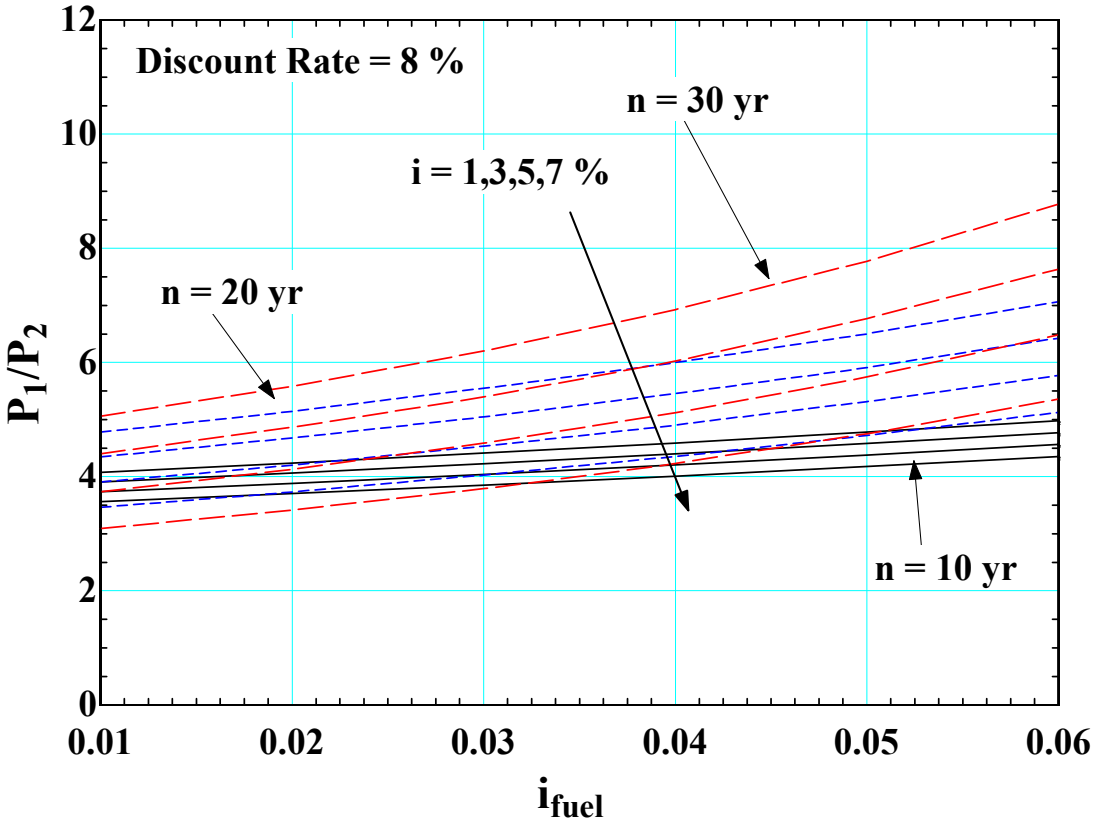
Discount Rate = 8 %
n = 30 yr
i = 1,3,5,7 %
n = 20 yr
n = 10 yr
P1/P2
ifuel
0
2
4
6
8
10
12
0.01
0.02
0.03
0.04
0.05
0.06

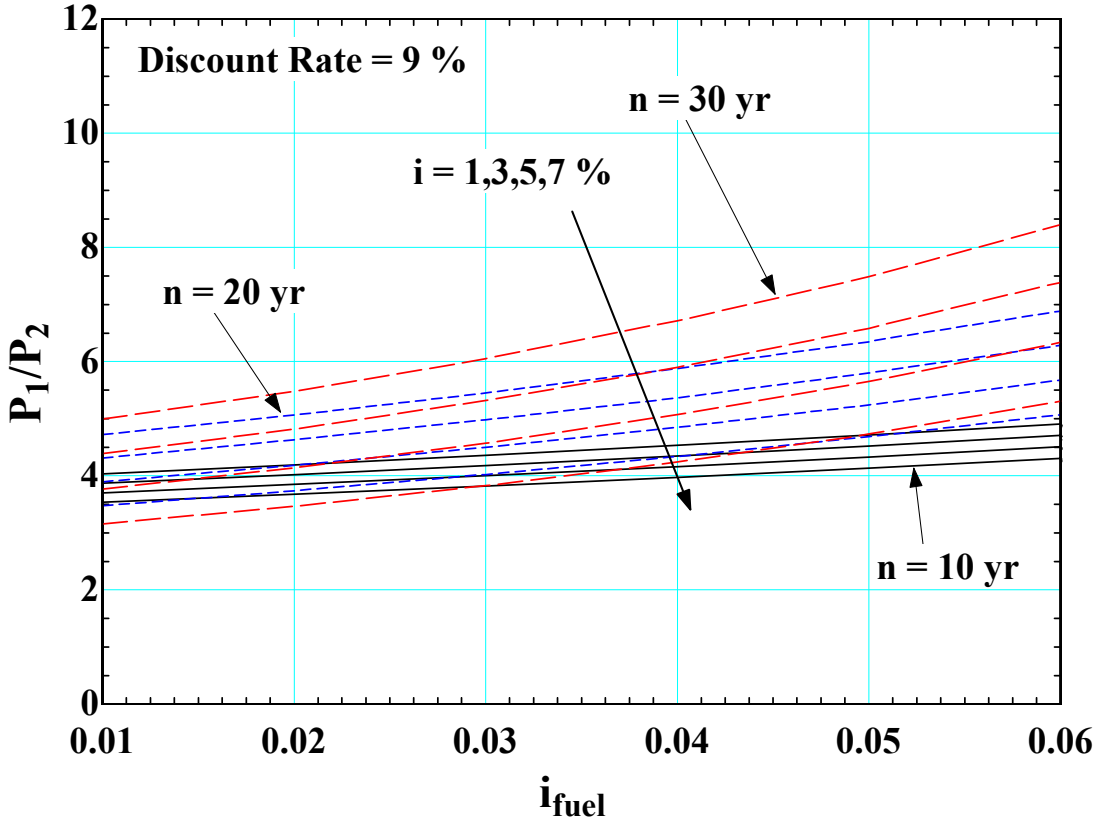
Discount Rate = 9 %
n = 30 yr
i = 1,3,5,7 %
n = 20 yr
n = 10 yr
P1/P2
ifuel
0
2
4
6
8
10
12
0.01
0.02
0.03
0.04
0.05
0.06

Appendix C – TRNSED Interface

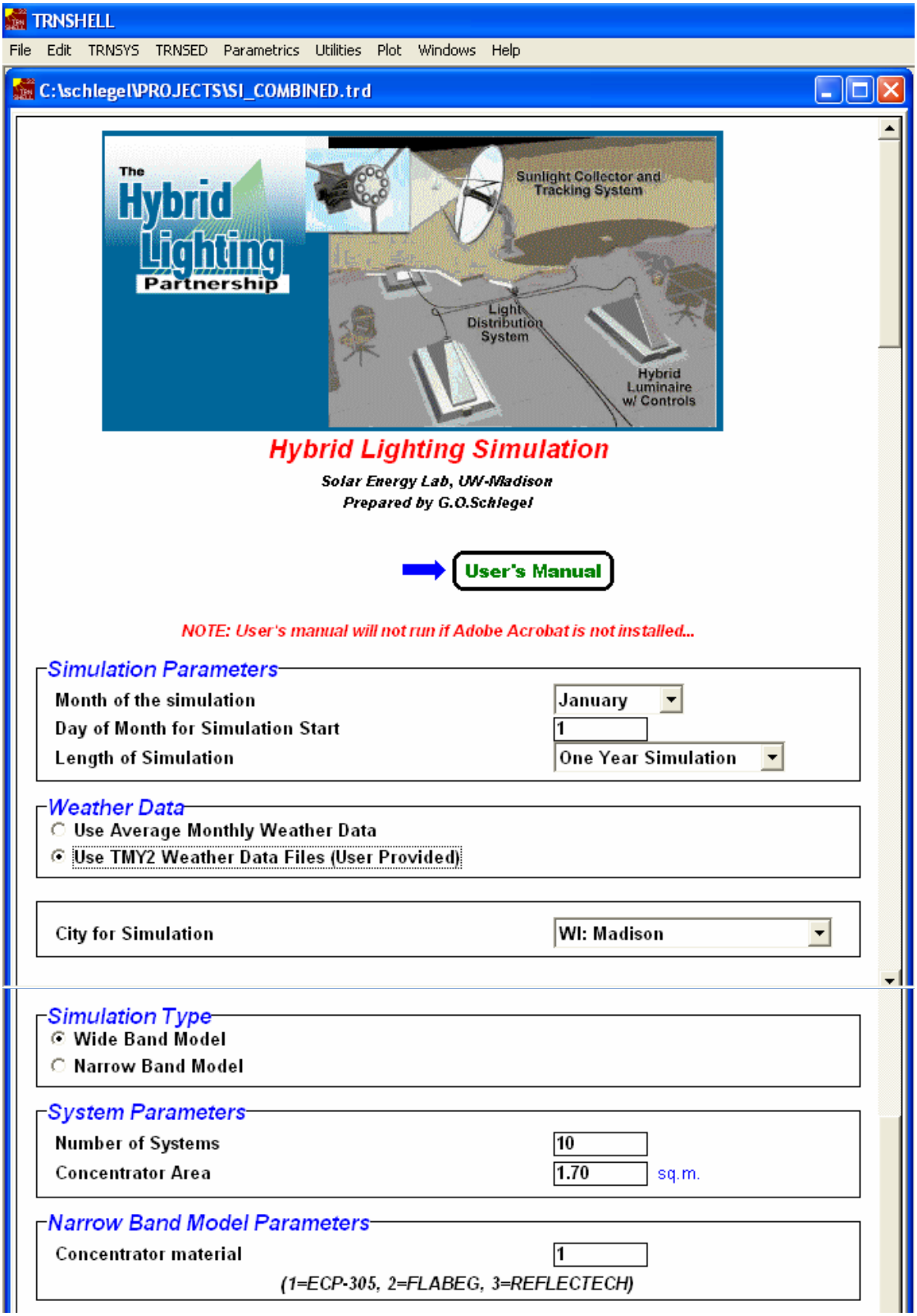

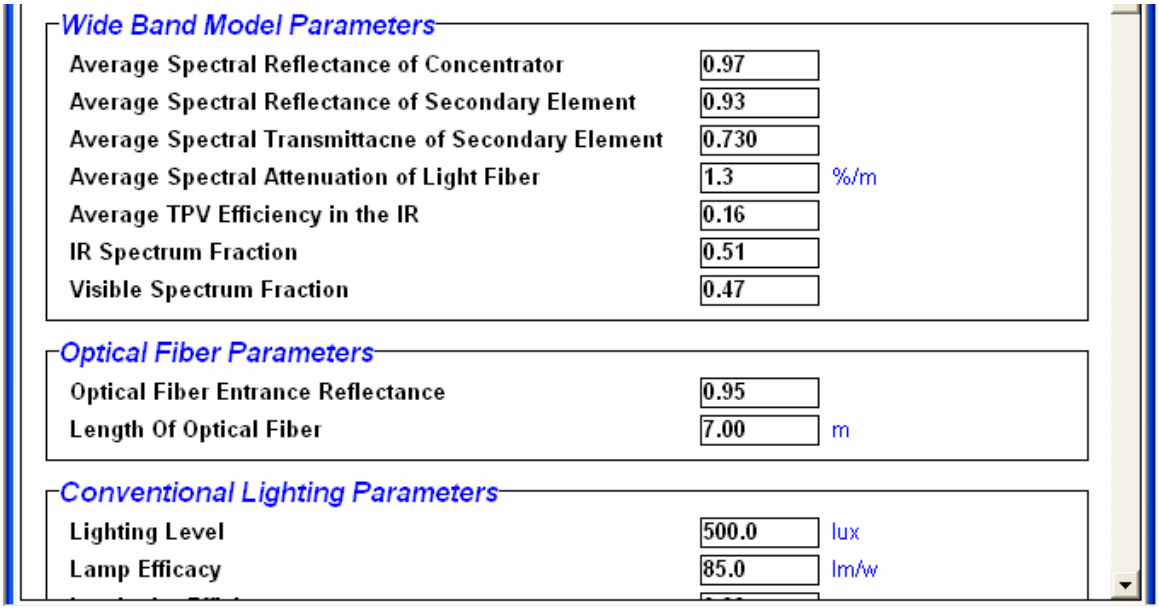
Wide Band Model Parameters
Average Spectral Reflectance of Concentrator 0.97
Average Spectral Reflectance of Secondary Element 0.93
Average Spectral Transmittacne of Secondary Element 0.730
Average Spectral Attenuation of Light Fiber 1.3 %/m
Average TPV Efficiency in the IR 0.16
IR Spectrum Fraction 0.51
Visible Spectrum Fraction 0.47
Optical Fiber Parameters
Optical Fiber Entrance Reflectance 0.95
Length Of Optical Fiber 7.00 m
Conventional Lighting Parameters
Lighting Level 500.0 lux
Lamp Efficacy 85.0 lm/w

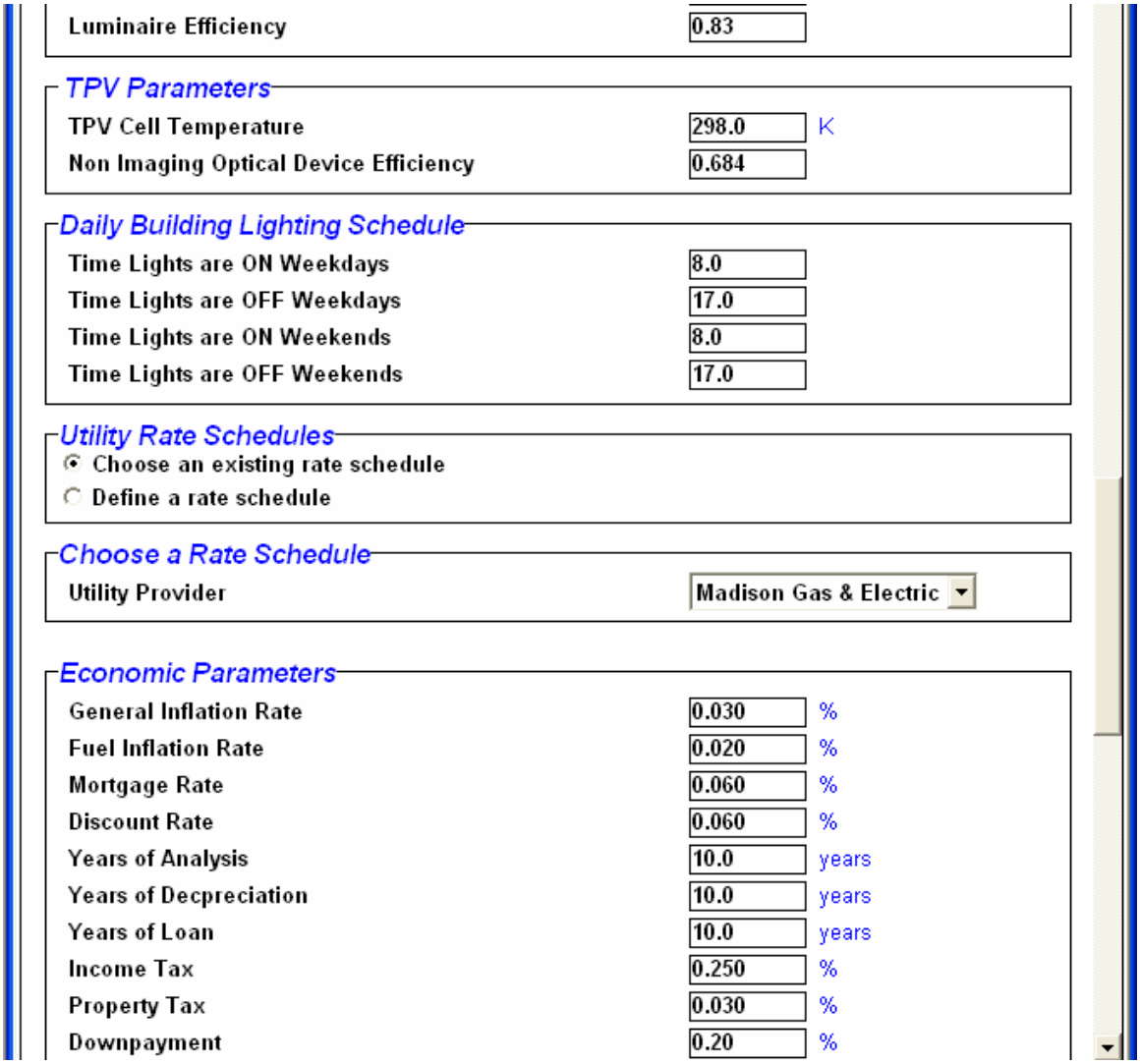
Luminaire Efficiency 0.83
TPV Parameters
TPV Cell Temperature 298.0 K
Non Imaging Optical Device Efficiency 0.684
Daily Building Lighting Schedule
Time Lights are ON Weekdays 8.0
Time Lights are OFF Weekdays 17.0
Time Lights are ON Weekends 8.0
Time Lights are OFF Weekends 17.0
Utility Rate Schedules
Choose an existing rate schedule
Define a rate schedule
Choose a Rate Schedule
Utility Provider Madison Gas & Electric
Economic Parameters
General Inflation Rate 0.030 %
Fuel Inflation Rate 0.020 %
Mortgage Rate 0.060 %
Discount Rate 0.060 %
Years of Analysis 10.0 years
Years of Decpreciation 10.0 years
Years of Loan 10.0 years
Income Tax 0.250 %
Property Tax 0.030 %
Downpayment 0.20 %

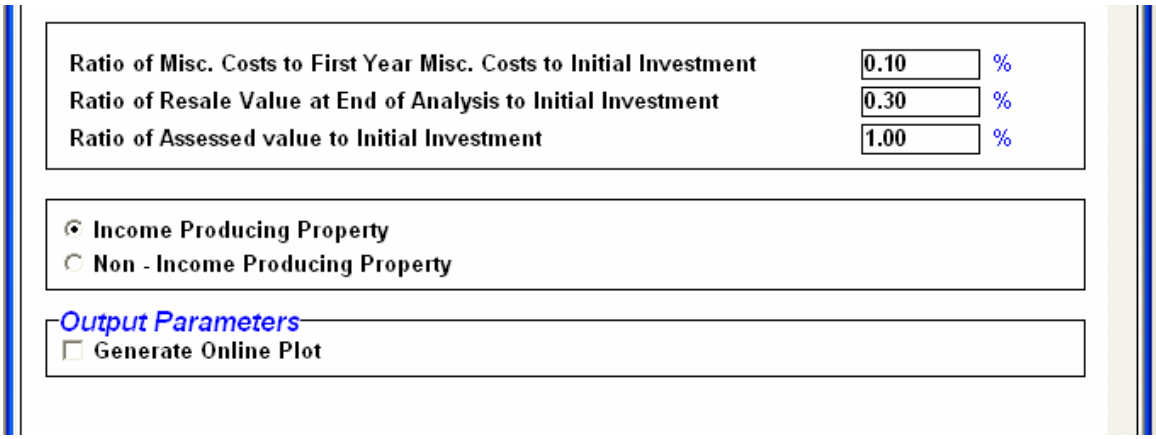

A user interface has been created using TRNSED. The TRNSED interface allows the user to modify different input and output parameters of the system to suit their particular needs without having to interface with the underlying FORTRAN code. Once the system parameters have been specified, the simulation is run by using the calculate command under the TRNSYS menu or pressing F8.

Parametric Table

The TRNSED interface has the ability to run a number of simulations simultaneously using the parametric table function. Under the parametric menu in TRNSED, create a new table by specifying the number of runs and the desired variables to change during the simulation sequence. Once the table is created the values of the variables need to be set which can be accomplished by typing directly in the table or accessing the modify table function in the parameterics menu. The simulation sequence is executed by selecting run table from the TRNSYS menu with the parametric table active. If the table is not active or hidden the run table option will not be available.

Simulation Parameters

Under the simulation parameters heading the length and starting day of the simulation can be modified. Variables included under simulations parameters include the month of the simulation, day of the month for simulation start, and length of the simulation. Both the day and month variables determine when the simulation will start while the length variable determines the length of the simulation after the start date.

Weather Data

The TRNSED interface allows the user to specify to use average monthly weather data or TMY2 weather data. If average monthly weather data are chosen the user must specify the desired city and average annual turbidity level. The cities are organized alphabetically and include 329 locations in both the United States and Canada. The TMY2 weather data selection also requires that the location be chosen from a similar list of locations. TMY2 data for Honolulu, HI, Seattle, WA, Reno, NV, Tucson, AZ, Madison, WI, and Atlanta, GA is included with the simulation software.

Additional TMY2 data files can be obtained for free from the National Renewable Energy Laboratory's website. The TMY2 files must be installed in the root directory of the TRNSED program in order for the simulation to operate. In addition to be installed in the root directory, file 'CitiesK1.dat' must be modified. The information in the file includes (from left to right): city list number, pull down menu text, latitude, longituide, shift in solar time, and tmy2 data file name. In addition to adding the necessary data, the first number in the file must be changed to reflect the number of cities listed in the entire data file.

Simulation Type

The TRSNED interface allows the user to determine if the simulation will use the narrow band model or the wide band model. The wide band model uses average spectral component data that the user specifies, while the narrow band model reads in the manufacturer's spectral data for each component.

Narrow Band Parameters

If the narrow band model is chosen, then the user must specify which concentrator material to be used in the simulation.

Wide Band Parameters

The wide band model requires that all of the average spectral component properties be specified including the concentrator reflectance, secondary element reflectance and transmittance, attenuation of the light fiber, TPV efficiency, and the fraction of the solar spectral

power distribution in the near IR spectrum(780-2500 nm) and visible spectrum (380-780 nm). Default values are based on manufacturer's spectral data.

System Parameters

Under the system parameters section the user can specify the number of modules per hybrid lighting system as well as the active collector area (the amount of concentrator area that is able to collect sunlight)

Optical Fiber Parameters

Two variables which describe the optical fibers include the entrance reflectance and the optical fiber length. The entrance reflectance allows the user to include losses which may occur due to alignment problems or additional filtering which may need to be added to the beginning of the fiber. The length refers to the average length of all of the fibers which are attached to the collection unit not the total length of all of the fiber.

Conventional Lighting Parameters

The conventional lighting parameters describe the necessary lighting characteristics in the building including the lighting level, lamp efficacy, and average hybrid lighting luminaire efficiency. Spectral data describing the luminaires was not available so all simulation use this average value.

Under the conventional lighting parameters subsection the user can also define which control strategy will be utilized in the simulation. The control system can be chosen from four options: 0 – ideal controls (no losses), 1 – dimmable ballasts which allow for under-illumination lighting levels, 2 – staging controls with constant output bulbs and ballasts, 3 - dimmable ballasts which allow for over-illumination lighting levels, 4 – dimmable ballast system with staging. If options 2 or 4 are chosen, then the number of stages that the lighting system will be divided into must be specified.

TPV Parameters

The non-imaging optical device efficiency can be specified here.

Daily Building Lighting Schedule

The lighting schedule allows the user to define when the lights will operate during the week and weekends. The lighting schedule for holidays is included in the weekend lighting schedule.

Electricity Rate Schedule

The electricity rate schedule allows the user to create their own rate schedule or choose an existing rate schedule from a list which includes: PG&E, MG&E, Southern Electric, Sierra Pacific Electric, Seattle City Light, Tucson Electric, and Hawaiian Electric. To define a rate schedule on-peak and off peak seasonal rates and times must be specified.

Natural Gas Rate Schedule

Natural gas rates are based on the annual average cost of natural gas by state (http://www.eia.doe.gov/emeu/states /_states.html). The annual average costs are inlcuded in the pre-defined rate schedules listed above but must be specified if using a user-defined rate schedule.

Economic Parameters

The economic parameters include all of the necessary variables to calculate the P_1, P_2 economic indicators. Below is a list of the variables followed by a brief description of each:

Years of Analysis – Length of the economic analysis in years.
Discount Rate – Rate of best alternative investment.
General Inflation Rate – The current estimated rate of inflation.
Initial Down Payment – Percentage of the total capital cost of the equipment paid at the time zero.
Mortgage Rate – Interest rate of the loan used to finance the capital cost of the equipment.
Years of Loan – Length of loan in years.
Years of Depreciation – Number of years that the equipment can be depreciated. The years of depreciation are typically the same as the length of the loan.
Incoming Producing – If the equipment is used on an income producing business.
Non-Income Producing – If the equipment is on a business that does not produce income or a non profit organization.
Income Tax Rate – Average income rate of the business.
Ratio of First Year Miscellaneous Costs to Initial Cost – The first year miscellaneous costs can include but are not limited to parasitic energy

costs, insurance, and maintenance. The miscellaneous costs are expressed as a ratio to the initial capital cost of the equipment.

Ratio of Resale Value at the End of the Analysis to Initial Cost – Estimated value of the equipment at the end of the analysis period which is expressed as a ratio to the initial capital cost of the equipment.

Ratio of Initial Valuation to Initial Cost – The ratio of the assessed value of the equipment at time zero to the initial capital cost. The value is typically 1 unless the equipment is immediately devalued for a particular reason.

Property Tax Rate – Average property tax rate of the location.

Output Parameters

The output parameters allow the user to specify whether they want to generate an online plot. The output from the on-line plotter includes the integrated lighting load with and without the hybrid lighting system as well as the electricity generated by the TPV integrated over the simulation length.

Parametric Table Output

If a parametric table is used the output integrated over the simulation length is appended to any existing data in the file TABLERES.OUT. The file is located in the TNRSYS15 directory. The outputs included in the data file in the following order are:

Lighting Load with Hybrid Lighting System [kWh]
Baseline Lighting Load [kWh]
Cooling Load with Hybrid Lighting System [kJ/hr]
Baseline Cooling Load [kJ/hr]
Heating Load with Hybrid Lighting System [kJ/hr]
Heating Load [kJ/hr]
Baseline Lighting Cost [$]
Lighting Cost with Hybrid Lighting System [$]
Baseline Cooling Cost [$]
Cooling Cost with Hybrid Lighting System [$]
Baseline Heating Cost [$]
Heating Cost with Hybrid Lighting System [$]
Revenue From TPV [$]
P_1
P_2
Annual Energy Savings [$/system]
Break Even Capital Cost [$/system]

Hourly Data Files

Each simulation run generates two files which contain values output at hourly intervals. The two output files are, HLsim.out which contains instantaneous hourly information and HLsim_int.out which contains data integrated over the simulation length. The variables included in the files in the following order are:

HLsim.out
Ambient Temperature [C]
Temperature of Zone 1 [C]
Temperature of Zone2 [C]
Beam Normal Radiation [kJ/hr-m^2]
Baseline Heating Load [kJ/hr]
Heating Load with Hybrid Lighting System [kJ/hr]
Baseline Cooling Load [kJ/hr]
Cooling Load with Hybrid Lighting System [kJ/hr]
Baseline Lighting Load [kWh]
Lighting Load with Hybrid Lighting System [kWh]
Light Output from Hybrid Lighting System [Lumens]
Output from TPV [Wh]

HLsim_INT.out
Lighting Load with Hybrid Lighting System [kWh]
Baseline Lighting Load [kWh]
Cooling Load with Hybrid Lighting System [kWh]
Baseline Cooling Load [kWh]
Heating Load with Hybrid Lighting System [kWh]
Baseline Heating Load [kWh]
Cost of Baseline Lighting Load [$]
Cost of Lighting Load with Hybrid Lighting System [$]
Cost of Baseline Cooling Load [$]
Cost of Cooling Load with Hybrid Lighting System [$]
Cost of Baseline Heating Load [$]
Cost of Heating Load with Hybrid Lighting System [$]
Revenue Produced by the TPV array [$]

Appendix D – Type 292 Hybrid Lighting Model Source Code

```
      SUBROUTINE TYPE292(TIME,XIN,OUT,T,DTDT,PAR,INFO,ICNTRL,*)

C*************************************************************************
C     HYBRID LIGHTING - SOLAR IRRADIANCE MODEL
      *
C
                        *
C     THIS COMPONENT GENERATES THE SPECTRAL SOLAR IRADIANCE DATA      *
C     BASED ON SMARTS2 OUTPUT FOR AIR MASS 2.25, BETA=.1, BETA=0.2    *
C     AND EXTRATERRESTRIAL SOLAR IRRADIANCE.  THE INTEGRATED            *
C     VALUE OF THE SMARTS2 DATA IS SCALED SO THE MAGNITUDE              *
C     OF THE BEAM COMPONENT MATCHES THE BEAM COMPONENT IN TRNSYS         *
C
                        *
C     THE COMPONENT ALSO CALCULATES THE SPECTRAL LOSSES ASSOCIATED      *
C     WITH THE HYBRID LIGHTING SYSTEM INCLUDING REFLECATNCE LOSSES      *
C     FROM THE PRIMARY MIRROR, REFLECTANCE AND TRANSMITTANCE LOSSES     *
C     FROM THE COLD MIRROR, TPV EFFICIENCY LOSSES, AND LIGHT FIBER      *
C     ATTENUATION LOSSES.  LUMINAIRE LOSSES ARE NOT MODELED AS          *
C     SPECTRALLY DEPENDENT.  LOSSES DUE TO SUPPLEMENTAL FILTERS WILL    *
C     BE INLCUDED AS THE INFORMATION IS OBTAINED
      *
C
                        *
C     ALL SPECTRAL DATA IS PREPROCESSED AND READ INTO FORTRAN IN 5      *
C     NANOMETER INCREMENTS FROM 280-2500 NM.  THE VISIBLE SPECTRUM      *
C     IS ASSUMED TO BE 380-780 NM, THE IR SPECTRUM IS 780-2500 NM,      *
C     AND THE UV SPECTRUM IS 280-380 NM.
      *
C*************************************************************************

C     DECLARATION OF VARIABLES
      IMPLICIT NONE
      REAL PAR,TIME,T,DTDT,IUNIT,ET,AMONE,ZETA,ZENARAD,PI,RHOECP,
     &ZETAB,AMONEB,RHORFT,RHOFBG,RHO,RHOCM,GRTWO,GTTWO,GTPV,G,GRONE,
     &GVIS,ETA_QE,ATTEN,PHOTOPIC,LIGHT,ELEC,CAREA,ALAMBDA,GBEAM,THETA,
     &RB,BEAMRATIO,IDI,HEXTRA,E,PHOTONI,GBEAMA,F,GEFF

      DOUBLE PRECISION XIN,OUT,ETA,LAT,AIRMASS,NTOTAL,LENGTH,KAPPA,
     &KAPPAB,ZENA,TURB,KAPPA2,TFD,TURBRATIO,FIBERLENGTH,KT,HHOR,HBEAM,
     &TPVAREA,VMAX,HOZ,SCALEFAC,HDIFF,TBEAM,IDICH,RBCH,SYSEFF,LIGHTEFF
     &,BEAMA,KAPPATAU,TAULAMBDA,RHO1,RHO2,TUBEREFL,VISPECTR,IRSPECTR,
     &FILTERIR,NUMBEROF,ATTENAVG,LUMEFFIC,TPVEFFIC,LIGHTLEV,BLDGAREA,
     &LAMPEFF,MODELFLAG,TBAR,IFLAG,N_D,DOWN,M_S,VAL,PRTAX,R_V,N_E,N_L,
     &INF,FUELINF,DIS,M,SEAREA,LFLGIN,SHEAT,SCOOL,LATENT,BHEAT,BCOOL,NLF
     &,BLATENT,CBLIGHT,CHLIGHT,BCCOST,HCCOST,BHCOST,HHCOST,TPVREV,VOC,
     &ISC,IMAX,VMAXARRAY,MUISC,MUVOC,TCREF,TC,EPSILON,NS,GT,GTREF,V,LF,
     &A,IL,IO,I,RS,P,ILREF,AREF,IOREF,RSREF,TAU,KAPPATAUAVG,LOADLNH,NAP,
     &LOADLH,XTRALGHT,LSCALE,LFLGOUT,SUNLIGHT,XTRAHEAT,LLNH,LLH,OPTEFF,
     &LATENTCOOL,BLATENTHEAT,BLATENTCOOL,LATENTHEAT,HEAT,COOL,BASECOOL,
     &BASEHEAT,AES,BECC,P1,PWF,NMIN,NMIN1,A1,A2,A3,A4,A5,A6,P2,ZERO,
     &NEWEFF,MULT,Z,SLAREA,SLTAU,NLEFF,ETAPV,PVAREA
```

```
      INTEGER INFO,CMODE,NP,NI,NO,ND,JJ,NRS,JH,JI,LUD,LUW,LUK,ICNTRL
     &,IFORM,LUR,REF,JK,RTOTAL,MIRROR,CLDMIR,CMTOTAL,LAMBDA
     &,VLAMBDA,ATTEN3M,ATTENTOTAL,VLTOTAL,TPV,TPVTOTAL,CONTROL

      LOGICAL FLAG
      PARAMETER (NI=21,NP=43,NO=19,ND=0)
      CHARACTER*3 YCHECK(NI),OCHECK(NO),CARD
      CHARACTER FILNAM*40,COMP*4
      DIMENSION PAR(NP),XIN(NI),OUT(NO),INFO(15),ET(445),KAPPAB(445),
     &G(445),KAPPA(445),AMONE(445),RHOECP(445),GRONE(445),AMONEB(445),
     &KAPPA2(445),RHORFT(445),RHOFBG(445),RHO(445),RHOCM(445),GRTWO(445)
     &,GTTWO(445),LAMBDA(445),GTPV(445),GVIS(445),ETA_QE(445),ATTEN(445)
     &,PHOTOPIC(445),ALAMBDA(445),GBEAM(445),E(445),PHOTONI(445),
     &GBEAMA(445),KAPPATAU(445),TAULAMBDA(445),F(445),GEFF(445)
      COMMON /LUNITS/ LUR,LUW,IFORM,LUK
      COMMON /SYSTMX/ COMP
      DATA IUNIT/0/PI/3.1415926/
C-----------------------------------------------------------------------

C           IF ITS THE FIRST CALL TO THIS UNIT, DO SOME BOOKKEEPING
                 IF (INFO(7).GE.0) GO TO 100

C           FIRST CALL OF SIMULATION, CALL THE TYPECK SUBROUTINE TO CHECK
THAT THE
C           USER HAS PROVIDED THE CORRECT NUMBER OF INPUTS,PARAMETERS, AND
DERIVS
                 INFO(6)=NO
                 INFO(9)=1
                 CALL TYPECK(1,INFO,NI,NP,ND)

C           GET THE VALUES OF THE PARAMETERS FOR THIS COMPONENT
                 LAT=PAR(1)
                 LUD=PAR(2)
                 REF=PAR(3)
                 MIRROR=PAR(4)
                 CLDMIR=PAR(5)
                 VLAMBDA=PAR(6)
                 ATTEN3M=PAR(7)
                 FIBERLENGTH=PAR(8)
                 TPV=PAR(9)
               CAREA=PAR(10)
                 RHO1=PAR(11)
                 RHO2=PAR(12)
                 TUBEREFL=PAR(13)
                 VISPECTR=PAR(14)
                 IRSPECTR=PAR(15)
                 FILTERIR=PAR(16)
                 NUMBEROF=PAR(17)
                 ATTENAVG=PAR(18)
                 LUMEFFIC=PAR(19)
                 TPVEFFIC=PAR(20)
                 LIGHTLEV=PAR(21)
                 BLDGAREA=PAR(22)
                 LAMPEFF=PAR(23)
                 MODELFLAG=PAR(24)
                 TBAR=PAR(25)
                 IFLAG=PAR(26)
```

```
                  N_D=PAR(27)
                  DOWN=PAR(28)
                  M_S=PAR(29)
                  VAL=PAR(30)
                  PRTAX=PAR(31)
                  R_V=PAR(32)
                  N_E=PAR(33)
                  N_L=PAR(34)
                  INF=PAR(35)
                  FUELINF=PAR(36)
                  DIS=PAR(37)
                  M=PAR(38)
                  OPTEFF=PAR(39)
                  CONTROL=PAR(40)
                  MULT=PAR(41)
                  SLAREA=PAR(42)
                  SLTAU=PAR(43)

C     SET DUMMY ECONOMIC PARAMETER OUTPUTS
      P1=0
      P2=0
      AES=0
      BECC=0

C     PROTECT AGAINST WEIRD TYPE 56 EFFECTS IF NUMBEROF=0
      IF (NUMBEROF.EQ.0.00) THEN
            NUMBEROF=0.0001
      ENDIF

C     CHECK TO SEE WHICH MODEL IS BEING RUN AND DIRECT TRAFFIC ACCORDINGLY
      IF (MODELFLAG.GT.0)THEN
            GOTO 100
            ELSE
            GOTO 50
      ENDIF


C**********************************************************************
C    OPEN DATA FILE
                  *
C**********************************************************************


50    IF (COMP .EQ. 'MICR') THEN
C       CHECK TO SEE IF FILE IS ALREADY OPENED.  IF NOT, GET NAME AND OPEN
         INQUIRE(UNIT=LUD,OPENED=FLAG)
         IF (.NOT. FLAG) THEN
           WRITE(LUW,221) INFO(1), INFO(2)
221        FORMAT(//2X,'**** UNIT ',I3,' TYPE ',I3,' SOLAR IRRADIANCE MO
     &       DEL'/4X,'ENTER FILE NAME FOR SOLAR IRRADIANCE DATA.')
           READ(LUK,222,ERR=223) FILNAM
222        FORMAT(A40)
           OPEN(LUD,FILE=FILNAM,STATUS='OLD',ERR=223)
           GO TO 25
223        WRITE(LUW,224) 143,INFO(1),INFO(2)
224        FORMAT(//,1X,'***** ERROR *****',8X,'TRNSYS ERROR # ',I3,/1X,
     .     'UNIT ',I3,' TYPE ',I3,' WEATHER GENERATOR',/1X,
```

```
     .     'ERROR READING INPUT WEATHER FILE FOR TYPE 54 SUBROUTINE')
           CALL MYSTOP(143)
           RETURN
25         CONTINUE
         ENDIF
       ELSE
         INQUIRE(UNIT=LUD,EXIST=FLAG)
         IF (.NOT. FLAG) THEN
           OPEN(LUD,STATUS='OLD')
         ENDIF
       END IF
      REWIND LUD

C     READ IRRADIANCE DATA
      READ(LUD,*) NTOTAL
C                 READ(LUD,*,END=520,ERR=520) NTOTAL
C                 NRS=NTOTAL-1
      DO 70 JJ=1,NTOTAL
      READ(LUD,*) LAMBDA(JJ),ET(JJ),AMONE(JJ),AMONEB(JJ)
C                 READ(LUD,*,END=520,ERR=520) ET,AM

C     CALCULATE ARRAYS OF DECAY COEFFICIENTS
C     AMONEB IS THE TOTAL HORIZONTAL IRRADIANCE AT AM=2.25, BETA=0.2
C     AMONE IS THE TOTAL HORIZONTAL IRRADIANCE AT AM=2.25, BETA=0.1
      LENGTH=2.25
      ZETA=AMONE(JJ)/ET(JJ)
      ZETAB=AMONEB(JJ)/ET(JJ)
      IF (ZETA.GT.0) THEN
            KAPPA(JJ)=(-1/LENGTH)*LOG(ZETA)
      ELSE
            KAPPA(JJ)=5
      ENDIF

      IF (ZETAB.GT.0) THEN
            KAPPAB(JJ)=(-1/LENGTH)*LOG(ZETAB)
            KAPPA2(JJ)=KAPPAB(JJ)-KAPPA(JJ)
      ELSE
            KAPPA2(JJ)=0
      ENDIF

70    CONTINUE
      CLOSE(UNIT=LUD)

C     READ PRIMARY MIRROR REFLECTANCE DATA
      READ(REF,*) RTOTAL
      DO 80 JK=1,RTOTAL
            READ(REF,*) RHOECP(JK),RHORFT(JK), RHOFBG(JK)

      IF (MIRROR.NE.1) THEN
            IF (MIRROR.NE.2) THEN
                  RHO(JK)=RHOFBG(JK)
            ELSE
                  RHO(JK)=RHORFT(JK)
            ENDIF
      ELSE
            RHO(JK)=RHOECP(JK)
      ENDIF
```

```
80    CONTINUE

C     READ COLDMIRROR REFLECTANCE DATA (0-100 %)
      READ(CLDMIR,*) CMTOTAL
      DO 85 JK=1,CMTOTAL
            READ(CLDMIR,*) RHOCM(JK)
85    CONTINUE

C     READ VISIBILITY CURVE DATA, V-LAMBDA (0-1)
      READ(VLAMBDA,*) VLTOTAL
      DO 86 JK=1,VLTOTAL
            READ(VLAMBDA,*) PHOTOPIC(JK)
86    CONTINUE

C     READ FIBER ATTENUATION DATA, (0-100 %/FT)
      READ(ATTEN3M,*) ATTENTOTAL
      DO 87 JK=1,ATTENTOTAL
            READ(ATTEN3M,*) ATTEN(JK)
            IF (ATTEN(JK).GT.99.99) THEN
                  TAULAMBDA(JK)=0
            ELSE
                  KAPPATAU(JK)=-1.0*LOG(1.0-(ATTEN(JK)/100))
                  TAULAMBDA(JK)=EXP(-1.0*KAPPATAU(JK)*FIBERLENGTH*3.28084)
            ENDIF
87    CONTINUE

C     READ THERMAL PHOTOVOLAIC CELL QUANTUM EFFICIENCY DATA, (0-1)
      READ(TPV,*) TPVTOTAL
      DO 88 JK=1,TPVTOTAL
            READ(TPV,*) ETA_QE(JK)
88    CONTINUE
                        RETURN 1

C           END OF THE FIRST ITERATION BOOKKEEPING

C     ****************************************************************
C     *
                         *
C     *                                     MAIN PROGRAM
                   *
C     *
                         *
C     ****************************************************************

100    CONTINUE

C     GET THE VALUES OF THE INPUTS TO THIS COMPONENT
                  ZENA=XIN(1)
                  HEXTRA=XIN(2)
                  HHOR=XIN(3)
                  TURB=XIN(4)

C     CHEATER INPUTS
                  HDIFF=XIN(5)
                  HBEAM=XIN(6)
                  TBEAM=XIN(7)
```

```
C     INPUTS FROM THE TYPE FORMERLY KNOWN AS 291
                  LFLGIN=XIN(8)
                  SHEAT=XIN(9)
                  SCOOL=XIN(10)
                  LATENT=XIN(11)
                  BHEAT=XIN(12)
                  BCOOL=XIN(13)
                  BLATENT=XIN(14)

C     COSTING INPUTS - SHOULD ONLY BE READ IN ONCE AT END OF SIMULATION
                  CBLIGHT=XIN(15)
                  CHLIGHT=XIN(16)
                  BCCOST=XIN(17)
                  HCCOST=XIN(18)
                  BHCOST=XIN(19)
                  HHCOST=XIN(20)
                  TPVREV=XIN(21)

C     IF ITS THE LAST CALL CALCULATE THE ECONOMIC PARAMETERS
      IF (INFO(8).EQ.-1) THEN
            GOTO 700
      ENDIF
C     CHECK TO SEE WHICH MODEL IS BEING RUN AND DIRECT TRAFFIC ACCORDINGLY
      IF (MODELFLAG.EQ.1)THEN
            NLEFF=200
            GOTO 500
      ENDIF
      IF (MODELFLAG.EQ.2) THEN
            NLEFF=100
            GOTO 550
      ENDIF
      NLEFF=200


C     ****************************************************************
C     *
                        *
C     *                                       NARROW BAND MODEL
             *
C     *
                        *
C     ****************************************************************

C     RESET THE INTEGRATION VARIABLES
      LIGHT=0
      LIGHTEFF=0
      SYSEFF=0
      ELEC=0
      BEAMA=0
      HOZ=0
C     TURBIDITY RATIO DEFINED AS
C     (ACTUAL TURBIDTY-TURBIDITY FIT DIFF)/TURB FIT DIFF
      TFD=0.1
      TURBRATIO=(TURB-TFD)/TFD
C     CALCULATE VALUE OF AIR MASS
      IF (ZENA.GT.89) THEN
```

```
            AIRMASS = 0
C     IRRADIANCE CALCULATION, INITIALIZE ARRAYS
      DO 90 JI=1,NTOTAL
            G(JI)=0
            GEFF(JI)=0
            GBEAM(JI)=0
            GBEAMA(JI)=0
            GRONE(JI)=0
            GRTWO(JI)=0
            GTTWO(JI)=0
            GVIS(JI)=0
90    CONTINUE
            ELSE
            ZENARAD=ZENA*(PI/180)
            AIRMASS=1/COS(ZENARAD)
C     Using Erbs et al, from Solar Eng of Thermal Processes (2.10.1)
            KT=HHOR/HEXTRA
            IF    (KT.GT.0.80) THEN
                  IDI=0.165
                  ELSE
                        IF (KT.GT.0.39) THEN
                        IDI=0.9511-(0.1604*KT)+(4.388*(KT**2))-
(16.638*(KT**3)
     &                  )+(12.336*(KT**4))
                              ELSE
                              IDI=1.0-(0.09*KT)
                        ENDIF
            ENDIF
C     RATIO OF BEAM RADIATION ON A TILTED SURFACE TO A HORIZONTAL SURFACE
C     ASSUME THE CONCENTRATING COLLECTOR TRACKS PERFECTLY (THETA=0).
C     EQUATION 1.8.1 SOLAR ENGINEERING OF THERMAL PROCESSES
C     LIMITED RB TO AVOID ARTIFICIALLY LARGE IRRADIANCES IN THE MORNING AND
C     EVENING
            RB=1/COS(ZENARAD)
            IDICH=HDIFF/HHOR
            RBCH=TBEAM/MAX(0.1,HBEAM)
C     TOTAL HORIZONTAL IRRADIANCE CALCULATION, G IS W/M2-NM,
C     GBEAM IS IN W/M2-NM
            DO 91 JI=1,NTOTAL
                  G(JI)=ET(JI)*EXP(-1*(KAPPA(JI)+(KAPPA2(JI)*TURBRATIO))*
     &            AIRMASS)
C     ONLY THE BEAM NORMAL RADIATION CAN BE USED
                  GBEAM(JI)=RBCH*(G(JI)-(G(JI)*IDICH))
C     CALCULATE INTEGRATED VALUES OF EXTRATERRETRIAL, TOTAL HORIZONTAL,
C     AND BEAM RADIATION, ALL VALUES IN kJ/HR-M2
                  HOZ=HOZ+G(JI)*5*3.6
91          CONTINUE
C     WHEN THE INTEGRATED RADIATION BOTH BEAM AND TOTAL HORIZONTAL
C     IS DIFFERENT THAN THE RESULTS FROM THE RADIATION PROCESSOR
C     SCALEFAC SCALES THE SMARTS2 INTEGRATED BEAM RESULTS TO MATCH
C     THE LEVELS OF THE RADIATION PROCESSOR.
            IF (HHOR.GT.HOZ) THEN
                  SCALEFAC=HHOR/(HOZ)
                  ELSE
                  SCALEFAC=(HOZ)/HHOR
            ENDIF
            DO 92 JK=1,NTOTAL
```

```
C     SCALE BEAM RADIATION, AND INTEGRATE TO COMPARE WITH TRNSYS OUTPUT
                  GBEAMA(JK)=GBEAM(JK)*SCALEFAC
                  BEAMA=BEAMA+GBEAMA(JK)*5
C     PRIMARY MIRROR REFLECTANCE LOSSES
                  GRONE(JK)=GBEAMA(JK)*RHO(JK)*.01
C     COLD MIRROR LOSSES R - REFLECTANCE, T - TRANSMITTANCE,IGNORING
ABSORPTION
                  GRTWO(JK)=GRONE(JK)*RHOCM(JK)*.01
                  GTTWO(JK)=GRONE(JK)*(1-(RHOCM(JK)*.01))
C     EFFICACY CALCULATION
                  IF (LAMBDA(JK).LT.380) THEN
                        GVIS(JK)=0
                        GEFF(JK)=0
                        ELSE
                        IF (LAMBDA(JK).GT.780) THEN
                              GVIS(JK)=0
                              GEFF(JK)=0
                              ELSE
                              GEFF(JK)=GRTWO(JK)*TAULAMBDA(JK)

      GVIS(JK)=GRTWO(JK)*TAULAMBDA(JK)*PHOTOPIC(JK)*683
                        ENDIF
                  ENDIF
92          CONTINUE
      ENDIF

C
C     ****************************************************************
C     *
                        *
C     *           THERMAL PHOTOVOLTAIC LIGHT CURRENT CALCULATION
*
C     *
                        *
C     ****************************************************************
C
C     THE ARRAY USED IN THE HYBRID LIGHTING SYSTEM IS MADE OF GASB CELLS.
C     THE FIRST STEP OF THE CALCULATION IS TO CONVERT THE INCCOMING
C     IRRADIANCE INTO PHOTONS, NEXT APPLY THE QE, CALCULATE THE AMOUNT OF
C     RESULTING FREE ELECTRONS, AND CALCULATE THE ASSOCIATED CURRENT.
C     1240 IS A CONSTANT WHICH FACTORS INTO ACCOUNT PLANCK'S CONSTANT(h),
C     THE CHARGE OF AN ELECTRON(e), AND THE SPEED OF LIGHT IN A VACUUM(c).
C     0.01 IS INCLUDED TO REPRESENT ONE CELL OF THE 100 CELL ARRAY

      DO 93 JK=1,NTOTAL
      PHOTONI(JK)=(CAREA/1240)*(GTTWO(JK)*ETA_QE(JK)*LAMBDA(JK)*0.01)
      ELEC=ELEC+PHOTONI(JK)*5
93    CONTINUE

C     ****************************************************************
C     *
                        *
C     *                                   I-V MODEL
                  *
C     *
                        *
C     ****************************************************************
```

```
      VOC=47.72
      IMAX=5.13
      VMAXARRAY=34.52
      MUISC=0.00031
      MUVOC=-0.001205
      TCREF=298
      TC=273+25
      EPSILON=0.382
      NS=100

C     NO REFERENCE IRRADIANCE WAS AVAILABLE FOR THE ARRAY, GUESS VALUE
C     OF 850 W/M2 WORKS WELL, (SEE FRAAS,L. ET AL., PP.3, 2002.)
      GT=BEAMA
      GTREF=850

C     IRRADIANCE TO MATCH THE MEASURED SHORT CIRCUIT CURRENT.
      ISC=ELEC

C     RESET TPV ARRAY ELECTRICAL CURRENT GUESS VALUE
      I=5

C     PROTECTION AGAINST SMALL LIGHT CURRENT
      IF (ISC.LT.0.05) THEN
            P=0
            LIGHT=0
            GOTO 600
      ELSE

C     DUFFIE & BECKMAN, EQ 23.2.3.,23.2.11.,23.2.4.
C     "REFERENCE CONDITIONS"
      ILREF=ISC
      AREF=(MUVOC*TCREF-VOC+EPSILON*NS)/(((MUISC*TCREF)/ILREF)-3)
      IOREF=ILREF*exp(-VOC/AREF)

C     CELL TEMPERATURE CONDITIONS
C     DUFFIE & BECKMAN, EQ 23.2.6.,23.2.7.,23.2.8.,23.2.5
      A=(TC/TCREF)*AREF
      IL=(GT/GTREF)*(ILREF+MUISC*(TC-TCREF))
      IO=IOREF*((TC/TCREF)**3*exp(((EPSILON*NS)/AREF)*(1-(TCREF/TC))))
      RSREF=(AREF*LOG(1-MIN(0.9,IMAX/ILREF))-VMAXARRAY+VOC)/IMAX

C     ASSUME SERIES RESISTANCE TO BE INDEPENDENT OF TEMPERATURE
      RS=RSREF

C     ASSUME LOAD MATCHES MAX ARRAY VOLTAGE
      V=VMAXARRAY

C     DUFFIE & BECKMAN, EQ 23.2.1
C     NEGLECT LAST TERM OF EQUATION 23.2.1 DUE TO LARGE SHUNT RESISTANCE
C     BOTH VERSIONS OF EQUATIONS ARE THE SAME
C     V=A*LOG(MAX(0.01,(IL+IO-I)/IO))-I*RS
      I=IL-IO*(exp((V+I*RS)/A)-1)
C     LIMIT CURRENT TO POSTIIVE VALUES
      I=MAX(0.0,I)
C     THE COOLING FAN CONSUMES 5 WATTS OF POWER, OPTEFF IS THE OPTICAL
C     LOSSES ASSOCIATED WITH THE NON-IMAGING OPTICAL DEVICE
      P=((I*V)-5)*NUMBEROF*OPTEFF
```

```
C     INTEGRATE RESULTS OF VISIBLE ENERGY
C     LIGHT IS IN LUMENS/M2
      DO 94 JK=1,NTOTAL
      LIGHT=LIGHT+GVIS(JK)*5
      LIGHTEFF=LIGHTEFF+GEFF(JK)*5
94    CONTINUE
      LIGHT=LIGHT*NUMBEROF*CAREA*LUMEFFIC
      SYSEFF=(LIGHTEFF)/((TBEAM/3.6))
      ENDIF
      GOTO 600

C     ****************************************************************
C     *
                        *
C     *                                   WIDE BAND MODEL
                  *
C     *
                        *
C     ****************************************************************

500   KAPPATAUAVG=-1.0*LOG(1.0-(ATTENAVG/100))
      TAU=EXP(-1.0*KAPPATAUAVG*FIBERLENGTH)
C     200 IS THE APPROXIMATE EFFICACY OF FILTERED SOLAR RADIATION
      LIGHT=NUMBEROF*RHO1*RHO2*TUBEREFL*VISPECTR*(TBEAM/3.6)*CAREA*TAU*
     &LUMEFFIC*200
      P=NUMBEROF*RHO1*FILTERIR*(TBEAM/3.6)*IRSPECTR*CAREA*TPVEFFIC*
     &OPTEFF
      SYSEFF=RHO1*RHO2*TUBEREFL*TAU*LUMEFFIC
      GOTO 600

C     DAYLIGHTING COMPARISON; 100 IS APPROXIMATE EFFICACY OF UNFILTERED
C     SUNLIGHT, 0.65 IS THE WELL EFFICIENCY, 0.7 IS A FACTOR TO ACCOUNT
C     FOR DIRT ON THE SKYLIGHT.  SEE IESNA LIGHTING HANDBOOK, 2000.
550   LIGHT=NUMBEROF*(HHOR/3.6)*SLAREA*SLTAU*100*.65*.7
      GOTO 600

C     ****************************************************************
C     *
                        *
C     *                                   FORMERLY TYPE 291
             *
C     *
                        *
C     ****************************************************************

C     CALCULATE LOADS ASSOC WITH LIGHTING - LOADLNH IN LUMENS
600   IF (LFLGIN .LT. 1.0) THEN
            LOADLNH=0
            ELSE
            LOADLNH=((BLDGAREA)*LIGHTLEV)
      ENDIF

C     WILL HAVE TO ADD SOMETHING HERE TO IF HLS CAN BE TURNED OFF
C     CHECK TO SEE IF VAR LIGHT IS LARGER THAN NORMAL LOAD
      IF(LIGHT .GT. LOADLNH) THEN
            LOADLH=0
```

```
            XTRALGHT=LIGHT-LOADLNH
      ELSE
            LOADLH=LOADLNH-LIGHT
            XTRALGHT=0
      ENDIF

C     SCALE OF THERMAL LOAD ASSOCIATED WITH LIGHTING LOAD, BASED ON
C     ILLUMINATION LEVEL IN LUX, EFFICACY OF LAMP USED IN BLDG, AND A
C     BUILDING LIGHTING GAIN OF 10 W/M2.
      LSCALE=(LIGHTLEV/LAMPEFF)/10

C     NORMALIZED OUTPUT FOR TYPE 56 RECALCULATION OF HEATING/COOLINGLOADS
C     LFLGOUT IS SENT TO THE TYPE 56 BLDG MODEL WHICH HAS A THERMAL GAIN
C     DUE TO LIGHTING OF 10 W/M2 WHICH CANCELS OUT THE SEEMINGLY RANDOM
C      10 W/M2 IN THE DENOMINATOR OF LSCALE.
      IF (LOADLNH .GT. 0) THEN
            LF=(LOADLH/LOADLNH)
C           LFLGOUT=LSCALE*LF

C     SUNLIGHT IS SENT TO TYPE 56 TO CALCULATE FRACTION OF HEAT OF ORIGINAL
C     LIGHTING WHICH IS CONTAINED IN NATURAL LIGHT.  ASSUMED THE EFFICACY OF
C     FILTERED SUNLIGHT TO BE 200 LM/W.
C     THE GAIN IN THE TYPE 56 BLDG MODEL SHOULD BE SET UP WITH A
C     SCHEDULE OF 1 (ALWAYS ON), AND A SCALE OF 1*SUNLIGHT.
            SUNLIGHT=((1-(LOADLH/LOADLNH))*(LOADLNH/NLEFF))*3.6
      ELSE
            LF=0
C           LFLGOUT=1*LSCALE
            SUNLIGHT=0
      ENDIF

C     ON DAYS WHEN THERE IS TOO MUCH LIGHT THE THERMAL ENERGY OF THE
C     ADDTIONAL LIGHT IS ADDED TO THE BUILDING LOAD, UNITS OF KJ/HR.
C     THE GAIN IN THE TYPE 56 BLDG MODEL SHOULD BE SET UP WITH A
C     SCHEDULE OF 1 (ALWAYS ON), AND A SCALE OF 1*XTRAHEAT.
      XTRAHEAT=(XTRALGHT/NLEFF)*3.6

C     CONVERT LIGHTING LOADS FROM LUMEN-HRS TO KWH
      LLNH=(LOADLNH/LAMPEFF)/1000

C     DETERMINE CONTROL STARTEGY AND DIRECT TRAFFIC
      IF (CONTROL.EQ.0) THEN
            GOTO 800
            ELSE
                  IF (CONTROL.EQ.1) THEN
                        GOTO 900
                        ELSE
                              IF (CONTROL.EQ.2) THEN
                                    GOTO 1000
                                    ELSE
                                          IF (CONTROL.EQ.3) THEN
                                                GOTO 950
                                                ELSE
                                                      GOTO 1100
                                          ENDIF
                              ENDIF
                  ENDIF
```

```
      ENDIF


C     HYBRID LIGHTING LOAD WITHOUT DIMMABLE BALLASTS
800   LLH=(LOADLH/LAMPEFF)/1000
      LFLGOUT=LSCALE*LF
      GOTO 1200

C     HYBRID LIGHTING LOAD WITH DIMMABLE BALLASTS
C     BASED ON ELECTRONIC BALLASTS AND F32T8 LAMPS
C     BASICALLY THE LIGHTING EFFICACY DECREASES WHEN THE BULBS
C     ARE DIMMED
C     IF THE LIGHT FRACTION IS LESS THAN 0.20 THE BUILDING WILL
C     BE UNDER-ILLUMINATED IN THE SPIRIT OF CONSERVATION.
900   IF(LF.EQ.0.00) THEN
      LLH=0
      LFLGOUT=0
            ELSE
            IF (LF.LT.0.20) THEN
            LLH=0
            LFLGOUT=0
            ELSE
                  NAP=(((LF*100)+29.701847)/(1.81576002*71.43))
                  NEWEFF=MIN(LAMPEFF,(LAMPEFF*(LF/NAP)))
                  LLH=LOADLH/(NEWEFF*1000)
                  LFLGOUT=(LIGHTLEV/(NEWEFF*10))*LF
            ENDIF
      ENDIF
      GOTO 1200

C     IF THE LIGHT FRACTION IS LESS THAN 0.20 THE BUILDING WILL
C     BE OVER-ILLUMINATED IN THE SPIRIT OF WASTE.
950   IF(LF.EQ.0.00) THEN
      LLH=0
      LFLGOUT=0
            ELSE
            IF (LF.LT.0.20) THEN
            LLH=(LOADLNH*.20)/(44*1000)
            LFLGOUT=(LIGHTLEV/(44*10))*.2
            ELSE
                  NAP=(((LF*100)+29.701847)/(1.81576002*71.43))
                  NEWEFF=MIN(LAMPEFF,(LAMPEFF*(LF/NAP)))
                  LLH=LOADLH/(NEWEFF*1000)
                  LFLGOUT=(LIGHTLEV/(NEWEFF*10))*LF
            ENDIF
      ENDIF
      GOTO 1200

C     STAGING CONTROLS
1000  IF (LF.EQ.0) THEN
            LLH=0
            LFLGOUT=0
            ELSE
                  IF (LF.GT.(1-(1/MULT))) THEN
                        LLH=LLNH
                        LFLGOUT=LSCALE
                        ELSE
```

```
                        DO 1001 Z=2,MULT
                              IF (LF.GT.(1-(Z*(1/MULT)))) THEN
                                    LLH=(1-((Z-1)*(1/MULT)))*LLNH
                                    LFLGOUT=(1-(Z*(1/MULT)))*LSCALE
                                    GOTO 1002
                              END IF
1001                    CONTINUE

1002              ENDIF
      ENDIF
      GOTO 1200

C     STAGING CONTROLS WITH DIMMABLE BALLASTS

1100  IF (LF.EQ.0) THEN
            LLH=0
            LFLGOUT=0
            ELSE
                  IF (LF.GT.(1-(1/MULT))) THEN
                        NAP=(((LF*100)+29.701847)/(1.81576002*71.43))
                        NEWEFF=MIN(LAMPEFF,(LAMPEFF*(LF/NAP)))
                        LLH=LOADLH/(NEWEFF*1000)
                        LFLGOUT=(LIGHTLEV/(NEWEFF*10))*LF
                        ELSE
                              DO 1101 Z=2,MULT
                              IF (LF.GT.(1-(Z*(1/MULT)))) THEN
                                    NLF=LF/(1-((Z-1)*(1/MULT)))

      NAP=(((NLF*100)+29.701847)/(1.81576002*71.43))
                                    NEWEFF=MIN(LAMPEFF,(LAMPEFF*(NLF/NAP)))
                                    LLH=LOADLH/(NEWEFF*1000)
                                    LFLGOUT=(LIGHTLEV/(NEWEFF*10))*LF
                                    GOTO 1102
                              ENDIF
1101                          CONTINUE
1102              ENDIF
      ENDIF

C     DETERMINE WHETHER THE LATENT LOAD IS ASSOCIATED WITH COOLING(+)
C     OR HEATING(-)
1200  IF (LATENT .GT. 0) THEN
            LATENTCOOL=LATENT
            LATENTHEAT=0
      ELSE
            LATENTHEAT=ABS(LATENT)
            LATENTCOOL=0
      ENDIF

      IF (BLATENT .GT. 0) THEN
            BLATENTCOOL=BLATENT
            BLATENTHEAT=0
      ELSE
            BLATENTHEAT=ABS(BLATENT)
            BLATENTCOOL=0
      ENDIF

C     CALCULATION OF THE TOTAL HEATING & COOLING LOADS
```

```
C     CONVERSION FROM KJ TO KWH
      HEAT=((SHEAT+LATENTHEAT)/3600.00)
      COOL=((SCOOL+LATENTCOOL)/3600.00)
      BASEHEAT=(BHEAT+BLATENTHEAT)/3600
      BASECOOL=(BCOOL+BLATENTCOOL)/3600
      GOTO 300

C     ****************************************************************
C     *
                         *
C     *                                    P1,P2 ANALYSIS
                  *
C     *
                         *
C     ****************************************************************

C     DUFFIE & BECKMAN,EQ.11.8.2
700   ZERO=0
      P1=(1-(IFLAG*TBAR))*PWF(N_E,INF,DIS)

C     DUFFIE & BECKMAN,EQ.11.8.3
      NMIN=MIN(N_E,N_L)
      NMIN1=MIN(N_E,N_D)
      A1=DOWN+(1-DOWN)*PWF(NMIN,ZERO,DIS)/PWF(N_L,ZERO,M)
      A2=TBAR*(1-DOWN)*(PWF(NMIN,M,DIS)*(M-1/PWF(N_L,ZERO,M))+PWF(NMIN,
     &ZERO,DIS)/PWF(N_L,ZERO,M))
      A3=M_S*(1-IFLAG*TBAR)*PWF(N_E,INF,DIS)
      A4=PRTAX*VAL*(1-TBAR)*PWF(N_E,INF,DIS)
      A5=IFLAG*TBAR*PWF(NMIN1,ZERO,DIS)/MAX(N_D,1.0)
      A6=R_V*(1-IFLAG*TBAR)/(1+DIS)**N_E
      P2=A1-A2+A3+A4-A5-A6

C     AES IS THE ANNUAL ENERGY SAVINGS PER SYSTEM
C     BECC IS THE BREAK EVEN CAPITAL COST OF ONE SYSTEM
      AES=((CBLIGHT-CHLIGHT)+(BCCOST-HCCOST)+(BHCOST-HHCOST)+TPVREV)
     &/NUMBEROF
      BECC=(P1/P2)*AES

C     SET THE OUTPUTS FROM TYPE 291
300   OUT(1)=LFLGOUT
      OUT(2)=LLH
      OUT(3)=LLNH
      OUT(4)=COOL
      OUT(5)=BASECOOL
      OUT(6)=HEAT
      OUT(7)=BASEHEAT
      OUT(8)=LSCALE
      OUT(9)=SUNLIGHT
      OUT(10)=XTRAHEAT

C     SET THE OUTPUTS FROM ORGINAL TYPE 292
      OUT(11)=LIGHT
      OUT(12)=P

C     ECONOMIC OUTPUTS
      OUT(13)=P1
      OUT(14)=P2
```

```
      OUT(15)=AES
      OUT(16)=BECC
      OUT(17)=LATENTCOOL/3600
      OUT(18)=LATENTHEAT/3600
      OUT(19)=SYSEFF
      RETURN 1
      END

C     ****************************************************************
C     *
                        *
C     *                                    FUNCTION DEFINTION
                  *
C     *
                        *
C     ****************************************************************

C     DUFFIE & BECKMAN,EQ.11.5.1
      FUNCTION PWF(N,INF,DIS)
      DOUBLE PRECISION N,INF,DIS,PWF
      IF (DIS.EQ.INF) THEN
            PWF=N/(1+INF)
      ELSE
            PWF=(1/(DIS-INF))*(1-(((1+INF)/(1+DIS))**N))
      ENDIF
      END FUNCTION
```

Appendix E – Building Input Description File

```
*********************************************
*  PreBid   5.0.8
*********************************************
*   BUILDING DESCRIPTIONS FILE TRNSYS
*   FOR BUILDING:   C:\schlegel\PROJECTS\lighthum.bui
*   GET BY WORKING WITH PreBid 5.0 for Windows
*********************************************
*
---------------------------------------------
*  C o m m e n t s
---------------------------------------------
---------------------------------------------
*  P r o j e c t
---------------------------------------------
*+++ PROJECT
*+++ TITLE=GREG'S TRIAL
*+++ DESCRIPTION=TRIAL
*+++ CREATED=GOS
*+++ ADDRESS=2
*+++ CITY=3
*+++ SWITCH=UNDEFINED
---------------------------------------------
*  P r o p e r t i e s
---------------------------------------------
PROPERTIES
 DENSITY=1.204 : CAPACITY=1.012 : HVAPOR=2454.0 : SIGMA=2.041e-007 :
RTEMP=293.15
*
+++++++++++++++++++++++++++++++++++++++++++++
TYPES
+++++++++++++++++++++++++++++++++++++++++++++
*
---------------------------------------------
*  L a y e r s
---------------------------------------------
LAYER WALL_BOARD
 CONDUCTIVITY=   1.04 : CAPACITY=      1 : DENSITY=    800
LAYER MINERAL_WO
 CONDUCTIVITY=   0.13 : CAPACITY=    0.9 : DENSITY=     80
LAYER SPRUCE_PIN
 CONDUCTIVITY=   0.47 : CAPACITY=      2 : DENSITY=    600
LAYER PLYWOOD
 CONDUCTIVITY=   0.54 : CAPACITY=    1.2 : DENSITY=    800
LAYER POLY_VINYL
 CONDUCTIVITY=   0.83 : CAPACITY=      1 : DENSITY=   1500
LAYER INSUL125
 CONDUCTIVITY= 0.1548 : CAPACITY=   0.84 : DENSITY=     91
LAYER BET240
 CONDUCTIVITY=  7.326 : CAPACITY=   0.92 : DENSITY=   2100
LAYER STWOLL064
 CONDUCTIVITY= 0.1692 : CAPACITY=   0.84 : DENSITY=     75
LAYER ASBESTZ
```

```
 CONDUCTIVITY=   1.62 : CAPACITY=   1.05 : DENSITY=   1300
LAYER HOHLBLOCK
 CONDUCTIVITY=  2.016 : CAPACITY=   1.05 : DENSITY=   1300
-----------------------------------------------
*  I n p u t s
-----------------------------------------------
INPUTS LIGHT HLIGHT SCHLIGHT SCHHLIGHT SUNLIGHT XTRALGHT
-----------------------------------------------
*  S c h e d u l e s
-----------------------------------------------
SCHEDULE DAY
 HOURS =0.0  6.0  18.0  24.0
 VALUES=0 1. 0 0
SCHEDULE WEEKEND
 HOURS =0.0  24.0
 VALUES=0 0
SCHEDULE DAY519
 HOURS =0.0  5.0  19.0  24.0
 VALUES=0 1. 0 0
SCHEDULE DAY717
 HOURS =0.0  7.0  17.0  24.0
 VALUES=0 1. 0 0
SCHEDULE DAY817
 HOURS =0.0  8.0  17.0  24.0
 VALUES=0 1. 0 0
SCHEDULE TRIAL1
 DAYS=1 2 3 4 5 6 7
 HOURLY=DAY DAY DAY DAY DAY WEEKEND WEEKEND
-----------------------------------------------
*  W a l l s
-----------------------------------------------
WALL OUTSIDE
 LAYERS   = WALL_BOARD MINERAL_WO SPRUCE_PIN PLYWOOD POLY_VINYL
 THICKNESS= 0.123      0.123      0.123      0.123   0.123
 ABS-FRONT= 0.6   : ABS-BACK= 0.6
 HFRONT   = 11 : HBACK= 64
WALL CEILING
 LAYERS   = WALL_BOARD INSUL125 INSUL125 INSUL125
 THICKNESS= 0.123      0.123    0.123    0.123
 ABS-FRONT= 0.6   : ABS-BACK= 0.6
 HFRONT   = 11 : HBACK= 64
WALL TRIALEXT
 LAYERS   = WALL_BOARD MINERAL_WO SPRUCE_PIN PLYWOOD POLY_VINYL
 THICKNESS= 0.006      0.102      0.051      0.006   0.013
 ABS-FRONT= 0.6   : ABS-BACK= 0.6
 HFRONT   = 11 : HBACK= 64
WALL AWAND_S
 LAYERS   = BET240 STWOLL064 ASBESTZ
 THICKNESS= 0.24   0.064     0.025
 ABS-FRONT= 0.6   : ABS-BACK= 0.6
 HFRONT   = 11 : HBACK= 64
WALL IWAND_S
 LAYERS   = HOHLBLOCK
 THICKNESS= 0.24
 ABS-FRONT= 0.6   : ABS-BACK= 0.6
 HFRONT   = 11 : HBACK= 11
```

```
-----------------------------------------------
*  W i n d o w s
-----------------------------------------------
-----------------------------------------------
*  D e f a u l t  G a i n s
-----------------------------------------------
GAIN PERS_ISO04
 CONVECTIVE=180 : RADIATIVE=90 : HUMIDITY=0.11
GAIN COMPUTER04
 CONVECTIVE=690 : RADIATIVE=138 : HUMIDITY=0
GAIN LIGHT02_01
 CONVECTIVE=INPUT 36000*SCHLIGHT : RADIATIVE=INPUT 54000*SCHLIGHT :
HUMIDITY=0
GAIN LIGHT02_02
 CONVECTIVE=INPUT 36000*SCHHLIGHT : RADIATIVE=INPUT 54000*SCHHLIGHT :
HUMIDITY=0
-----------------------------------------------
*  O t h e r  G a i n s
-----------------------------------------------
GAIN GAIN001
 CONVECTIVE=0.5 : RADIATIVE=0.5 : HUMIDITY=0
GAIN NATLIGHT
 CONVECTIVE=0.1 : RADIATIVE=0.9 : HUMIDITY=0
GAIN GAIN002
 CONVECTIVE=0.25 : RADIATIVE=0.75 : HUMIDITY=0
-----------------------------------------------
*  C o m f o r t
-----------------------------------------------
-----------------------------------------------
*  I n f i l t r a t i o n
-----------------------------------------------
INFILTRATION INFIL001
 AIRCHANGE=0.4
INFILTRATION CONSTANT
 AIRCHANGE=0.2
-----------------------------------------------
*  V e n t i l a t i o n
-----------------------------------------------
VENTILATION VENT001
 TEMPERATURE=OUTSIDE
 AIRCHANGE=SCHEDULE 0.43*DAY817+0.17
 HUMIDITY=OUTSIDE
VENTILATION VENT002
 TEMPERATURE=OUTSIDE
 AIRCHANGE=SCHEDULE 0.18*DAY+0.06
 HUMIDITY=OUTSIDE
VENTILATION OFF
 TEMPERATURE=OUTSIDE
 AIRCHANGE=0
 HUMIDITY=OUTSIDE
-----------------------------------------------
*  C o o l i n g
-----------------------------------------------
COOLING COOL001
 ON=26
 POWER=633035
 HUMIDITY=60
```

```
-----------------------------------------------
*  H e a t i n g
-----------------------------------------------
HEATING TRIAL0
 ON=SCHEDULE 3*DAY519+17
 POWER=1.4e+006
 HUMIDITY=30
 RRAD=0
HEATING TRIAL1
 ON=SCHEDULE 5*DAY519+15
 POWER=999999999
 HUMIDITY=0
 RRAD=0
HEATING CONSTANT
 ON=20
 POWER=999999999
 HUMIDITY=40
 RRAD=0
*
-----------------------------------------------
*  Z o n e s
-----------------------------------------------
ZONES ZONE1 ZONE3
-----------------------------------------------
*  O r i e n t a t i o n s
-----------------------------------------------
ORIENTATIONS NORTH SOUTH EAST WEST HORIZONTAL
*
+++++++++++++++++++++++++++++++++++++++++++++
BUILDING
+++++++++++++++++++++++++++++++++++++++++++++
*
-----------------------------------------------
*  Z o n e  ZONE1  /  A i r n o d e  ZONE1
-----------------------------------------------
ZONE ZONE1
AIRNODE ZONE1
WALL  =TRIALEXT   : SURF=  1 : AREA=       200 : EXTERNAL : ORI=NORTH :
FSKY=0.5
WALL  =TRIALEXT   : SURF=  2 : AREA=       200 : EXTERNAL : ORI=EAST :
FSKY=0.5
WALL  =TRIALEXT   : SURF=  3 : AREA=       200 : EXTERNAL : ORI=SOUTH :
FSKY=0.5
WALL  =TRIALEXT   : SURF=  4 : AREA=       200 : EXTERNAL : ORI=WEST :
FSKY=0.5
WALL  =TRIALEXT   : SURF=  5 : AREA=      2500 : EXTERNAL : ORI=HORIZONTAL :
FSKY=1
 REGIME
 GAIN        = PERS_ISO04 : SCALE= SCHEDULE 150*DAY817+25
 GAIN        = COMPUTER04 : SCALE= SCHEDULE 150*DAY817
 GAIN        = LIGHT02_01 : SCALE= INPUT 1*LIGHT
 INFILTRATION= CONSTANT
 VENTILATION = VENT002
 COOLING     = COOL001
 HEATING     = TRIAL0
```

```
 CAPACITANCE = 12000   : VOLUME= 10000   : TINITIAL= 20      : PHINITIAL= 40
: WCAPR= 1

-----------------------------------------------
*  Z o n e  ZONE3  /  A i r n o d e  ZONE3
-----------------------------------------------
ZONE ZONE3
AIRNODE ZONE3
WALL  =TRIALEXT   : SURF=  6 : AREA=       200 : EXTERNAL : ORI=NORTH :
FSKY=0.5
WALL  =TRIALEXT   : SURF=  7 : AREA=       200 : EXTERNAL : ORI=EAST :
FSKY=0.5
WALL  =TRIALEXT   : SURF=  8 : AREA=       200 : EXTERNAL : ORI=SOUTH :
FSKY=0.5
WALL  =TRIALEXT   : SURF=  9 : AREA=       200 : EXTERNAL : ORI=WEST :
FSKY=0.5
WALL  =TRIALEXT   : SURF= 10 : AREA=      2500 : EXTERNAL : ORI=HORIZONTAL :
FSKY=1
 REGIME
 GAIN        = PERS_ISO04 : SCALE= SCHEDULE 150*DAY817+25
 GAIN        = COMPUTER04 : SCALE= SCHEDULE 150*DAY817
 GAIN        = LIGHT02_02 : SCALE= INPUT 1*HLIGHT
 GAIN        = NATLIGHT   : SCALE= INPUT 1*SUNLIGHT
 GAIN        = NATLIGHT   : SCALE= INPUT 1*XTRALGHT
 INFILTRATION= CONSTANT
 VENTILATION = VENT002
 COOLING     = COOL001
 HEATING     = TRIAL0
 CAPACITANCE = 12000   : VOLUME= 10000   : TINITIAL= 20      : PHINITIAL= 40
: WCAPR= 1
-----------------------------------------------
*  O u t p u t s
-----------------------------------------------
OUTPUTS
 TRANSFER : TIMEBASE=1.000
 AIRNODES = ZONE1
 NTYPES =  30 : QHEAT   sensible heating demand of zone (positive values)
        =  31 : QCOOL   sensible cooling demand of zone (positive values)
        =  10 : QLATD   latent energy demand of zone, humidification(-),
dehumidifcation (+)
 AIRNODES = ZONE3
 NTYPES =  30 : QHEAT   sensible heating demand of zone (positive values)
        =  31 : QCOOL   sensible cooling demand of zone (positive values)
        =  10 : QLATD   latent energy demand of zone, humidification(-),
dehumidifcation (+)
 AIRNODES = ZONE1
 NTYPES =   1 : TAIR    air temperature of zone
 AIRNODES = ZONE3
 NTYPES =   1 : TAIR    air temperature of zone
 AIRNODES = ZONE1
 NTYPES =   9 : RELHUM  relativ humidity of zone air
 AIRNODES = ZONE3
 NTYPES =   9 : RELHUM  relativ humidity of zone air
-----------------------------------------------
*  E n d

END
```

Appendix F – Hybrid Lighting Model TRNSED File

```
*|<Background> WHITE
*|<COLOR1> RED
*|<SIZE1> 14
*|<ALIGN1> CENTER
*|<STYLE1> BOLD ITALIC
*|<STYLE2> BOLD
*|<SIZE2> 10
*|<ALIGN2> LEFT
*|<SIZE3> 10
*|<TAB2> 4 IN
*|<PICTURE> HLTITLE.BMP  CENTER
*|*Hybrid Lighting Simulation
*|<COLOR1> BLACK
*|<SIZE1> 8
*|*Solar Energy Lab, UW-Madison
*|*Prepared by G.O.Schlegel
*|<COLOR1> red
*|<SIZE1> 9

**|<APPLINK1> TRNINFO.bmp brochure.pdf CENTER
*|<APPLINK1> MANUAL.bmp  OLHLSM.pdf  LEFT
*|*NOTE: User's manual will not run if Adobe Acrobat is not installed...
*|<COLOR1> BLUE
*|<SIZE1> 12

ASSIGN "C:\schlegel\PROJECTS\SI_COMBINED.LST" 6
ASSIGN "C:\schlegel\PROJECTS\lighthum.bld" 26
ASSIGN "C:\schlegel\PROJECTS\lighthum.trn" 27
ASSIGN "C:\trnsys15\prebid\Lib\American\W4-lib.dat" 28
ASSIGN "C:\schlegel\PROJECTS\SI_COMBINED.out" 17
ASSIGN "C:\schlegel\PROJECTS\SI_COMBINED_Int.out" 18
ASSIGN "C:\schlegel\Hybrid Lighting\SOLAR3.DAT" 32
ASSIGN "C:\schlegel\Hybrid Lighting\CONCENTRATOR.DAT" 33
ASSIGN "C:\schlegel\Hybrid Lighting\COLDMIRROR.DAT" 34
ASSIGN "C:\schlegel\Hybrid Lighting\vlambda.DAT" 29
ASSIGN "C:\schlegel\Hybrid Lighting\atten.DAT" 30
ASSIGN "C:\schlegel\Hybrid Lighting\GASB.DAT" 31
ASSIGN "C:\schlegel\PROJECTS\WDATA.DAT" 25
ASSIGN "C:\schlegel\PROJECTS\type56.out" 35



**********************************************************************
**
*** Control cards
**********************************************************************
**
* START, STOP and STEP
*|[SIMPAR|Simulation Parameters
EQUATIONS 7
I_MONTH= 0
*|<Month of the simulation                    |Month1.dat|1|2|1000
I_DAY1= 1.0000000000000E+00
*|Day of Month for Simulation Start           |||0|1|1|31|1000
```

```
I_DAY=I_MONTH/24+I_DAY1
I_LENGTH= 365
*|<Length of Simulation                          |Length.dat|2|1|1000
WEEKS=I_LENGTH/7.
START=24*(I_DAY-1)+1
STOP=START+I_LENGTH*24-1
EQUATIONS 1
STEP=1.0
*Timestep |hours|hours|0|1|1|1000000.00000|1000
*SIMULATION Start time   End time    Time step
SIMULATION  START  STOP  STEP
*|]

*|(WEATHER|Weather Data
*|Use Average Monthly Weather Data|MONTHLY
*|Use TMY2 Weather Data Files (User Provided)|TMY2
*|)

*|[TMY2|
EQUATIONS 4
CITY= 230
*|<City for Simulation                |CitiesK.dat |2|1|1000
LAT= 43.13
*|<Latitude of City                   |CitiesK.dat |0|3|1000
TIMESHIFT= 0.67
*|<Adjustment to solar time           |CitiesK.dat |0|5|1000
GNDTEMP= 1
*|<Average ground temperature                    |CitiesK.dat|0|7|1000
Assign madisn.tm2 13
*|<City Path                                     |CitiesK.dat |0|9|1000
*|]

*|#*|[MONTHLY|
*|#EQUATIONS 3
*|#CITY= 218
*|#*|<City for Simulation                  |Cities.dat |2|1|1000
*|#LAT= 31.62
*|#*|<Latitude of City                |Cities.dat |0|3|1000
*|#GNDTEMP= 1
*|#*|<Average Ground Temperature             |Cities.dat|0|6|1000
*|#Assign  13
*|#*|<City Path                                 |Cities.dat |0|5|1000
*|#CONSTANTS 2
*|#TIMESHIFT= 0.0
*|#TURB= 1.0000000000000E-01
*|#*|Average Annual Turbidity Level |||0.0|0.4|0|1.0|1
*|#*|]

*|(SIMTYPE|Simulation Type
*|Wide Band Model|SMARTS2|_BAND
*|Narrow Band Model|BAND|_SMARTS2
*|)

*|[CONCPAR|System Parameters
CONSTANTS 2
NUMBEROF= 1.0000000000000E+01
*|Number of Systems                        |||0|1|0|1000|1
```

```
CONCENT1= 1.7000000000000E+00
*|Concentrator Area                        |sq.m.|sq.ft.|0|10.76|0.0|100.00|4
*|]

*|[NARROW|Narrow Band Model Parameters
CONSTANTS 1
CONCTYPE= 1.0000000000000E+00
*|Concentrator material  |||0|1|0|1000|1
*|<COLOR1> BLACK
*|<SIZE1> 10
*|*(1=ECP-305, 2=FLABEG, 3=REFLECTECH)
*|<COLOR1> BLUE
*|<SIZE1> 12
*|]

*|[WIDE|Wide Band Model Parameters
CONSTANTS 7
RHO1= 9.7000000000000E-01
*|Average Spectral Reflectance      of Concentrator   |||0.0|1.0|0|1.00|1
RHO2= 9.3000000000000E-01
*|Average Spectral Reflectance      of Secondary Element
      |||0.0|1.0|0|1.00|1
FILTERIR= 7.3000000000000E-01
*|Average Spectral Transmittacne of Secondary Element
      |||0.0|1.0|0|1.000|1|%/m|%/ft|0.0|1.0|0|1.00|1
ATTEN= 1.3000000000000E+00
*|Average Spectral Attenuation of Light Fiber   |%/m|%/ft|0|0.305|0|100.0|1
TPVEFFIC= 1.6000000000000E-01
*|Average TPV Efficiency in the IR        |||0.0|1.0|0|1.00|1
IRSPECTR= 5.1000000000000E-01
*|IR Spectrum Fraction              |||0.0|1.0|0|1.00|1
VISIBLES= 4.7000000000000E-01
*|Visible Spectrum Fraction               |||0.0|1.0|0|1.00|1
*|]

*|[LTPAR|Optical Fiber Parameters
Constants 2
TUBEREFL= 9.5000000000000E-01
*|Optical Fiber Entrance Reflectance                        |||0|1|0|1.00|5
TLENGTH= 7.0000000000000E+00
*|Length Of Optical Fiber                    |m|ft|0|3.28084|0.0|1000000.00|6
*|]


*|[BLDGPAR|Conventional Lighting Parameters
CONSTANTS 3
LIGHTLEV= 5.0000000000000E+02
*|Lighting Level                          |lux|fc|0|.0929|0.00|1000.0|13
LAMPEFFI= 8.5000000000000E+01
*|Lamp Efficacy                           |lm/w|lm/w|0|1|0.0|683.0|14
LUMEFF= 8.3000000000000E-01
*|Luminaire Efficiency               |||0|1|0|1.00|15
*|]

*|[TPVPAR| TPV Parameters
CONSTANTS 2
T_C= 2.9800000000000E+02
```

```
*|TPV Cell Temperature |K|K|0|1|0.0|1000.0|18
OPTEFF= 6.8400000000000E-01
*|Non Imaging Optical Device Efficiency  |||0|1|0.000|1.000|18
*|]

*|[LIGHTSCH|Daily Building Lighting Schedule
CONSTANTS 4
WDLON= 8.0000000000000E+00
*|Time Lights are ON Weekdays |||0|1|0|24.0|16
WDLOFF= 1.7000000000000E+01
*|Time Lights are OFF Weekdays      |||0|1|0|24.0|16
WELON= 8.0000000000000E+00
*|Time Lights are ON Weekends |||0|1|0|24.0|16
WELOFF= 1.7000000000000E+01
*|Time Lights are OFF Weekends      |||0|1|0|24.0|16
*|]

*|(RATES|Utility Rate Schedules
*|Choose an existing rate schedule|EXISTING
*|Define a rate schedule|ELECPRICE
*|)

*|[EXISTING|Choose a Rate Schedule
EQUATIONS 16
SHHRON= 10
*|<Utility Provider                    |Rates.dat |2|3|17
SHON= 0.0636
*|<
|Rates.dat |0|4|17
SUMHRON = 10.0
*|<
|Rates.dat |0|5|17
SUMON= 0.0636
*|<                              |Rates.dat |0|6|17
SUMHROFF= 21.0
*|<                              |Rates.dat |0|7|17
SUMOFF= 0.0366
*|<                              |Rates.dat |0|8|17
SHHROFF= 21.0
*|<
|Rates.dat |0|9|17
WINHRON= 10.0
*|<                              |Rates.dat |0|10|17
WINON= 0.0567
*|<                              |Rates.dat |0|11|17
WINHROFF= 21.0
*|<                              |Rates.dat |0|12|17
WINOFF= 0.03066
*|<                              |Rates.dat |0|13|17
edaily= 1.0355
*|<                              |Rates.dat |0|14|17
emonthly= 865
*|<                              |Rates.dat |0|15|17
STARTSUM= 3625
*|<                              |Rates.dat |0|16|17
STARTWIN= 6553
*|<                              |Rates.dat |0|17|17
```

```
NGPRICE= 0.0247
*|<                              |Rates.dat |0|18|17
*|]

*|#*|[ELECPRICE|Utility Rate Schedules
*|#*|<COLOR1> red
*|#*|<SIZE1> 9
*|*Weekends are considered off-peak
*|*
*|#*|<COLOR1> BLUE
*|#*|<SIZE1> 12
*|#CONSTANTS 15
*|#SHHRON= 8.5000000000000E+00
*|#*|Summer Shoulder Start Time           |hr|hr|0|1|0|24.00|17
*|#SHON= 1.8000000000000E-01
*|#*|Summer Shoulder Rate           |$/kWh|$/kWh|0|1|0|1.0000|17
*|#SHHROFF= 2.1500000000000E+01
*|#*|Summer Shoulder End Time       |hr|hr|0|24|0|24.00|17
*|#SUMON= 1.8000000000000E-01
*|#*|Summer On Peak Rate            |$/kWh|$/kWh|0|1|0|1.0000|17
*|#SUMHRON= 1.2000000000000E+01
*|#*|Summer Peak Start Time         |||0|1|0|24.00|17
*|#SUMOFF= 1.8000000000000E-01
*|#*|Summer Off Peak Rate           |$/kWh|$/kWh|0|1|0|1.0000|17
*|#SUMHROFF= 1.8000000000000E+01
*|#*|Summer Peak End Time           |||0|1|0|24.00|17
*|#WINON= 1.8000000000000E-01
*|#*|Winter On Peak Rate            |$/kWh|$/kWh|0|1|0|1.0000|17
*|#WINHRON= 8.5000000000000E+00
*|#*|Winter Peak Start Time         |||0|1|0|24.00|17
*|#WINOFF= 1.8000000000000E-01
*|#*|Winter Off Peak Rate           |$/kWh|$/kWh|0|1|0|1.0000|17
*|#WINHROFF= 2.1500000000000E+01
*|#*|Winter Peak End Time           |||0|1|0|24.00|17
*|#EDAILY= 0.0000000000000E+00
*|#*|Daily Customer Charge (if applicable)  |$/day|$/day|0|1|0|100.00|17
*|#EMONTHLY= 0.0000000000000E+00
*|#*|Monthly Demand Charge (if applicable)  |$/peak kW|$/peak
kW|0|1|0|1000.00|17
*|#STARTSUM= 2.8810000000000E+03
*|#*|Hour of Year Summer Prices Begin          |hr|hr|0|1|0|8760|18
*|#STARTWIN= 7.2970000000000E+03
*|#*|Hour of Year Winter Prices Begin          |hr|hr|0|1|0|8760|18
*|#NGPRICE= 2.0000000000000E-02
*|#*|Average Annual Natural Gas Price
|$/kwh|$/kwh|0|1|0.000|1.000|18
*|#*|]

*|[ECON1|Economic Parameters
EQUATIONS 13
INF= 3.0000000000000E-02
*|General Inflation Rate  |%|%|0|1|0|1.000|18
FUELINF= 2.0000000000000E-02
*|Fuel Inflation Rate  |%|%|0|1|0|1.000|18
M= 6.0000000000000E-02
*|Mortgage Rate  |%|%|0|1|0|1.000|18
DIS= 6.0000000000000E-02
```

```
*|Discount Rate  |%|%|0|1|0|1.000|18
N_E= 1.0000000000000E+01
*|Years of Analysis  |years|years|0|1|0|100.0|18
N_D= 1.0000000000000E+01
*|Years of Decpreciation  |years|years|0|1|0|100.0|18
N_L= 1.0000000000000E+01
*|Years of Loan  |years|years|0|1|0|100.0|18
TBAR= 2.5000000000000E-01
*|Income Tax  |%|%|0|1|0|1.000|18
PRTAX= 3.0000000000000E-02
*|Property Tax  |%|%|0|1|0|1.000|18
DOWN= 2.0000000000000E-01
*|Downpayment  |%|%|0|1|0|1.00|18
*|]
*|[ECON2|
*|<TAB2>5 IN
M_S= 1.0000000000000E-01
*|Ratio of Misc. Costs to First Year Misc. Costs to Initial Investment
|%|%|0|1|0|1.00|18
R_V= 3.0000000000000E-01
*|Ratio of Resale Value at End of Analysis to Initial Investment
|%|%|0|1|0|1.00|18
VAL= 1.0000000000000E+00
*|Ratio of Assessed value to Initial Investment  |%|%|0|1|0|1.00|18
*|]

*|(INCOME|
*|Income Producing Property|INCF
*|Non - Income Producing Property|NINCF
*|)

*|{OUT|Output Parameters
*|Generate Online Plot|ONLINE
*|}

*<><><><><><><><><><><><><><><><><><><><><><><><><><><><><><><><><><><><<>

* User defined CONSTANTS
VERSION 15
*                              Integration  Convergence
TOLERANCES 0.00001 0.00001
*                              Max iterations     Max warnings      Trace
limit
LIMITS 30 30 30
*                              TRNSYS numerical integration solver method
DFQ 1
*                              TRNSYS output file width, number of characters
WIDTH 80
*                              NOLIST statement
LIST
*                              MAP statement
MAP
*                              Solver statement
SOLVER 0

*****************************************************************************
**
```

```
*** Units
**********************************************************************
**
EQUATIONS 1
TPVKWH=[24,10]/1000
*|[TMY2|
EQUATIONS 1
TURB=[18,22]
*|]
* EQUATIONS "KT"
EQUATIONS 2
EXTRA = max(1,[19,1])
KT = [19,4]/EXTRA
*----------------------------------------------------------------------
--
* EQUATIONS "Electric Eqn"
EQUATIONS 9
rate = [17,9]*([10,1]*[13,1]+([11,1]*(1-[13,1])))+(1-[17,9])*(((1-
[17,8])*[9,1]+[17,8]*[10,1])*[13,1]+(((1-[17,8])*[12,1]+[17,8]*[11,1])*(1-
[13,1])))
base = [31,3]*rate+0.5*((edaily/24)+(emonthly/720))
hybrid=[31,2]*rate+0.5*((edaily/24)+(emonthly/720))

*|#*|[SMARTS2|
*|#MODELFLAG=1
*|#*|]
*|[BAND|
MODELFLAG =-1
*|]

*|#*|[NINCF|
*|#IFLAG=0
*|#*|]
*|[INCF|
IFLAG=1
*|]
TPVR =([31,12]/1000)*rate
COP = 3
HCCost = ([31,4]/COP)*rate+0.5*((edaily/24)+(emonthly/720))
BCCOST = ([31,5]/COP)*rate+0.5*((edaily/24) +(emonthly/720))
*----------------------------------------------------------------------
--
* EQUATIONS "Light Conv"
EQUATIONS 3
lightout = [23,1]/1000
hlightout = [23,2]/1000
TPVOUT=[23,7]/1000000
*----------------------------------------------------------------------
--
* EQUATIONS "Equa"
EQUATIONS 3
Aux = [24,9]+[24,2]+[24,1]
NoSolar = [24,8]+[24,3]+[24,4]
Load = [24,5]+[24,7]+[24,6]
*----------------------------------------------------------------------
--
* EQUATIONS "Sens Conv"
```

```
EQUATIONS 5
hcoolout = [23,4]/1000
coolout = [23,3]/1000
hheatout = [23,6]/1000
heatout = [23,5]/1000
TPVMWH=TPVKWH/1000
*-------------------------------------------------------------------------------
--
* EQUATIONS "Gas Prices"
CONSTANTS 5
NGSUM= NGPRICE
NGWIN= NGPRICE
NGDAILY= 0
NGON= 2.8810000000000E+03
NGoff= 7.2970000000000E+03
EQUATIONS 3
Eta = .80
HHCOST = ([31,6]/Eta)*[14,1]+NGDAILY/24
BHCOST = ([31,7]/Eta)*[14,1]+NGDAILY/24
*-------------------------------------------------------------------------------
--
* EQUATIONS "Light"
EQUATIONS 4
SchLight = [17,9]*[16,1]+(1-[17,9])*((1-[17,8])*[15,1]+([17,8]*[16,1]))
SchHLight = SchLight
Light = [31,8]
Hlight = [31,1]

*-------------------------------------------------------------------------------
--
*****Schedules*****
*-------------------------------------------------------------------------------
--
UNIT 9 TYPE 14     $/kwh, WD, SUM Schedule T14h
PARAMETERS 20
0 SUMOFF SHHRON  SUMOFF SHHRON SHON SUMHRON SHON SUMHRON SUMON SUMHROFF SUMON
SUMHROFF SHON SHHROFF SHON SHHROFF SUMOFF 24 SUMOFF
*-------------------------------------------------------------------------------
--
UNIT 10 TYPE 14    $/kwh, WE,SUM Schedule, T14h
PARAMETERS 4
0 SUMOFF 24 SUMOFF
*-------------------------------------------------------------------------------
--
UNIT 11 TYPE 14    $/kwh, WE,WIN Schedule, T14h-2
PARAMETERS 4
0 WINOFF 24 WINOFF
*-------------------------------------------------------------------------------
--
UNIT 12 TYPE 14    $/kwh, WD, WIN Schedule, T14h-3
PARAMETERS 12
0 WINOFF WINHRON WINOFF WINHRON WINON WINHROFF WINON WINHROFF WINOFF 24
WINOFF
*-------------------------------------------------------------------------------
--
UNIT 13 TYPE 14    SEASON
PARAMETERS 12
```

```
0 0 STARTSUM 0 STARTSUM 1 STARTWIN 1 STARTWIN 0 8760 0
*-------------------------------------------------------------------------------
--
* Model "Natural Gas Schedule T14h" (Type 14)
UNIT 14 TYPE 14    Natural Gas Schedule T14h
PARAMETERS 12
0 NGWIN NGON NGWIN NGON NGSUM NGOFF NGSUM NGOFF NGWIN 8760 NGWIN
*-------------------------------------------------------------------------------
--
*Weekday Lighting Schedule
UNIT 15 TYPE 14    Light Wday
PARAMETERS 12
1 0 WDLON 0 WDLON 1 WDLOFF 1 WDLOFF 0 24 0
*-------------------------------------------------------------------------------
--
*Weekend Lighting Schedule
UNIT 16 TYPE 14    Light Sched T14h
PARAMETERS 12
1 0 WELON 0 WELON 1 WELOFF 1 WELOFF 0 24 0
*-------------------------------------------------------------------------------
--
UNIT 17 TYPE 95    holidays_T95a
PARAMETERS 4
0 1998 0 1
*-------------------------------------------------------------------------------
--
****TRNSYS TYPES****
*-------------------------------------------------------------------------------
--
*|#*|[MONTHLY|
*|#UNIT 18 TYPE 54       TYPE54a
*|#PARAMETERS 19
*|#1 25 CITY 2 1 1 4.0 4.0 4.0 4.0 4.0 4.0 4.0 4.0 4.0 4.0 4.0 4.0 0.0
*|#*-----------------------------------------------------------------------
-----
*|#UNIT 19 TYPE 16       TYPE16g
*|#PARAMETERS 9
*|#4 1 3 START LAT 4871.0 0.0 2 -1
*|#INPUTS 13
*|#18,7 18,8 18,99 18,100 0,0 0,0 0,0 0,0 0,0 0,0 0,0 0,0 0,0 0,0
*|#0.0 0.0 0.0 1.0 0.2 90 0.0 90 90 90 180 90 270
*|#*-----------------------------------------------------------------------
-----
*|#UNIT 20 TYPE 16       TYPE16g-2
*|#PARAMETERS 9
*|#4 4 3 START LAT 4871.0 0.0 2 -1
*|#INPUTS 7
*|#18,7 18,8 18,99 18,100 0,0 0,0 0,0
*|#0.0 0.0 0.0 1.0 0.2 90 0.0
*|#*-----------------------------------------------------------------------
-----
*|#UNIT 21 TYPE 69       TYPE69b
*|#PARAMETERS 2
*|#0 0
*|#INPUTS 5
*|#18,4 18,5 18,8 0,0 0,0
*|#0 20 0 0 0
```

```
*|#*|]
*-------------------------------------------------------------------------
--
*|[TMY2|
UNIT 18 TYPE 89    TYPE89b-2
PARAMETERS 2
-2 13
*-------------------------------------------------------------------------
--
UNIT 19 TYPE 16    TYPE16g
PARAMETERS 9
*HorMode  TrackMode TiltMode  StartDay  Latitude  SolConst  Shift     NotUsed
SolarTime
4 1 3 START LAT 4871.0 TIMESHIFT 2 1
INPUTS 13
18,4 18,3 18,99 18,100 0,0 0,0 0,0 0,0 0,0 0,0 0,0 0,0 0,0 0,0
*** INITIAL INPUT VALUES
0.0 0 0.0 1.0 0.2 90 0.0 90 90 90 180 90 270
*-------------------------------------------------------------------------
--
UNIT 20 TYPE 16    TYPE16g-2
PARAMETERS 9
4 4 3 START LAT 4871.0 TIMESHIFT 2 1
INPUTS 7
18,4 18,3 18,99 18,100 0,0 0,0 0,0
0.0 0.0 0.0 1.0 0.2 90 0.0
*-------------------------------------------------------------------------
--
UNIT 21 TYPE 69    TYPE69b
PARAMETERS 2
0 0
INPUTS 5
18,5 18,9 18,3 0,0 0,0
0 20 0 0 0
*|]

*-------------------------------------------------------------------------
--
***TYPE 56***
*-------------------------------------------------------------------------
--
UNIT 22 TYPE 56    type56
PARAMETERS 5
26 27 28 0 0.50
INPUTS 24
*|[TMY2|
18,5 18,10
*|]
*|#*|[MONTHLY|
*|#18,4 18,6
*|#*|]
21,1 19,17 19,7 19,22 19,12 19,4 19,18 19,8 19,23 19,13 19,5 19,20 19,10
19,25 19,15 19,2
Light
HLIGHT
SCHlight
SCHHLIGHT
```

```
31,9
31,10
*** INITIAL INPUT VALUES
0 0 0 0 0 0 0 0 0 0 0 0 0 0 0 0 0 0 0 0 0 0 0 0 0 0
*-------------------------------------------------------------------------------
--

UNIT 23 TYPE 24    TYPE24
PARAMETERS 1
* 1 Reset time
stop
INPUTS 7
31,2 31,3 31,4 31,5 31,6 31,7 31,12
*** INITIAL INPUT VALUES
0.0 0.0 0.0 0.0 0.0 0.0 0.0
*-------------------------------------------------------------------------------
--
UNIT 24 TYPE 24    TYPE24-2
PARAMETERS 1
* 1 Reset time
stop
INPUTS 12
HCCost HHCOST BCCOST BHCOST 31,3 31,6 31,4 base hybrid TPVR
31,12
20,8
*** INITIAL INPUT VALUES
0.0 0.0 0.0 0.0 0.0 0.0 0.0 0.0 0.0 0.0 0.0 0
*-------------------------------------------------------------------------------
--
*|#*|[ONLINE|
*|#UNIT 25 TYPE 65       Lighting-Int
*|#PARAMETERS 10
*|#* 1 Nb. of left-axis variables
*|#2
*|#* 2 Nb. of right-axis variables
*|#1
*|#* 3 Left axis minimum
*|#0.0
*|#* 4 Left axis maximum
*|#100
*|#* 5 Right axis minimum
*|#0.0
*|#* 6 Right axis maximum
*|#10000
*|#* 7 Number of plots per simulation
*|#1
*|#* 8 X-axis gridpoints
*|#14
*|#* 9 Shut off Online w/o removing
*|#0
*|#* 10 Logical Unit for ouput file
*|#-1
*|#INPUTS 3
*|#* Light Conv:lightout ->Left axis variable-1
*|#Lightout
*|#* Light Conv:hlightout ->Left axis variable-2
*|#hlightout
```

```
*|#* [unconnected] Right axis variable
*|#TPVOUT
*|#*** INITIAL INPUT VALUES
*|#Baseline w/Hybrid TPV
*|#LABELS  5
*|#MWh MWh MWh
*|#Lighting Energy (MWh)
*|#TPV ENERGY (MWh)
*|#Lighting Energy
*|#*-------------|-------------------------------------------------------------
------
*|#UNIT 26 TYPE 65       Sensible - Int
*|#PARAMETERS 10
*|#* 1 Nb. of left-axis variables
*|#2
*|#* 2 Nb. of right-axis variables
*|#2
*|#* 3 Left axis minimum
*|#0
*|#* 4 Left axis maximum
*|#100
*|#* 5 Right axis minimum
*|#0.0
*|#* 6 Right axis maximum
*|#500
*|#* 7 Number of plots per simulation
*|#1
*|#* 8 X-axis gridpoints
*|#12
*|#* 9 Shut off Online w/o removing
*|#0
*|#* 10 Logical Unit for ouput file
*|#-1
*|#INPUTS 4
*|#* Sens Conv:hcoolout ->Left axis variable-1
*|#hcoolout
*|#* Sens Conv:coolout ->Left axis variable-2
*|#coolout
*|#* Sens Conv:hheatout ->Right axis variable-1
*|#hheatout
*|#* Sens Conv:heatout ->Right axis variable-2
*|#heatout
*|#*** INITIAL INPUT VALUES
*|#w/Hybrid Baseline w/Hybrid Baseline
*|#LABELS  5
*|#MWh MWh
*|# Cooling Energy (MWh)
*|# Heating Energy (MWh)
*|#Sensible Energy
*|#*|]
*-------------------------------------------------------------------------------
--

UNIT 28 TYPE 25    TYPE25b
PARAMETERS 6
STEP START STOP 17 1 1
INPUTS 17
```

```
18,5 22,7 22,8 20,8 31,7 31,6 31,5 31,4 31,2 31,3 31,11 TPVKWH 31,17 31,18
22,9 22,10 31,19
TAMB TZONE1 TZONE2 Beam BHeat HHeat BCool HCool HLight BLight Lumens TPVOUT
LC LH RH1 RH2 SYSEFF
C C C kj/hr-m2 kj/hr kj/hr kj/hr kj/hr kWh kWh lumens kWh KWH KWH % % %
*--------------------------------------------------------------------------
--
UNIT 29 TYPE 25
PARAMETERS 6
STEP START STOP 18 1 1
INPUTS 14
23,1 23,2 23,3 23,4 23,5 23,6 24,8 24,9 24,3 24,1 24,4 24,2 24,10 24,12
HLIGHT BLIGHT HCOOL BCOOL HHEAT BHEAT CBLIGHT CHLIGHT CBCOOL CHCOOL CBHEAT
CHHEAT CTPV Beam
KWH KWH KWH KWH KWH KWH $ $ $ $ $ $ $ kJ
*--------------------------------------------------------------------------
--
UNIT 31 TYPE 292   Type292
PARAMETERS 39
* 1 Latitude
LAT
* 2 Logical unit of Smarts2v91 Solar Irradiance file
32
* 3 Logical unit of concentrator reflectance data
33
* 4 Concentrator Type
CONCTYPE
* 5 Logical unit of cold mirror spectral data file
34
* 6 Logical unit of visibility curve (v lambda) data
29
* 7 Logical unit of optical fiber data file
30
* 8 optical fiber length
TLENGTH
* 9 Logical unit of TPV response data file
31
* 10 Collector Area
CONCENT1
*1 concentrator relfectance
RHO1
* 2 Filter Visisble Reflectance
RHO2
* 3 tube reflectance
TUBEREFL
* 4 Visible spectrum fraction
VISIBLES
* 5 IR spectrum fraction
IRSPECTR
* 7 Filter IR transmittance
FILTERIR
* 19 Number of Collectors
NUMBEROF
* 20 Attenuation (%/length)
ATTEN
* 21 Luminaire Efficiency
LUMEFF
```

```
* 22 TPV EFFICIENCY
TPVEFFIC
* 23 LIGHT LEVEL
LIGHTLEV
* 24 BLDG AREA
2500
* 25 LAMP EFFICACY
LAMPEFFI
MODELFLAG
TBAR IFLAG N_D DOWN M_S VAL PRTAX R_V N_E
N_L INF FUELINF DIS M, OPTEFF
INPUTS 21
* TYPE16h-2:Solar zenith angle ->Zenith Angle
20,2
* TYPE16h-2:Extraterrestrial on horizontal ->Extra Terrestrial Radiation
20,1
* TYPE16h-2:Total horizontal radiation ->Total Horizontal Radiation
20,4
*TURBIDITY INPUT
TURB
20,6
20,5
20,8
* Light:SchLight ->LIGHTING FLAG
SchLight
22,4 22,5 22,6 22,1 22,2 22,3
24,8 24,9 24,3 24,1 24,4 24,2 24,10
*** INITIAL INPUT VALUES
0 0 0 0.1 0 0 0 0 0 0 0 0 0 0 0 0 0 0 0 0 0

UNIT 32 TYPE 580 TYPE580
PARAMETERS 3
21 1 0
INPUTS 18
23,1 23,2 23,3 23,4 23,5 23,6 24,8 24,9 24,3 24,1 24,4 24,2 24,10 31,13 31,14
31,15 31,16 23,7
0 0 0 0 0 0 0 0 0 0 0 0 0 0 0 0 0 0

UNIT 33 TYPE 25    TYPE25b
PARAMETERS 6
STEP START STOP 35 1 1
INPUTS 6
base 31,3 bhcost 31,6 bccost 31,5
lightingcost lightingenergy heatingcost heatingenergy coolingcost cooling
energy
$ kwh $ kwh $ kwh

END
```

Bibliography

American Society of Heating, Refrigeration, and Air-conditioning Engineers (ASHRAE), *2001 ASHRAE Handbook - Fundamentals*, 2001.

American Society of Heating, Refrigeration, and Air-conditioning Engineers (ASHRAE), *Ventilation for Acceptable Indoor Air Quality, ASHRAE Standard 62-2001*, 2001.

Berk, A., Bernstein, L. S., and Robertson, D. C., *MODTRAN: A moderate resolution model for LOWTRAN,* Rep. GL-TR-89-0122, Air Force Geophysical Lab., Hanscom, MA, 1989.

BP Solar, (http://www.bpsolar.com/), 2003

Department of Energy, *Annual Energy Outlook 2001 Market Trends – Energy Demand*, available at http://www.eia.doe.gov/oiaf/aeo/demand.html#comm, Dec. 2000.

Department of Energy, Energy Information Administration, available at http://www.eia.doe.gov/emeu/states /_states.html, 2003.

Duffie, J.A. and Beckman, W.A., *Solar Engineering of Thermal Processes*, 2nd Ed., John Wiley and Sons, 1991.

Dye, D., Wood, B.D., Fraas, L.M., Muhs, J.D., *Optical Design of an Infrared Non-Imaging Device for a Full Spectrum Solar Energy System*, International Solar Energy Conference, Kohala Coast, Hawaii Island, March 15-18, 2003.

Earl, D.D., Muhs, J.D., *Modeling and Evaluation of Chromatic Variations in a Hybrid Solar/Electric Lighting System*, International Solar Energy Conference, Kohala Coast, Hawaii Island, March 15-18, 2003a.

Earl, D.D., Maxey, C.L., Muhs, J.D., *Performance of New Hybrid Solar Lighting Luminaire Design*, International Solar Energy Conference, Kohala Coast, Hawaii Island, March 15-18, 2003b.

Fay, C*., Daylighting and Productivity, A Literature Review*, International Solar Energy Conference, Kohala Coast, Hawaii Island, March 15-18, 2003.

Fraas, L.M., Pyle, W.R., Ryason, P.R., *Concentrated and Piped Sunlight for Indoor Illumination*, Applied Optics, Vol.22, No.4, February 1983, p. 578-582.

Fraas, L.M., Daniels, W.E., Muhs, J.D., *Infrared Photovoltaics for Combined Solar Lighting and Electricity for Buildings*,17th European PV Solar Energy Conference, Munich, Germany, October 22-26, 2001.

Fraas, L.M., Avery, J.E., Nakamura, T., *Electricity from Concentrated Solar IR in Solar Lighting Applications*, 29th IEEE Photovoltaic Specialists Conference, May 20-24, 2002.

Gueymard, C., *Prediction and Performance Assessment of Mean Hourly Global Radiation*, Solar Energy, Vol. 68, No. 3, March, 2000.

Illuminating Engineering Society of North America (IESNA)*, The IESNA Lighting Handbook: Reference and Application,* Illuminating Engineering Society of North America, New York, N.Y., 2000.

Iqbal, M., *An Introduction to Solar Radiation*, Academic Press, Toronto, 1983.

Kneizys, F. X., Shettle, E. P., et al., *Atmospheric transmittance/radiance: Computer code LOWTRAN 5,* Rep. AFGL TR-80-0067, Air Force Geophysics Lab., Hanscom AFB, MA, 1980.

Lin, J.L., Burger, D.R., *TPV Cell IV Curve Testing with Varying Black Body Emission Temperatures, Intensities, and Cell Temperatures*, Solar Energy Materials and Solar Cells, Vol. 40 (1996), pp. 177-181.

Maxey, L.D., Cates, M.R., Jaiswal, S.L., *Efficient Optical Couplings for Fiber-Distributed Solar Lighting*, International Solar Energy Conference, Kohala Coast, Hawaii Island, March 15-18, 2003b.

Means Company, Inc., *Means Building Construction Cost Data,* 53rd Annual Edition, Phillip R. Waier, P.E., Senior Editor, 1995.

Muhs, J.D., *Hybrid Lighting Doubles the Efficiency and Affordability of Solar Energy in Commercial Buildings*, CADDET- Energy Efficient News Letter, No. 4, 2000a, p. 6 - 9.

Muhs, J.D., *Design and Analysis of Hybrid Solar Lighting and Full Spectrum Solar Energy Systems*, Proceedings of the American Solar Energy Society, Solar 2000, June16-21, 2000b, American Solar Energy Society.

National Lighting Product Information Program (NLPIP), *Dimming Electronic Ballasts, Specifier Reports*, available at http:\\www.lrc.rpi.edu, Vol.7, Number 3, October 1999.

Klein, S.A., et al., *TRNSYS, A Transient Simulation Program*, Solar Energy Laboratory, University of Wisconsin – Madison, USA, 2000.

Kneizys, F. X., Shettle, E. P., et al., *Atmospheric transmittance/radiance: Computer code LOWTRAN 5,* Rep.AFGL TR-80-0067, Air Force Geophysics Lab., Hanscom AFB, MA, 1980.

Tekelioglu, M., Wood, B.D., *Thermal Management of the Polymethylmethacrylate (PMMA) Core Optical Fiber for use in Hybrid Solar Lighting*, International Solar Energy Conference, Kohala Coast, Hawaii Island, March 15-18, 2003.